

AWARD NUMBER: W81XWH-16-1-0392

TITLE: Investigating the Role of PCM1 and Mib1 in Regulating Ciliogenesis and in Prostate Cancer

PRINCIPAL INVESTIGATOR: Lei Wang

CONTRACTING ORGANIZATION: NEW YORK UNIVERSITY
New York, NY 10016

REPORT DATE: November 2018

TYPE OF REPORT: Final

PREPARED FOR: U.S. Army Medical Research and Materiel Command
Fort Detrick, Maryland 21702-5012

DISTRIBUTION STATEMENT: Approved for Public Release;
Distribution Unlimited

The views, opinions and/or findings contained in this report are those of the author(s) and should not be construed as an official Department of the Army position, policy or decision unless so designated by other documentation.

REPORT DOCUMENTATION PAGE

Form Approved
OMB No. 0704-0188

Public reporting burden for this collection of information is estimated to average 1 hour per response, including the time for reviewing instructions, searching existing data sources, gathering and maintaining the data needed, and completing and reviewing this collection of information. Send comments regarding this burden estimate or any other aspect of this collection of information, including suggestions for reducing this burden to Department of Defense, Washington Headquarters Services, Directorate for Information Operations and Reports (0704-0188), 1215 Jefferson Davis Highway, Suite 1204, Arlington, VA 22202-4302. Respondents should be aware that notwithstanding any other provision of law, no person shall be subject to any penalty for failing to comply with a collection of information if it does not display a currently valid OMB control number. **PLEASE DO NOT RETURN YOUR FORM TO THE ABOVE ADDRESS.**

1. REPORT DATE November 2018	2. REPORT TYPE Final	3. DATES COVERED 15 Jul 2016 - 14 Jul 2018
4. TITLE AND SUBTITLE Investigating the Role of PCM1 and Mib1 in Regulating Ciliogenesis and in Prostate Cancer		5a. CONTRACT NUMBER W81XWH-16-1-0392
		5b. GRANT NUMBER
		5c. PROGRAM ELEMENT NUMBER
6. AUTHOR(S) Lei Wang		5d. PROJECT NUMBER
		5e. TASK NUMBER
E-Mail: Lei.Wang2@nyumc.org		5f. WORK UNIT NUMBER
7. PERFORMING ORGANIZATION NAME(S) AND ADDRESS(ES) AND ADDRESS(ES) NEW YORK UNIVERSITY 550 1ST AVE NEW YORK NY 10016-6402		8. PERFORMING ORGANIZATION REPORT NUMBER
9. SPONSORING / MONITORING AGENCY NAME(S) AND ADDRESS(ES) U.S. Army Medical Research and Materiel Command Fort Detrick, Maryland 21702-5012		10. SPONSOR/MONITOR'S ACRONYM(S)
		11. SPONSOR/MONITOR'S REPORT NUMBER(S)
12. DISTRIBUTION / AVAILABILITY STATEMENT Approved for Public Release; Distribution Unlimited		
13. SUPPLEMENTARY NOTES		
14. ABSTRACT <p>The purpose of this research is to reveal the relationship between assembly of the primary cilium and prostate cancer by investigating two centrosomal proteins, pericentriolar material 1 (PCM1) and Mind bomb 1 (Mib1), and to test the possibility that these proteins can serve as robust prostate cancer biomarkers and, potentially, targets for drug discovery. The primary cilium serves as a cellular antenna, and this organelle inhibits cell proliferation. The loss of this key signaling organelle was reported in various cancers, including prostate cancer. Therefore, we hypothesize that the absence of a primary cilium can potentially trigger cell proliferation and prostate cancer development. Pericentriolar material 1 is essential for ciliogenesis, and the <i>PCM1</i> gene is deleted in ~15% of prostate cancers. Our results indicate that ablation of pericentriolar material 1 leads to aberrant expression of its interacting partner, Mind bomb 1, an enzyme that is a negative regulator of ciliogenesis. Based on these data, we hypothesize that elevated levels of Mind bomb1 provoked by pericentriolar material 1 depletion in prostate cancer promote abnormal cell growth and malignancy by preventing the assembly of cilia. To test this hypothesis, we will investigate the impact of pericentriolar material 1 deletions in prostate cancer and determine whether there is a correlation between increased Mind bomb 1, the loss of cilia, and the stage of prostate tumor progression. Next, we will test whether pericentriolar material 1 depletion and aberrant levels of Mind bomb 1 promote prostate cancer development. Finally, we will investigate whether Mind bomb 1 removal induces ciliogenesis and inhibits growth of prostate cancer to determine the suitability of Mind bomb 1 as a target of anti-cancer drugs.</p>		

15. SUBJECT TERMS Primary cilium, prostate cancer, PCM1, MIB1					
16. SECURITY CLASSIFICATION OF:			17. LIMITATION OF ABSTRACT	18. NUMBER OF PAGES	19a. NAME OF RESPONSIBLE PERSON
a. REPORT	b. ABSTRACT	c. THIS PAGE	Unclassified	44	USAMRMC
Unclassified	Unclassified	Unclassified			19b. TELEPHONE NUMBER <i>(include area code)</i>

Standard Form 298 (Rev. 8-98)
Prescribed by ANSI Std. Z39.18

Table of Contents

	<u>Page</u>
1. Introduction.....	2
2. Keywords.....	2
3. Accomplishments.....	2
4. Impact.....	11
5. Changes/Problems.....	12
6. Products.....	12
7. Participants & Other Collaborating Organizations.....	12
8. Special Reporting Requirements.....	13
9. Appendices.....	13

1. INTRODUCTION:

The purpose of this research is to reveal the relationship between assembly of the primary cilium and prostate cancer by investigating two centrosomal proteins, pericentriolar material 1 (PCM1) and Mind bomb 1 (Mib1), and to test the possibility that these proteins can serve as robust **prostate cancer biomarkers** and, potentially, **targets for drug discovery**. The primary cilium serves as a cellular antenna, and this organelle inhibits cell proliferation. The loss of this key signaling organelle was reported in various cancers, including prostate cancer. Therefore, we hypothesize that the absence of a primary cilium can potentially trigger cell proliferation and prostate cancer development. PCM1 is essential for ciliogenesis, and the *PCM1* gene is deleted in ~15% of prostate cancers. Our results indicate that ablation of PCM1 leads to aberrant expression of its interacting partner, Mib1, an enzyme that is a negative regulator of ciliogenesis. Based on these data, we hypothesize that elevated levels of Mib1 provoked by PCM1 depletion in prostate cancer promote abnormal cell growth and malignancy by preventing the assembly of cilia. To test this hypothesis, we will investigate the impact of PCM1 deletions in prostate cancer and determine whether there is a correlation between increased Mib1, the loss of cilia, and the stage of prostate tumor progression. Next, we will test whether PCM1 depletion and aberrant levels of Mib1 promote prostate cancer development. Finally, we will investigate whether Mib1 removal induces ciliogenesis and inhibits growth of prostate cancer to determine the suitability of Mib1 as a target of anti-cancer drugs. Collectively through our research proposal, we will be able to understand a novel regulatory pathway in the formation of primary cilia and its implications in prostate cancer development. These efforts will ultimately allow us to devise innovative and effective therapeutic approaches against malignant prostate cancer. First, our investigation may allow us to find **new bio-markers** to detect cancer. In addition, since we are examining a “druggable” protein with enzymatic activity, our results could ultimately allow discovery of **potential anti-cancer drugs** for effective therapeutic approaches against malignant prostate cancer, which is a leading, fatal disease threatening the male population worldwide.

2. KEYWORDS:

Primary cilium, prostate cancer, PCM1, Mib1

3. ACCOMPLISHMENTS:

What were the major goals of the project? What was accomplished under these goals?

Training-Specific Tasks:

Subtask 2: Present research at the monthly department group meetings

Completed

Subtask 3: Attend a national scientific meeting in relevant scientific field

I attended the Cold Spring Harbor Asia conference on Cilia & Centrosomes and presented my work as poster “Tethering of an E3 ligase by PCM1 regulates the abundance of centrosomal KIAA0586/Talpid3 and promotes ciliogenesis”. I attended the 13th international zebrafish conference to study the use of zebrafish in tumor biology.

Milestone Achieved: Presentation of project data at a national meeting

Specific Aim 1 Major Task 1: To investigate whether PCM1 deletion in prostate cancer is correlated with an increase in Mib1 and the loss of cilia

Subtask 1: Measurement of PCM1 and Mib1 expression in normal prostate and prostate cancer tissue arrays.

Results: We studied the expression of PCM1 and Mib1 proteins in human prostate cancer (PCa) tissue samples by immunohistochemical analysis of a human PCa TMA derived from a cohort of PCa patients ($n = 131$) in various clinicopathological groups. TMAs were obtained from the DOD-sponsored PCBN repository at Johns Hopkins University. In collaboration with prostate cancer pathologists and a biostatistician, we first examined the expression of PCM1 and Mib1 in normal and malignant prostatic epithelial cells in prostate tissue. The mean protein intensity of cytoplasmic PCM1 and Mib1 were significantly increased in PCa compared to the adjacent normal tissues ($p < 0.001$) (Figure 1). We did not observe a significant association between the change in Mib1 and PCM1 expression level with Gleason primary score (Figure 2), Gleason sum score (Figure 3) or prostate cancer stage (Figure 4). Then we compared expression of PCM1 and Mib1 proteins in non-hormone resistant tumor groups to hormone-resistant tumor group and found no significant difference (Figure 6 and Table 1). Finally, we examined the expression of PCM1 and Mib1 in normal and high grade PIN epithelial cells. **The mean protein intensity of cytoplasmic PCM1 and Mib1 were significantly increased in high-grade prostate intraepithelial neoplasia (HGPIN) compared to the adjacent normal tissues** ($p < 0.001$) (Figure 5).

Figure 1. Protein intensity of PCM1 and Mib1 in normal and PCa tissues. Paired Wilcoxon rank test. * $P < 0.05$.

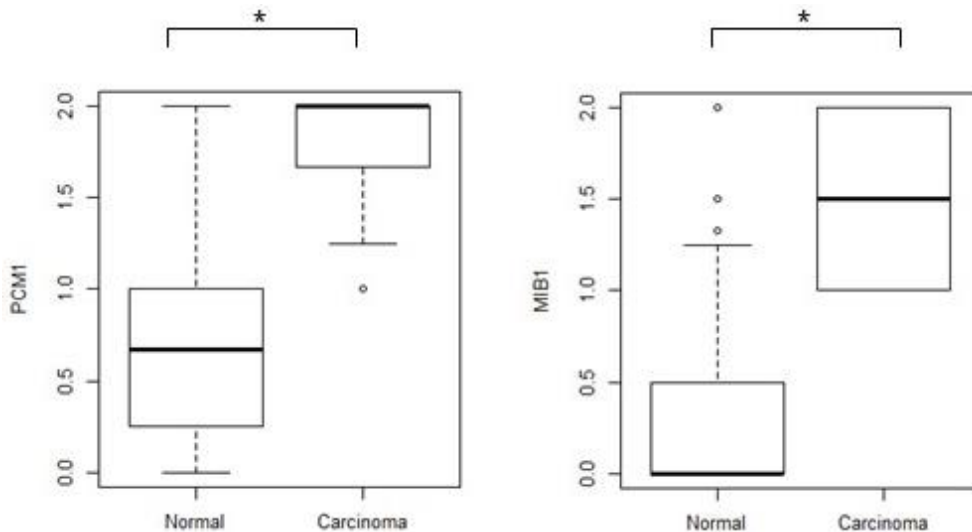


Figure 2. Simple linear regression model was used to study association of protein expression changes (tumor - normal) and Gleason-Primary score.

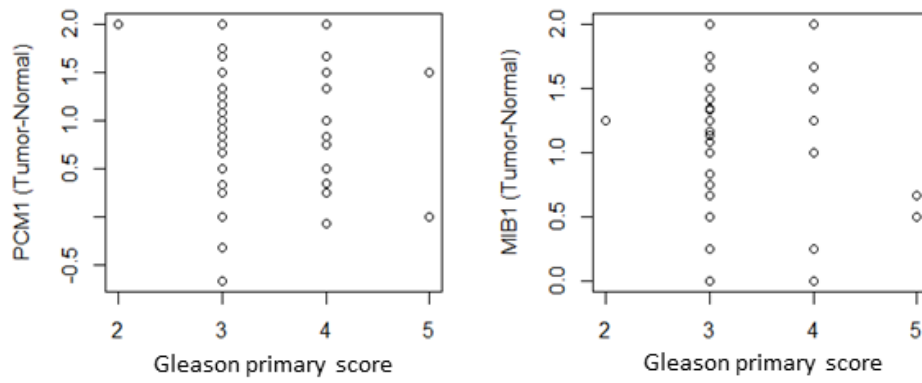


Figure 3. Simple linear regression model was used to study association of protein expression changes (tumor - normal) and Gleason-Sum score.

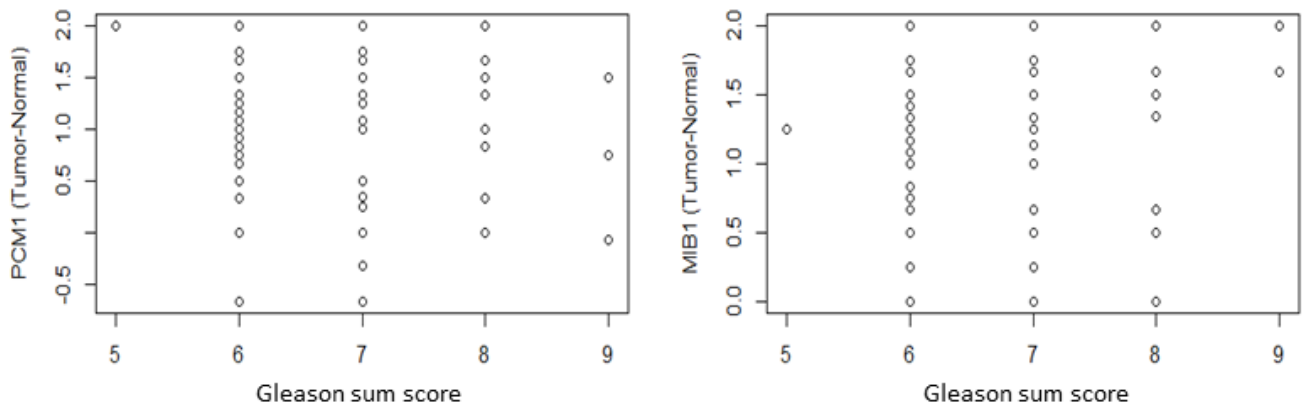


Figure 4. Analysis of variance (ANOVA) was used to test the association between protein expression changes and TNM stage.

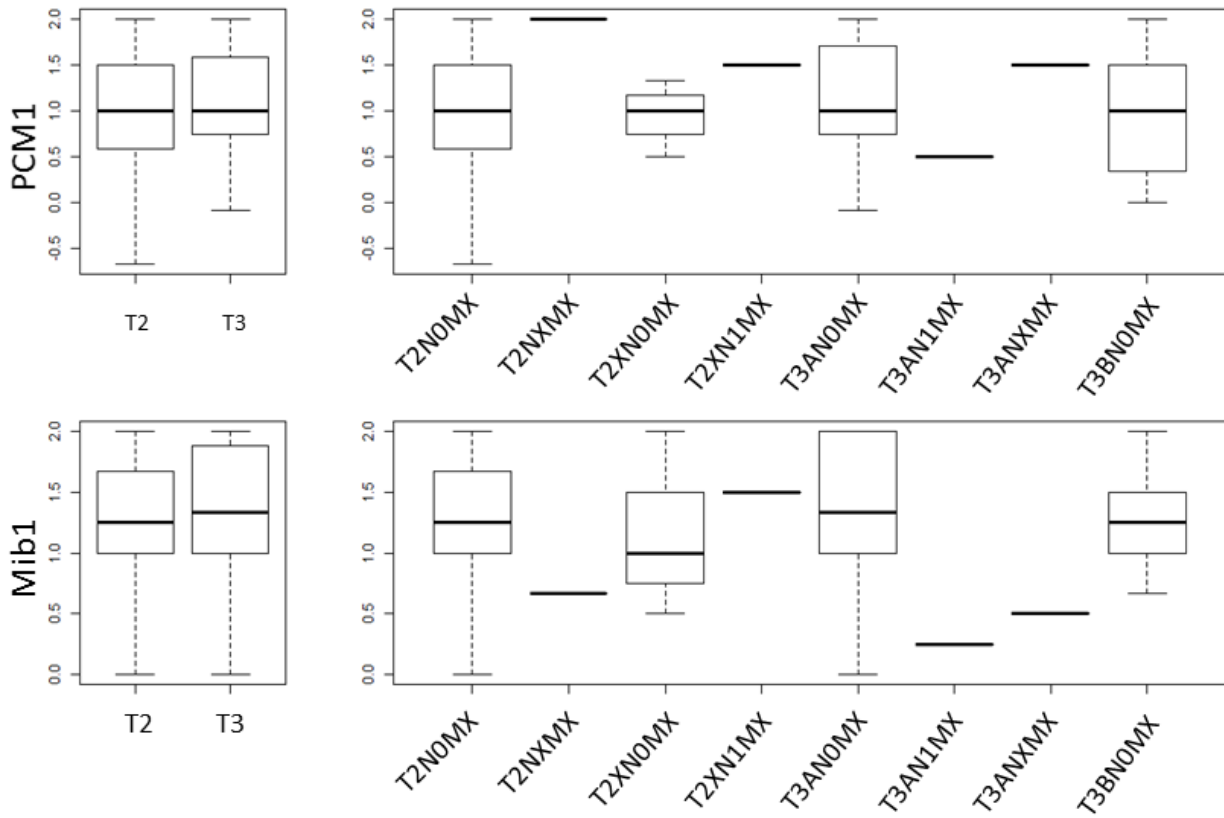


Figure 5. Protein intensity of PCM1 and Mib1 in normal and HGPIN tissues. Paired Wilcoxon rank test. * P<0.05.

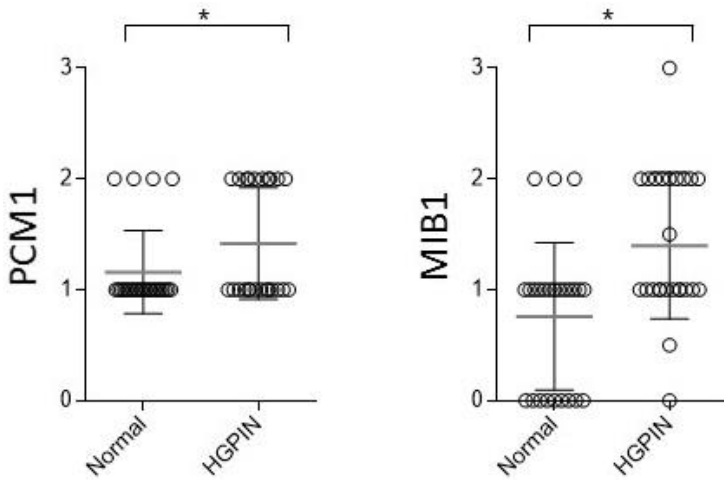


Figure 6. Comparison of non-resistant tumor groups and resistant tumor group (i.e., group I, III, IV vs group II).

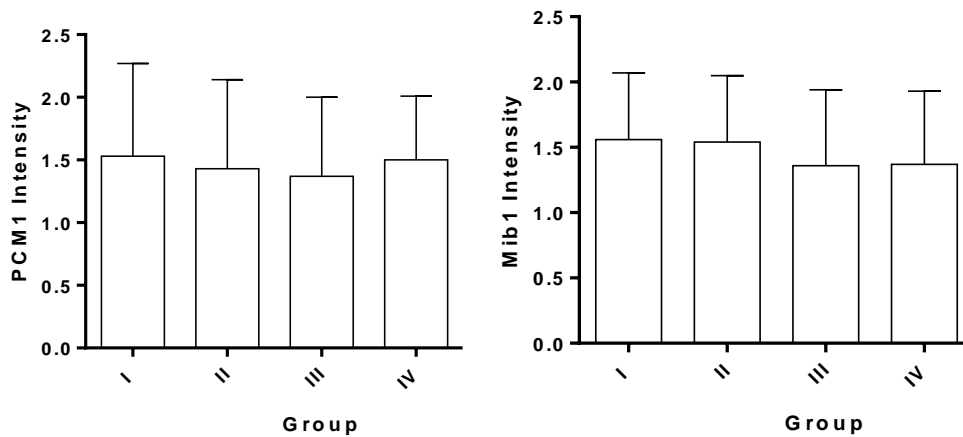


Table 1. Sample size summary.

Group	Type	Sample size
I	Tumor from Hormone Naïve, TURP	15
II	Tumor from Hormone Refractory, TURP	40
III	Tumor from Neo Adjuvant, Radicals	27
IV	Tumor from No therapy, Radicals	28

Subtask 2: Measurement of ciliation and proliferation in PCM1 positive and negative prostate cancer tissue and cell lines

Results: We hypothesize that epithelial cells in tumors will lose their primary cilia. Therefore, we measured the expression level and ciliation potential of PCM1 and Mib1 in normal, benign prostate epithelia cell lines and PCa cell lines. Consistent with our findings in TMAs, PCM1 was found to be over-expressed in certain PCa and benign cell lines (NEI-8, RC165 and BPH-1) compared to a normal prostate cell line (RWPE-1) and stem cell line, WPE. Mib1 was also over-expressed in certain PCa and benign cell lines (LnCaP, RC165 and BPH-1) compared to normal prostate cell lines (RWPE-1 and WPE). Moreover, **Pca and benign cell lines (LnCaP, LnCaP-AI, NEI-8, RC165 and BPH-1) have lower ciliation rates compared to normal prostate cell lines (RWPE-1 and WPE, Figure 7).** We also examine the correlation between PCM1, Mib1 expression levels and ciliation in patient tissues by co-staining CK5, acetylated tubulin (Ace-Tubulin, a marker for cilia), and γ -Tubulin (a marker for centrosomes) in TMAs. Consistent with our data from PCa cell lines above, **primary cilia number was significantly decreased in epithelial cells of tumor samples ($p < 0.001$)** (Figure 8). The normal prostate has a bilayered epithelium of basal cells (CK5 positive) and luminal cells (CK5 negative). We observed that primary cilia were enriched 17.8-fold on normal CK5⁺ cells (median=33.8%) compared to normal

CK5⁻ cells (median=1.9% Figure 9), suggesting that **primary cilia mainly present in basal cells**. We also found that **decreased cilia number in epithelia cells is due to decreased CK5⁺ population but not decreased ciliation rate in CK5⁺ cells**. Because the ciliation rate of CK5⁺ and CK5⁻ epithelial cells in tumor is equal to that in normal tissue (Figure 10). We also tried to examine the correlation between increased Mib1 intensity and ciliation rate in the patient sample, but found no correlation between them (Figure 11). This may due to the small sample number of patients with CK5⁺ cells and the lack of accuracy of using Mib1 intensity to measure Mib1 expression level, which could be improved in the future.

Milestone(s) Achieved: Correlate loss of cilia, over-expression of Mib1 and loss of PCM1 with stage of tumor

Figure 7. Measurement of ciliation and protein level of PCM1 and Mib1 in prostate cell lines. “++”, “+” and “-” indicate ~20%, ~10% and ~0% of cells were ciliated respectively.

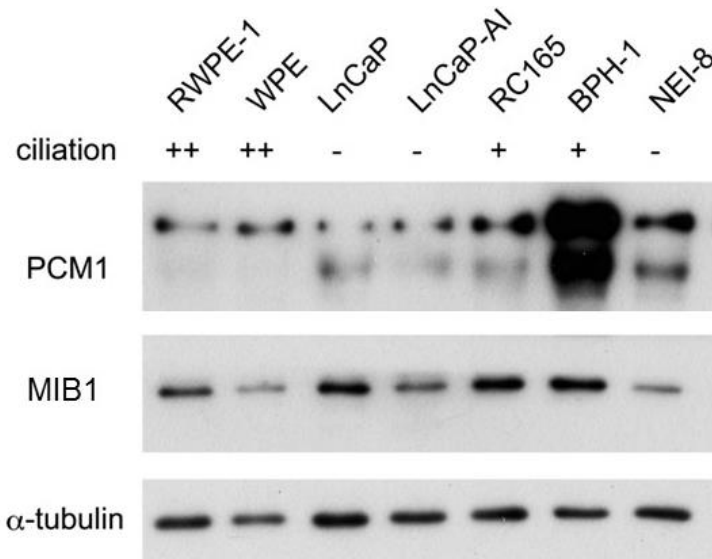


Figure 8. Triple-staining of prostate tissue for CK5, Ace-tubulin, and γ -tubulin. Staining of pilot TMA is shown, and each marker is indicated at top right of each panel. Ciliation rate of epithelial cells in normal and tumor tissue is shown. Cilia are indicated by arrows. Scale bar=10 μ m.

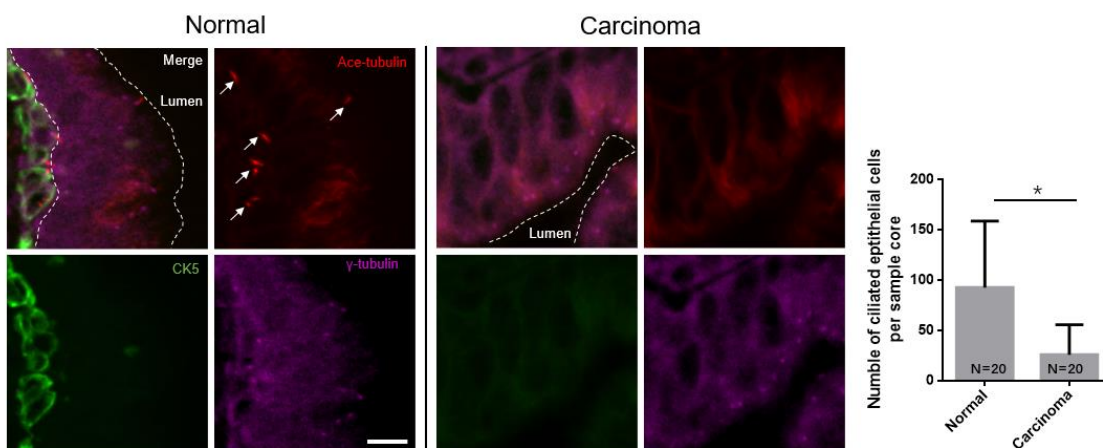


Figure 9. Measurement of ciliation in luminal and basal epithelial cells.

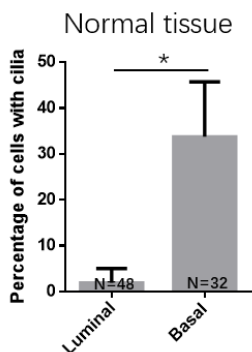


Figure 10. Quantification of basal cell number and comparison of ciliation of epithelial cells in normal and tumor tissue.

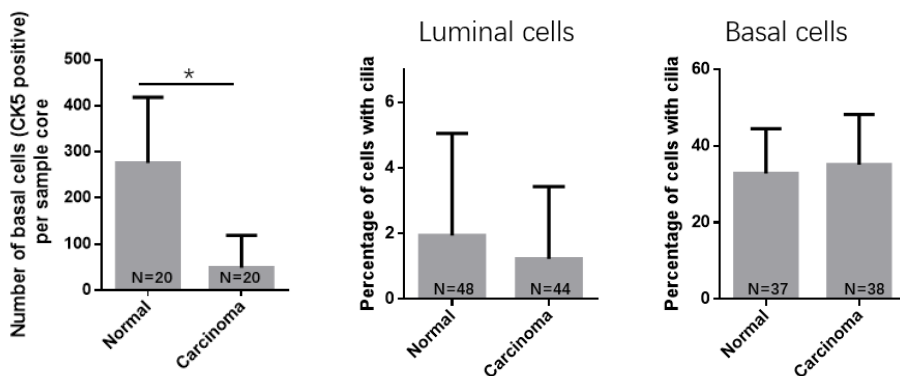
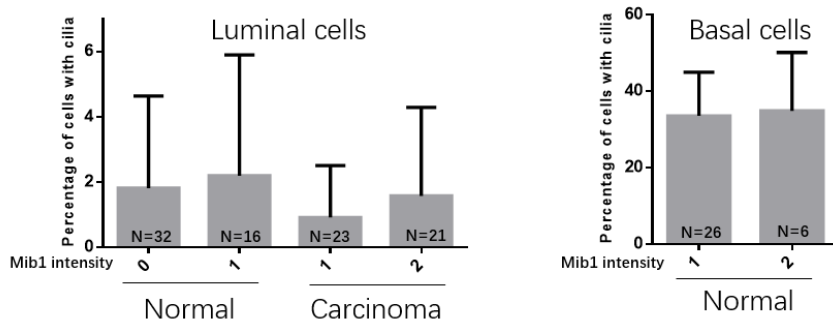


Figure 11. Analysis of the association between Mib1 expression changes and ciliation rate.



Specific Aim 2: To investigate the impact of PCM1 and Mib1 loss and Mib1 over-expression in prostate cancer development

Major Task 2: The impact of deleting *PCM1* or *Mib1* in prostate cell lines and zebrafish xenograft model.

Subtask 1: Establishment of prostate normal and cancer cell lines depleted for *PCM1* or *Mib1*

Subtask 2: Investigation of ciliation, proliferation and malignancy of the cell lines and tumor formation.

Since our TMA and cell lines data show that Mib1 protein is over-expressed in prostate tumors, our

work will have considerable impact if we are able to demonstrate that deleting of Mib1 in Pca or benign cell lines rescues ciliogenesis and inhibits cell growth. We chose LNCap and RC165, which have higher Mib1 expression level compared to normal prostate cell lines (Figure 7), to test our hypothesis. The establishment of Mib1 knockout LNCap and RC165 cell lines is in progress. We will test ciliogenesis, cell growth, and tumor formation using these cell lines.

Major Task 3: The impact of stably over-expressing Mib1 in prostate cell lines and zebrafish xenograft model.

Since our TMA and cell lines data show that Mib1 protein is over-expressed in prostate tumors, our work will have considerable impact if we are able to demonstrate that overexpression of Mib1 inhibits ciliogenesis and promotes cell growth. To further test this possibility, we ectopically expressed Mib1 using a doxycycline (Dox)-inducible system in normal prostate cell lines, RWPE1 and WPE, and selected stable cell lines (Figure 12). We found that over-expression of Mib1 could indeed inhibit the ciliation rates and promote the proliferation of normal prostate cell lines (Figure 13 and 14).

Figure 12. Establishment of normal prostate cell lines stably over-expressing Mib1.

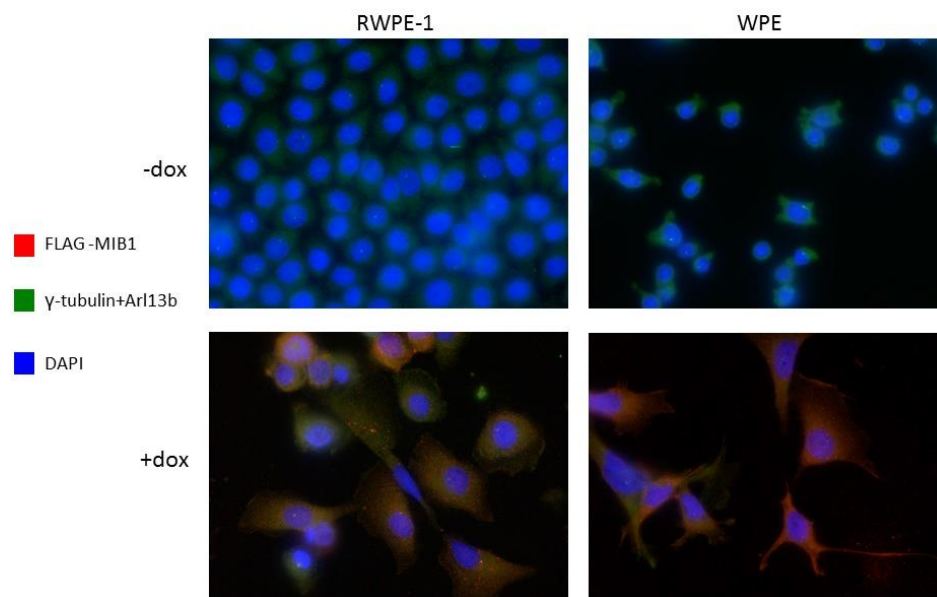


Figure 13. Over-expression of Mib1 inhibits ciliogenesis in normal prostate epithelial cell lines.

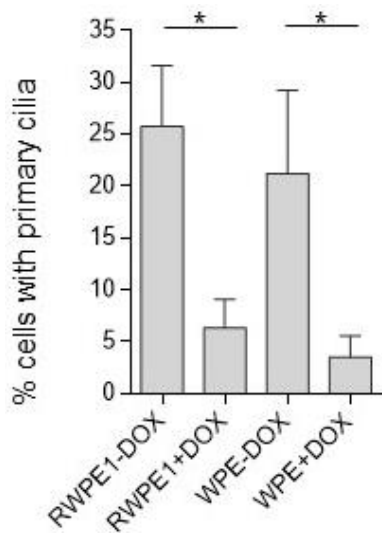
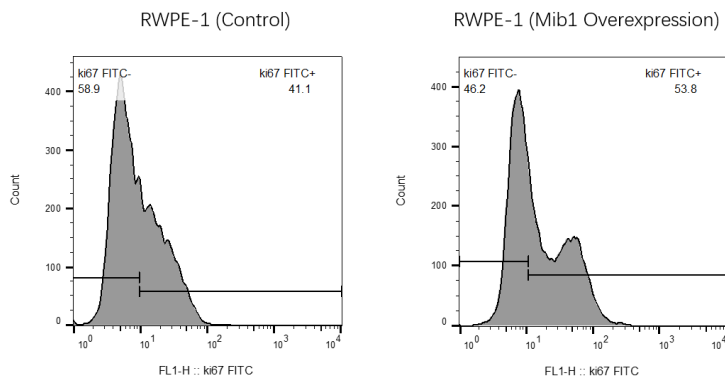


Figure 14. Over-expression of Mib1 promotes proliferation of normal prostate epithelial cell line.



Milestone(s) Achieved: Decrease of cilia rate and increase of proliferation of cell lines stably over- expressing Mib

Mentoring-Specific Tasks: Major Task 1: Mentoring and discussion about progression in prostate cancer research.

Subtask 1: Weakly meeting with mentor, Dr. Dynlacht

Completed

Subtask 2: Monthly meeting with mentor, Dr. Dynlacht and co- mentor, Dr. Lee

Completed

What opportunities for training and professional development has the project provided?

I am working at the NYU School of Medicine (NYUSoM) Cancer Institute as a postdoctoral fellow under the supervision of Dr. Dynlacht and my co-mentor, Dr. Peng Lee, an expert in prostate pathology and cancer. My work seeks to understand the relationship between primary cilia dysfunction and prostate cancer. This fellowship allowed me to acquire basic knowledge and technical expertise related to the biology of the prostate and prostate cancer biology, including approaches to study proliferation, invasion, migration, anchorage-independent growth, and apoptosis

in Dr. Peng Lee's laboratory. As time permits, I will extend the proposed research by introducing genetically engineered mouse models of prostate cancer, through which I will acquire essential expertise with mouse models to study prostate cancer. Dr. Cory Abate-Shen, our collaborator, will provide additional training opportunities and instruction. In addition, I learned biochemical and cell biological approaches in the Dynlacht laboratory, and Dr. Dynlacht provided mentoring and advice needed to proceed to the next, independent stage of my career. Most importantly, I will learn from both mentors critical thinking, experimental design, and grant writing to prepare for my independent research. In summary, this program would provide me with an outstanding opportunity to advance toward my career goals.

How were the results disseminated to communities of interest?

Manuscript in progress.

What do you plan to do during the next reporting period to accomplish the goals?

Nothing to report.

4. IMPACT

What was the impact on the development of the principal discipline(s) of the project?

Primary cilia play a repressive role in regulating cell proliferation and are frequently absent in numerous types of cancer, including prostate cancer. The purpose of this research is to reveal the relationship between assembly of the primary cilium and prostate cancer by investigating two centrosomal proteins, pericentriolar material 1 (PCM1) and Mind bomb 1 (Mib1). Further, defining the role and function of cilia during the course of prostate cancer malignancy will instigate novel insights into therapeutic approaches against prostate cancer. These insights will enable us to understand novel regulatory pathways in the formation of primary cilia and their implications for prostate cancer development. Our work may have major impacts on two fronts. First, our investigation may allow us to find new bio-markers (PCM1 and Mib1) to detect cancer. In addition, since we are examining a "druggable" protein with enzymatic activity, our results could ultimately allow discovery of potential anti-cancer drugs (Mib1) for effective therapeutic approaches against malignant prostate cancer, which is a leading, fatal disease threatening the male population worldwide.

What was the impact on other disciplines?

N/A

What was the impact on technology transfer?

If our research is successful, it could define PCM1 and Mib1 as important biomarkers and, potentially, targets of anti-cancer drugs for prostate cancer, thus relating to the Overarching Challenge of Diagnosis and Therapy for prostate cancer. Importantly, since Mib1 is an enzyme, it is a possible actionable target. If successful, in the future, we will work with our Office of Technology licensing to commence collaborations with potential pharmaceutical partners.

What was the impact on society beyond science and technology?

Nothing to report.

5. CHANGES/PROBLEMS:

Changes in approach and reasons for change

No changes in approach/nothing to report.

Actual or anticipated problems or delays and actions or plans to resolve them

None anticipated/nothing to report.

Changes that had a significant impact on expenditures

None.

Significant changes in use or care of human subjects, vertebrate animals, biohazards, and/or

select agents

None.

6. PRODUCTS:

Publications, conference papers, and presentations

I attended the Cold Spring Harbor Asia conference on Cilia & Centrosomes and presented my work as poster “Tethering of an E3 ligase by PCM1 regulates the abundance of centrosomal KIAA0586/Talpid3 and promotes ciliogenesis”.

Conference poster abstract:

To elucidate the role of centriolar satellites in ciliogenesis, we deleted the gene encoding the PCM1 protein, an integral component of satellites. PCM1 null human cells show marked defects in ciliogenesis, precipitated by the loss of specific proteins from satellites and their relocation to centrioles. We find that an amino-terminal domain of PCM1 can restore ciliogenesis and satellite localization of certain proteins, but not others, pinpointing unique roles for PCM1 and a group of satellite proteins in cilium assembly. Remarkably, we find that PCM1 is essential for tethering the E3 ligase, Mindbomb1 (Mib1), to satellites. In the absence of PCM1, Mib1 destabilizes Talpid3 through poly-ubiquitylation and suppresses cilium assembly. Loss of PCM1 blocks ciliogenesis by abrogating recruitment of ciliary vesicles associated with the Talpid3-binding protein, Rab8, which can be reversed by inactivating Mib1. Thus, PCM1 promotes ciliogenesis by tethering a key E3 ligase to satellites and restricting it from centrioles.

Publications:

Wang, L. and Dynlacht, B. D.; The regulation of cilium assembly and disassembly in development and disease; *Development*; 145: 2018; published; acknowledgement of federal support (yes).

Wang, L., Failler, M., Fu, W. and Dynlacht, B. D.; A distal centriolar protein network controls organelle maturation and asymmetry; *Nature Communications*; 9: 2018; 3938; 2018; published; acknowledgement of federal support (yes).

Website(s) or other Internet site(s)

Nothing to report.

Technologies or techniques

N/A

Inventions, patent applications, and/or licenses

N/A

Other Products

N/A

7. PARTICIPANTS & OTHER COLLABORATING ORGANIZATIONS

What individuals have worked on the project?

1. Name: Lei Wang

Role: PI

Nearest person month worked: 24 months

Contributions to Project: Dr. Wang performed all the experiments.

2. Name: Brian Dynlacht

Role: Mentor

Nearest person month worked: 2

Contribution to Project: Dr. Dynlacht provided mentoring and advice on cell biology and biochemistry.

3. Name: Peng Lee

Role: Co-mentor

Nearest person month worked: 2

Contribution to project: Dr. Lee provided mentoring and advice on prostate cancer and assisted in acquiring and analyzing patients samples.

Has there been a change in the active other support of the PD/PI(s) or senior/key personnel since the last reporting period?

Nothing to report.

What other organizations were involved as partners?

Nothing to report.

8. SPECIAL REPORTING REQUIREMENTS

Nothing to report.

9. APPENDICES:

Two publications:

Wang, L. and Dynlacht, B. D.; The regulation of cilium assembly and disassembly in development and disease; Development; 145: 2018; published; acknowledgement of federal support (yes).

Wang, L., Failler, M., Fu, W. and Dynlacht, B. D.; A distal centriolar protein network controls organelle maturation and asymmetry; Nature Communications; 9: 2018; 3938; 2018; published; acknowledgement of federal support (yes).

REVIEW

The regulation of cilium assembly and disassembly in development and disease

Lei Wang* and Brian D. Dynlacht*

ABSTRACT

The primary cilium is an antenna-like organelle assembled on most types of quiescent and differentiated mammalian cells. This immotile structure is essential for interpreting extracellular signals that regulate growth, development and homeostasis. As such, ciliary defects produce a spectrum of human diseases, termed ciliopathies, and deregulation of this important organelle also plays key roles during tumor formation and progression. Recent studies have begun to clarify the key mechanisms that regulate ciliary assembly and disassembly in both normal and tumor cells, highlighting new possibilities for therapeutic intervention. Here, we review these exciting new findings, discussing the molecular factors involved in cilium formation and removal, the intrinsic and extrinsic control of cilium assembly and disassembly, and the relevance of these processes to mammalian cell growth and disease.

KEY WORDS: Primary cilia, Ciliopathies, Cilium assembly, Cilium disassembly, Cancer

Introduction

Cilia and flagella are evolutionarily conserved hair-like microtubule-based structures that project from cells. These organelles are membrane bound and, although their membrane is contiguous with the plasma membrane, they retain a unique identity, with a compartmentalized structure dedicated to signaling. Ciliated cells can be monociliated or multiciliated. Furthermore, cilia can be categorized as motile or immotile, with the former possessing an ability to beat rhythmically and move extracellular fluids. In higher organisms, motile cilia are found in multiple organs, including the brain, lungs, middle ear and reproductive organs, where they drive fluid flow and/or produce signaling gradients that play diverse and important roles, e.g. in left-right patterning, neurogenesis, mucus clearance, hearing and movement of ova. In lower organisms, such as *Chlamydomonas* and paramecia, motile cilia or flagella are used for cell motility. Recent studies suggest that certain types of motile cilia also have sensory functions (Jain et al., 2012; Shah et al., 2009). By contrast, immotile cilia, also known as primary cilia, act as physical and chemical sensors and transducers of extracellular cues in a wide variety of cell and tissue types (Fig. 1).

The primary cilium is enriched in numerous ion channels, such as PKD1, PKD2, TRPV4 and AC6 (also known as ADCY6), that have been shown to play important roles in mechano-transduction (Pablo et al., 2017; Spasic and Jacobs, 2017). The primary cilium can sense fluid flow and extracellular stress, and can translate these signals to

control the left-right specification of organ development, calcium influx in kidney and liver cells, nitric oxide production in endothelial cells and osteogenic differentiation in mesenchymal stem cells. The primary cilium is also enriched in receptors that mediate transduction of Hedgehog (Hh), Wnt, Notch, Hippo, G protein-coupled receptors, receptor tyrosine kinases, mTOR, and TGF β signals (Elliott and Brugmann, 2018; Wheway et al., 2018). Given the important functions of cilia listed above, it is not surprising that defects in cilium assembly and signaling have been linked to at least 35 diseases, termed ciliopathies, that affect nearly all organ systems (for a review, see Reiter and Leroux, 2017). A detailed understanding of cilium assembly and cilium-associated signaling pathways is therefore crucial to the treatment of ciliopathies.

Progress over the past decade has begun to shed light on the cues that promote the assembly of primary cilia in mammalian cells. Such studies have shown that primary cilia are able to assemble upon cell cycle exit (Fig. 2) triggered by mitogen deprivation or differentiation (Aughstee, 2001; Choksi et al., 2014; Fu et al., 2014; Marion et al., 2009; Wheatley et al., 1996). For this reason, cilia assembly is often studied in well-established *in vitro* models, including mouse 3T3 fibroblasts and human retinal pigment epithelial (RPE1) cells (Tucker et al., 1979a,b), wherein ciliation can be efficiently induced through serum withdrawal. However, even in this simplified setting, the intracellular signaling events that promote ciliogenesis remain largely unknown at the molecular level. Nonetheless, in recent years, elegant cell biology and time-lapse microscopy experiments have demonstrated that ciliogenesis occurs sequentially, through a series of interdependent steps involving a number of intrinsic and extrinsic control mechanisms (Fig. 3). In this Review, we provide an overview of the process of ciliogenesis, with an emphasis on recent developments in understanding primary cilium assembly, disassembly and function in mammalian cells, and we include a discussion of the many unanswered questions that should be addressed in future studies.


An overview of the cilium assembly process

Ciliogenesis proceeds through two distinct pathways, termed the extracellular and intracellular pathways, depending upon whether cilium growth initiates at the cell surface or within the cytoplasm, respectively. The extracellular pathway is observed in epithelial cells of the kidney or lung, whereas intracellular assembly is observed in fibroblasts and retinal epithelial cells. In the well-studied intracellular pathway, cilium assembly initiates through a series of rapid and well-orchestrated events (Fig. 3), as demonstrated by time-lapse microscopy (Westlake et al., 2011), beginning with maturation of the mother centriole (MC) into a basal body, and culminating in docking of the basal body and growth of the axoneme at the plasma membrane.

First, within 15 min of serum withdrawal, small cytoplasmic vesicles (termed pre-ciliary vesicles, PCVs) that are believed to originate from the Golgi and the recycling endosome, accumulate in

Department of Pathology, New York University Cancer Institute, New York University School of Medicine, New York, NY 10016, USA.

*Authors for correspondence (lei.wang2@nyumc.org; brian.dynlacht@nyumc.org)

 L.W., 0000-0003-1802-7466; B.D.D., 0000-0001-9485-512X

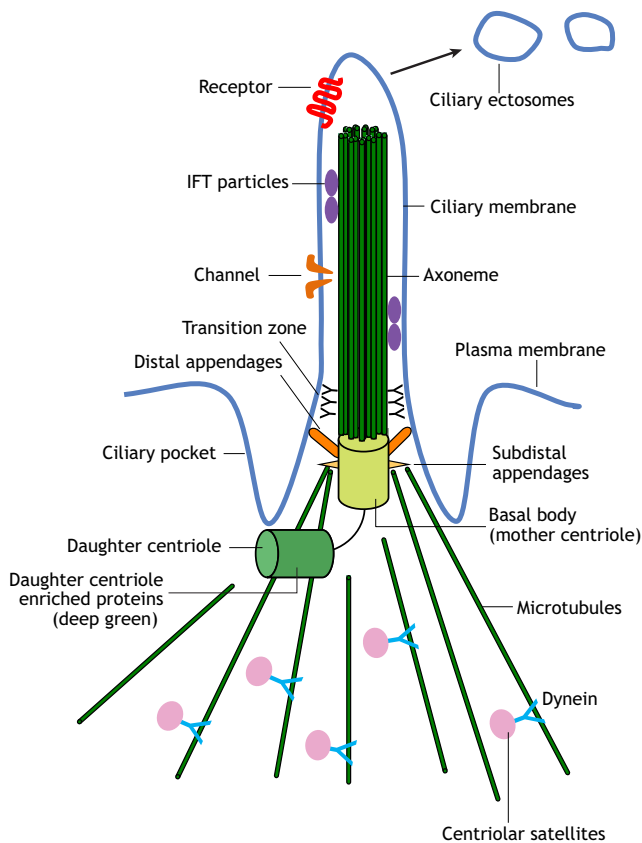


Fig. 1. Structure of the primary cilium. The overall architecture and key structural elements of the primary cilium are shown. IFT, intraflagellar transport.

the vicinity of MC distal appendages. These vesicles then appear to dock at the centriole, initiating the centriole-to-basal-body transition (Kobayashi et al., 2014; Lu et al., 2015b; Schmidt et al., 2012). After the initial docking of PCVs, the subsequent fusion of vesicles with the basal body produces a cap-like structure, or ciliary vesicle (CV) (Sorokin, 1962). The axoneme is assembled by extension of centriolar microtubules underneath this vesicular cap, and subsequent trafficking of post-Golgi vesicles enlarges the cap in coordination with microtubular growth, resulting in an axoneme compartmentalized by a double membrane. The nascent cilium subsequently docks to the plasma membrane through vesicular fusion with the membranous ciliary sheath, resulting in a projection from the cell surface.

Although the general events underlying ciliogenesis have been uncovered, a number of key questions remain unanswered. Namely, how are vesicles vectorially directed to the centrosome after mitogen deprivation? What are the proteins – on the vesicles and on the MC – that control the docking of PCVs to the centriole? What are the regulators that control the early events of cilium biogenesis, and how is axoneme elongation controlled? As we describe below, a number of recent studies have shed considerable light on these questions, revealing some of the proteins that convert centrioles to basal bodies and, eventually, to primary cilia.

Preparing cells for cilium assembly: mother centriole maturation

Assembly of the primary cilium requires a mature MC that is formed in two consecutive cell cycles from a daughter centriole (Fig. 2). In

the first cell cycle, new daughter centrioles are assembled from an existing (mother) and older (grandmother) centriole during the G1-to-S transition. These newborn daughter centrioles are distinguished by the recruitment of daughter centriole proteins such as CEP120, centrobilin and NEURL4 (Li et al., 2012; Mahjoub et al., 2010; Zou et al., 2005). In the next cell cycle, the newly formed daughter centriole in each cell gradually matures into a mother centriole, beginning with the loss of daughter centriole proteins at the G1/S phase and followed by the acquisition of distal appendages (DAs) and subdistal appendages (SDAs) in the late G2 phase. Both types of appendages play important roles for the future assembly of cilia: the DAs are essential for vesicle docking and for the recruitment of intraflagellar transport (IFT) machinery during the initiation of ciliogenesis, whereas the SDAs determine cilia positioning through the anchoring of centrioles to the cytoplasmic microtubular network (Sánchez and Dynlacht, 2016).

A number of proteins, including six DA proteins and approximately ten SDA proteins, which are hierarchically recruited to the distal end of the MC have been discovered thus far (Graser et al., 2007; Huang et al., 2017; Joo et al., 2013; Kodani et al., 2013; Kurtulmus et al., 2017 preprint; Mazo et al., 2016; Schmidt et al., 2012; Tanos et al., 2013; Wei et al., 2013). Using super-resolution microscopy, the DA proteins CEP83, CEP89, SCLT1 and CEP164 were shown to form the pinwheel-like spokes of DAs, whereas the interspoke matrix is populated by FBF1 (Yang et al., 2018). The recruitment of DA proteins requires several distal centriolar proteins, including C2CD3, OFD1 and MAPK15 (Kazatskaya et al., 2017; Singla et al., 2010; Ye et al., 2014). The pivotal importance of these distal centriolar proteins was demonstrated by the identification of mutations in the human *C2CD3* and *OFD1* genes, which produce ciliopathic syndromes with developmental abnormalities (Singla et al., 2010; Thauvin-Robinet et al., 2014). The recruitment of SDA proteins is regulated by a different set of proteins, including trichoplein (also known as TCHP) and CC2D2A (Ibi et al., 2011; Veleri et al., 2014); the ablation of CC2D2A impairs recruitment of the SDA proteins ODF2 and ninein, whereas trichoplein depletion abolishes the recruitment of ninein. Nevertheless, it remains unclear how MC maturation is regulated by this constellation of proteins, and how maturation is linked to the cell cycle and developmental programs. For example, OFD1 and C2CD3 are recruited to newly formed centrioles during centriole duplication, but they are not able to initiate DA assembly until the next cell cycle (Singla et al., 2010; Ye et al., 2014). Indeed, how centriolar asymmetry is generated in the first place – producing one mature MC and therefore only one primary cilium per cell – remains an unsolved mystery in the field.

Vesicle emergence, trafficking, docking and remodeling

After serum starvation, or in response to developmental signals (see below), PCVs are transported to the mature MC along microtubules in a kinesin- and dynein-dependent manner (Fig. 3) (Li et al., 2017; Wu et al., 2018). PCVs can originate from the Golgi or recycling endosomes, and their trafficking appears to depend on cues that trigger ciliogenesis (Sánchez and Dynlacht, 2016), as well as specific proteins such as kinesins, dyneins and myosins.

Golgi-derived PCVs are most likely transported by specific kinesins and dyneins, including KIF1C, which is recruited to the Golgi upon serum starvation (Lee et al., 2017). Upon depletion of KIF1C, ciliary membrane proteins are unable to traffic to the centriole and they accumulate at the Golgi. The dynein DYNC1H1 has also recently been shown to be required for PCV trafficking along microtubules (Wu et al., 2018). After trafficking to the

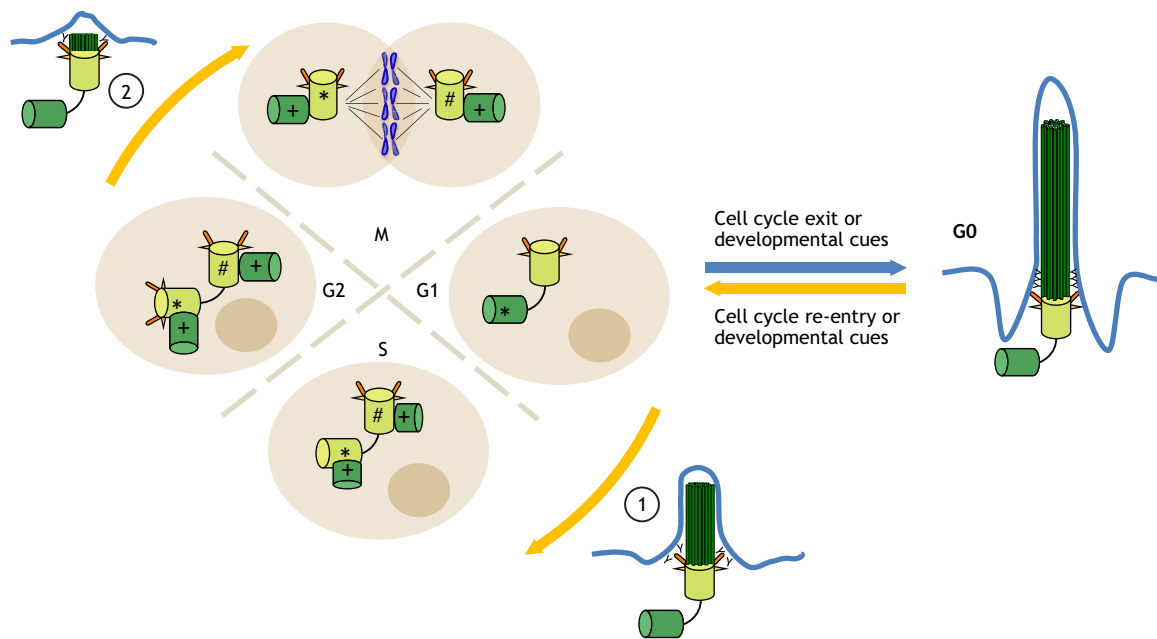


Fig. 2. A tale of two cycles: cell cycle-linked control of cilium formation and disassembly. A newly formed daughter centriole matures into a MC in two consecutive cell cycles. In the first cell cycle, new daughter centrioles (+) are assembled from an existing (mother) and older (grandmother, #) centriole. In the next cell cycle, the newly formed daughter centriole (*, dark green cylinder) gradually matures into a MC (*, light green cylinder), beginning with the loss of daughter centriole proteins at the G1/S phase and followed by the acquisition of distal appendages and sub-distal appendages in late G2 phase. The primary cilium then assembles when the cell exits the cell cycle (to enter G0) or receives developmental cues (blue arrow). Disassembly of the primary cilium occurs in a biphasic manner (yellow arrows), with the first wave occurring in G1 (1) and a second wave occurring before mitosis (2).

vicinity of centrioles, the docking of PCVs to the DAs relies upon a branched centrosomal actin network and, indeed, growing evidence suggests that the centrosome acts as an actin-organizing center in addition to its established role as a microtubule organizer (Farina et al., 2016). In support of this role, the actin nucleator complex ARP2/3 and the nucleation-promoting complex WASH localize on or near centrioles and promote assembly of a centrosomal actin network. Focal adhesion proteins also localize to centrioles and help to anchor them to the actin cytoskeleton (Antoniades et al., 2014). The actin cytoskeleton remodeling factors LIMK2 and TESK1 have also been visualized in the vicinity of centrioles (Kim et al., 2015a); interestingly, depletion of either of these kinases, which regulate the phosphorylation of cofilin 1, an actin-depolymerizing factor and positive regulator of ciliogenesis, provokes increased ciliation. These findings suggest that a dynamic balance between actin polymerization and depolymerization regulates ciliogenesis.

Recent observations suggest that the transport of PCVs to distal appendages via the actin network is also mediated by the motor protein myosin Va (Wu et al., 2018). Myosin Va⁺ PCVs can be found near centrioles as early as 30 min after serum starvation, and depletion of myosin Va, as with disruption of the centrosomal actin network, leads to the blockage of PCV docking. This finding suggests that myosin Va is among the earliest known markers of PCV trafficking. It is likely that microtubular and actin networks collaborate during PCV trafficking and docking. Although the details are largely lacking, putative regulators include MACF1A (May-Simera et al., 2016), which helps to organize the centrosomal microtubule-actin network through direct interaction with both microtubules and actin. As with myosin Va depletion, silencing of MACF1A leads to the blockage of PCV docking.

Apart from the Golgi-centriole pathway, components of the multi-subunit endosomal sorting complex required for transport (ESCRT) are essential for sustained docking of PCVs, supporting the involvement of the endosome trafficking pathway in CV growth (Ott et al., 2018). After PCV docking, the membrane-shaping protein EHD1 is recruited to PCVs to facilitate their fusion into a large CV, which caps the entire distal ends of MCs (Fig. 3). Although the cues are not fully understood, a sequence of events, triggered by Rab11 and Rabin8 (also known as RAB3IP), promotes the recruitment of the small GTPase Rab8a to CV to facilitate their extension (Bhattacharyya et al., 2016; Lu et al., 2015b; Wu et al., 2018). Rab8a facilitates the docking of PCVs to DAs by interacting with a group of distal centriolar proteins, including CEP164, Chibby (also known as CBY1), AHI1 and Talpid3 (also known as KIAA0586) (Burke et al., 2014; Hsiao et al., 2009; Kobayashi et al., 2014; Schmidt et al., 2012). Growing evidence also suggests that centriolar satellites, which are electron-dense cytoplasmic granules (Fig. 1), play an important role in PCV trafficking, fusion and extension. In particular, C2CD3 and OFD1, which localize to centriolar satellites as well as to the distal end of centrioles, have been shown to be required for DA assembly (Singla et al., 2010; Ye et al., 2014), whereas an integral centriolar satellite protein, PCM1, interacts with proteins of the BBosome complex and assists in BBosome trafficking, which in turn facilitates activation of Rab11-Rabin8-Rab8a signaling (Nachury et al., 2007; Westlake et al., 2011). PCM1 can also tether the centriolar satellite protein and E3 ligase Mib1, which regulates centrosomal levels of Talpid3, a protein required for Rab8a recruitment (Kobayashi et al., 2014; Wang et al., 2016). Rab8a recruitment, and hence PCV fusion and extension, is also regulated by CEP290, a protein that localizes to both centriolar satellites and the ciliary transition zone (Kim et al., 2008; Tsang et al., 2008). Furthermore, the WD-repeat containing

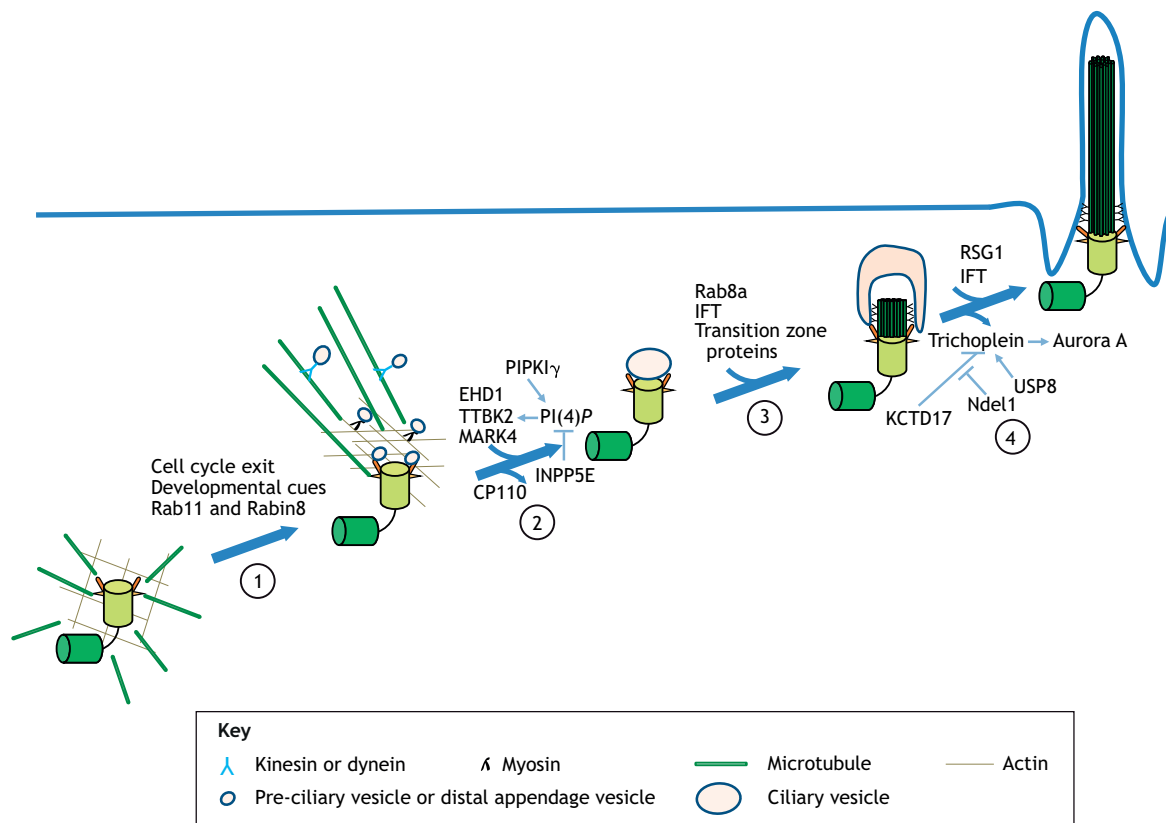


Fig. 3. The multiple phases and regulation of cilium assembly. The process of cilium assembly involves several successive stages. Cilium assembly is initiated upon cell cycle exit or after receiving developmental signals (1). PCVs are transported via microtubule-actin networks to the distal end of the MC and fuse into a larger CV (2). The process is accompanied by reorganization of the cytoskeleton, which drives the migration of centrosomes from the cytoplasm to the cell membrane. CP110 is removed. Next, IFT complexes are continuously recruited to the ciliary base to allow axoneme elongation, while Rab8a is recruited to the MC to facilitate ciliary membrane extension (3). The transition zone is then assembled, and this is followed by axoneme elongation and membrane fusion. Inhibition of the ciliary disassembly pathway also allows outgrowth of the cilium (4). Key proteins that play a regulatory role at each stage of the assembly process are shown. PI(4)P, PtdIns(4)P.

protein WDR8 functions in partnership with SXS2IP and CEP135 in both the assembly of centriolar satellites and PCV docking (Gupta et al., 2015; Klinger et al., 2014; Kurtulmus et al., 2016). It should be noted that centriolar recruitment of C2CD3, OFD1, CEP290 and WDR8 does not depend on their ability to localize to centriolar satellites (Kim et al., 2008; Kurtulmus et al., 2016; Lopes et al., 2011; Ye et al., 2014) and, therefore, additional work is needed to clarify which pool(s) are needed to regulate PCV docking. On the other hand, centriolar satellites are also involved in the organization of microtubular and actin networks through unknown mechanisms, and thus they could also contribute to microtubule-actin-mediated vesicle trafficking (Hori and Toda, 2017). To fully understand the earliest events that trigger ciliogenesis, it will be important to elucidate how vesicle transport is instigated upon receiving the initial cue to ciliate, to dissect how the cytoskeleton and transport between endoplasmic reticulum/endosomes and the centrosome are dynamically remodeled, and to identify the motors involved in each of these pathways.

Centrosome migration and cilium positioning

The morphology and positioning of the cilium vary extensively according to cell type, and the cilium can reside at the cell surface or assume a more submerged position (for a review, see Bernabé-Rubio and Alonso, 2017). For example, in mammals, the primary cilia in epithelial cells of kidney tubules are at the

cell surface (Latta et al., 1961), whereas those in smooth muscle cells, fibroblasts and pancreatic β cells are found at a more submerged position (Munger, 1958; Sorokin, 1962). Although the precise mechanisms that dictate cilium positioning remain unclear, some of the factors that regulate centrosome migration during ciliogenesis, and hence the final positioning of the cilium, are beginning to be identified.

During ciliogenesis, ciliary membrane assembly is accompanied by centrosome migration from the center of the cell towards the cell surface (Fig. 3), where the basal body then anchors to the plasma membrane via DAs (Sánchez and Dynlacht, 2016). This process is driven by mechanical forces produced during cytoskeleton remodeling. Indeed, time-lapse microscopy has revealed a dramatic increase in microtubule nucleation and stabilization around the centrosome, coinciding with migration of the centrosome (Pitaval et al., 2017). Microtubules cluster into large bundles between the centrosome and the basal pole of the cell, and point toward the apical pole of the cell, thus pushing the centrosome towards the apical membrane. In addition to the microtubule network, the actin network is also remodeled after serum starvation: the radial symmetry of the network is broken and actin filaments cluster to one side of the cell, resulting in the asymmetrical co-partitioning of microtubules with F-actin (Pitaval et al., 2017).

Beyond studies in tissue culture, the process of centrosome migration during ciliogenesis has been captured in a recent study of

Caenorhabditis elegans neuronal development (Li et al., 2017), wherein the centriole is transported along microtubules from the cell body to the tip of the dendrite in a dynein 1-dependent manner. These findings are significant because they suggest that actin and microtubules may cooperatively promote centrosome migration during ciliogenesis. A number of other ciliogenesis effectors have been implicated in centrosome migration, including FLNA, CEP83, CEP164, nesprin 2 (also known as Syne2), meckelin (also known as Tmem67), KIF3A, Pard3 and IFT20 (Adams et al., 2012; Li et al., 2017; Pitaval et al., 2017). As many of the genes encoding these proteins have been implicated in human ciliopathies (Reiter and Leroux, 2017), it will be interesting to investigate the role of centriole maturation, migration and positioning in these pathologies.

Cilia can also assume a more submerged position (Bernabé-Rubio and Alonso, 2017) and a recent study suggests that this positioning is determined by SDAs through their association with the Golgi (Mazo et al., 2016). In particular, it has been shown that the depletion of two SDA proteins, CEP128 and c-NAP1 (also known as CEP250), leads to dissociation of centrosomes from the Golgi, promoting the formation of cilia at the cell surface. It will be interesting to investigate whether, and how, this mechanism might be used in diverse cell types, and whether there are distinct functional outcomes associated with each position (surface versus submerged). Further studies are also needed to clarify the mechanisms that underlie centrosome migration and its relationship with other key events during ciliogenesis, described below.

Crucial control mechanisms in the basal body-to-cilium transition

A crucial mechanism in the decision to ciliate involves the removal of two proteins, CP110 (also known as CCP110) and CEP97, which are the first reported inhibitors of ciliogenesis. In cycling cells, CP110 and CEP97 localize at the distal ends of both mother and daughter centrioles to block inappropriate cilium formation (Spektor et al., 2007). After CV formation, the tau tubulin kinase TTBK2 is recruited by CEP164 to the DA of MCs, where it triggers removal of the CP110-CEP97 inhibitory complex (Fig. 3) (Cajane and Nigg, 2014; Goetz et al., 2012). It is noteworthy that the exact relationship between CV remodeling and CP110 removal remains to be defined, given that PCV docking and CV formation may not be essential for CP110 removal (Lee et al., 2017; Wu et al., 2018). Intriguingly, and in contrast to studies in cultured cells, it is also worth noting that ciliogenesis fails in *CP110* knockout mice, perhaps owing to a failure of SDA assembly and basal body anchoring to the membrane (Yadav et al., 2016). Interestingly, the recruitment of TTBK2 by CEP164 is regulated by phosphatidylinositol 4-phosphate [PtdIns(4)P] levels at the centrosome/ciliary base (Xu et al., 2016); PtdIns(4)P binds to CEP164 and TTBK2 and inhibits their interaction in proliferating cells. The centrosomal pool of PtdIns(4)P is regulated by phosphatidylinositol 5-phosphatase (INPP5E) and the PtdIns(4)P 5-kinase PIPKI γ . Upon serum starvation, INPP5E departs from the centrosome, and centrosomal PIPKI γ promotes TTBK2 recruitment and CP110 removal by depleting PtdIns(4)P at the centrosome. TTBK2 recruitment is also regulated by a centriolar satellite protein, MCRS1, which can directly bind to and recruit TTBK2 to the centriole (Lee et al., 2016b). An siRNA screen for kinases regulating ciliogenesis further identified a second kinase, MARK4, as another catalyst for CP110 removal (Kuhns et al., 2013). Recent studies have also shown that a small GTPase, RSG1, is recruited to MCs by TTBK2 and is required to initiate axoneme elongation (Agbu et al., 2018), which commences after CP110 removal (Fig. 3). Although this protein is important in

finalizing the maturation of basal bodies before axoneme elongation, future studies will be required to mechanistically dissect an exact role for RSG1 in this process.

Suppression of cilium disassembly, mediated by the kinase Aurora A (also known as Aurka), is also required for ciliogenesis (Inaba et al., 2016; Inoko et al., 2012; Kasahara et al., 2018, 2014). The SDA assembly regulator and ciliogenesis inhibitor trichoplein localizes at SDAs in cycling cells, where it activates Aurora A to promote cilium disassembly (Inoko et al., 2012) (discussed below). During ciliogenesis, however, KCTD17 acts as a substrate adaptor for Cul3-RING ubiquitin ligases (CRL3s) that polyubiquitylate and degrade trichoplein (Kasahara et al., 2014). Depletion of KCTD17 in RPE1 cells prevents removal of trichoplein and inactivation of Aurora A, resulting in the blockage of ciliogenesis before axoneme elongation. In cycling cells, Ndel1 protects trichoplein from CRL3/KCTD17-mediated degradation (Inaba et al., 2016). EGFR also directly phosphorylates USP8 to promote its deubiquitylase (DUB) activity, which in turn stabilizes trichoplein, thus tying together growth-promoting signals with cilium removal (Kasahara et al., 2018). On the other hand, the MST1/2-SAV1 complex of the Hippo pathway also participates in the dissociation of the Aurora A/HDAC6 cilia-disassembly complex by phosphorylating Aurora A (Kim et al., 2014). In the future, it will be important to investigate how the removal, destruction and/or mislocalization of negative regulators of ciliogenesis are integrated with cell cycle progression, and whether mutations that cripple these proteins are linked to human disease.

Axoneme elongation

The ciliary membrane and microtubules within the axoneme further elongate after the CV-capped basal body fuses with the plasma membrane (for a review, see Sánchez and Dynlacht, 2016). During this process of axoneme elongation, vast amounts of tubulin enter the cilium from the cytoplasm by diffusion and via IFT – the motor-dependent bi-directional cargo transport mechanism used within cilia for their formation, maintenance and function (Harris et al., 2018 preprint; Ishikawa and Marshall, 2017). Perturbation of cytoplasmic soluble tubulin levels or IFT transport can affect axoneme elongation and cilium length. Indeed, elegant studies in *Chlamydomonas* and mammalian cells suggest that increasing soluble tubulin production leads to longer cilia, whereas stabilization of tubulin leads to cilium shortening (Sharma et al., 2011; Wang et al., 2013b).

IFT requires various anterograde (IFT-B) and retrograde (IFT-A) transport complexes, and recent studies have begun to shed light on how these complexes are recruited to cilia. The recruitment of IFT-B to the ciliary base, for example, is mediated by TTBK2 and DA proteins (Goetz et al., 2012; Tanos et al., 2013). Super-resolution microscopy has also suggested that IFT molecules are concentrated within the matrix of DAs, wherein IFT complexes are formed with the assistance of the BBSome (Wei et al., 2012; Yang et al., 2018). The entry of IFT complexes into the cilium is also partially mediated by another small GTPase, RABL2B, which is recruited to the ciliary base by CEP19, a protein that is tethered at the distal end of the MC by CEP350 and FOP (also known as FGFR1OP). Active RABL2B then binds to the IFT-B complex, promoting entry of the latter into cilia (Kanie et al., 2017; Nishijima et al., 2017), and IFT complexes are subsequently transported via the kinesinII complex, the motor for anterograde movement, to the ciliary tip, where tubulins are integrated into the growing axoneme. The loading and unloading of cargos by kinesinII are regulated by its phosphorylation state. At the ciliary base, FLA8 (a subunit of the kinesinII motor, and a homolog

of KIF3B) in the unphosphorylated state allows IFT-B to bind to the kinesinII motor, which conveys it to the cilium tip. At the ciliary tip, CrCDPK1 phosphorylates FLA8 and disrupts the interaction between kinesinII and IFT particles, thereby facilitating cargo unloading (Liang et al., 2014).

Previous studies from several model organisms, primarily *Chlamydomonas* and *C. elegans*, have shown that the perturbation of IFT by disruption of IFT genes or motors blocks axonemal elongation and promotes assembly of short cilia. The velocity of IFT transport also contributes to the regulation of cilium length. Increased velocity of anterograde transport is associated with elongated cilia, whereas decreased velocity is linked to short cilia (Besschetnova et al., 2010; Marshall et al., 2005; Marshall and Rosenbaum, 2001). IFT is known to be regulated by a group of protein kinases, including DYF-5, DYF-18, PKG-1, GCK-2 and the DLK-1/p38 MAPK pathway (Burghoorn et al., 2007; Muthaiyan Shanmugam et al., 2018; Phirke et al., 2011; van der Vaart et al., 2015), although the mechanisms are unknown. Cilium length can also be regulated at the IFT cargo loading step. A recent study suggests that the loading of axonemal cargo onto IFT complexes decreases with increasing ciliary length (Pan and Snell, 2014; Wren et al., 2013), suggesting the existence of an uncharacterized feedback mechanism that senses the length of the cilium and thereby regulates cargo loading.

Axoneme elongation is also coordinated with ciliary membrane extension during ciliogenesis. Ciliary membrane growth can surpass the rate of axoneme extension when active Rab8a is overexpressed in mammalian cells or after depletion of IFT genes in trypanosomes (Absalon et al., 2008; Nachury et al., 2007). Abnormal ciliary membrane extension can also promote axoneme elongation and produce longer cilia (Lu et al., 2015a; Nachury et al., 2007). These studies indicate that there may be mechanisms that sense the length of the axoneme and, in turn, control the levels of regulators of membrane extension, including Rab8a and Arl13b. Moreover, the actin network, ectocytosis (Fig. 1) and endocytosis are also involved in the regulation of cilium length, probably by regulating ciliary membrane composition and protein transport or localization (Kaplan et al., 2012; Fu et al., 2016; Scheidel et al., 2018). Once fully assembled and elongated, the cilium retains its unique composition, in part, by virtue of gating mechanisms: at the base of the cilium, a soluble protein barrier and the transition zone function to maintain the protein composition of the cilium (for comprehensive reviews, see Jensen and Leroux, 2017; Nachury, 2018).

Despite these new findings regarding axoneme elongation, cilium length control and ciliary protein trafficking, much remains unknown, and additional studies will be required to determine how axoneme elongation is intricately coordinated with ciliary membrane extension and trafficking of signaling components. Finally, it should be noted that cilium length is also under the control of cilium disassembly pathways, which counteract assembly pathways during the cell cycle (see below).

Cilium disassembly

In contrast with cilium assembly, much less is known about the mechanisms that underlie cilia disassembly/resorption, which has to happen before mitosis. Experiments using cultured mammalian cells suggest that cilia disassemble in a biphasic manner, with the first major 'wave' occurring in G1 shortly after mitogenic stimulation of quiescent cells (Fig. 2) and a second wave occurring before mitosis (Pugacheva et al., 2007; Tucker et al., 1979b). Below, we summarize recent studies that have provided insights into cilium

disassembly, a process with immense implications in human disease, in particular cancer.

Disassembly of axonemal microtubules

Cilium disassembly requires the destabilization and depolymerization of axonemal microtubules (Figs 2 and 4). The mitotic kinase Aurora A appears to play a key role in promoting the latter process and thereby promotes both waves of cilium disassembly (Pugacheva et al., 2007). Aurora A is activated in response to cell cycle re-entry cues, whereupon it phosphorylates and stimulates the histone deacetylase HDAC6, which deacetylates and destabilizes tubulins within the axoneme. HDAC6 also de-acetylates cortactin and thus enhances actin polymerization, which also promotes cilium disassembly (Plotnikova et al., 2012; Pugacheva et al., 2007; Ran et al., 2015). The activation of Aurora A is under stringent control by complex signaling pathways that include calcium influx, which induces the binding of Ca²⁺/calmodulin (CaM) to Aurora A and its partner, NEDD9 (also known as HEF1). This stabilizes the interaction between these proteins and promotes Aurora A activation (Plotnikova et al., 2012). Moreover, PDGFR β promotes cilium disassembly by activating PLC γ , which causes release of intracellular Ca²⁺ and activation of CaM and Aurora A (Nielsen et al., 2015). Another histone deacetylase, HDAC2, has recently been shown to play a role in cilium disassembly (Kobayashi et al., 2017). Interestingly, HDAC2 positively regulates Aurora A expression, and its depletion promotes cilium assembly in cancer cells that have lost this organelle. Furthermore, Plk1, a G2/M phase kinase recruited to the pericentriolar matrix before mitotic entry, interacts with and activates HDAC6 to promote ciliary deacetylation and resorption (Lee et al., 2012; Wang et al., 2013a). These studies illustrate how HDACs can regulate cilium disassembly through discrete substrates and mechanisms, highlighting the potential of HDAC inhibition as a therapeutic strategy to reverse cilia loss.

The non-canonical Wnt signaling pathway also participates in Aurora A activation and, thus, ciliary disassembly. Wnt5a treatment induces the phosphorylation of Dvl2 by CK1 ϵ (also known as CSNK1E) and the formation of the Dvl2-Pik1 complex, which stabilizes NEDD9 and promotes Aurora A activation (Lee et al., 2012). Another protein, pitchfork (Pifo), promotes cilium disassembly through activation of Aurora A. Interestingly, heterozygous mutations in *Pifo* in mice and in humans lead to ciliopathy-related phenotypes, attesting to the biological consequences of perturbing cilium disassembly (Kinzel et al., 2010). Aurora A activity is also regulated by phosphoinositide signaling. Cultured cells grown in three dimensions develop a lumen with cilia and, in this context, the phosphatidylinositol phosphatase SHIP2 was found to bind Aurora A and NEDD9, and to promote their basolateral localization at the expense of their luminal expression associated with cilium resorption (Hamze-Komaiha et al., 2016). Moreover, INPP5E regulates Aurora A protein levels through transcriptional mechanisms that are mediated, at least in part, by AKT activity (Plotnikova et al., 2015). Finally, it was shown that serum stimulation can induce the formation of a cilium disassembly complex (CDC), which consists of Aurora A, CPAP (also known as CENPJ), Nde1 and OFD1, and in which CPAP functions as a scaffold protein that facilitates the recruitment of this complex to the ciliary base (Gabriel et al., 2016). Collectively, these studies illustrate how Aurora A acts as a nexus or focal point for a multitude of signals that impinge on the cilium to promote its disassembly (Fig. 4).

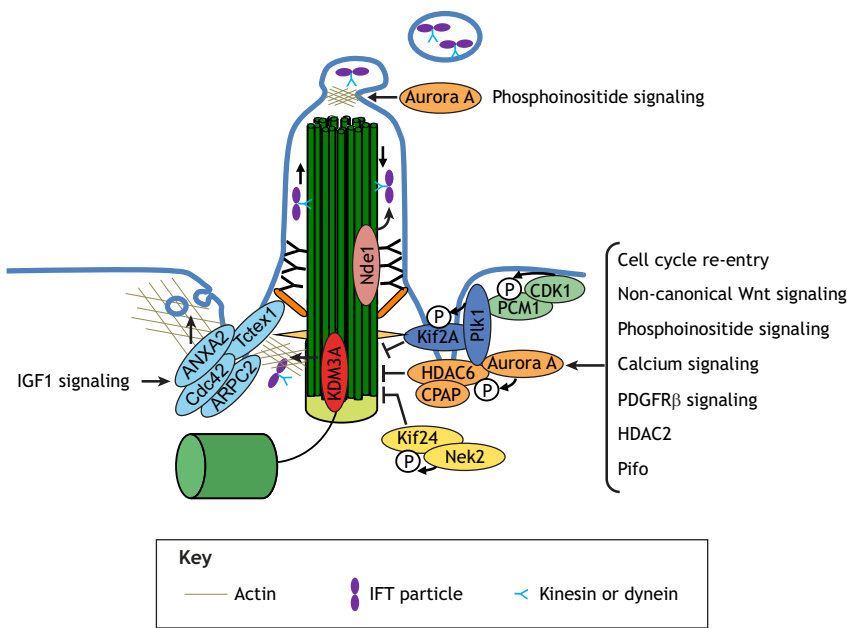


Fig. 4. The regulation of cilium disassembly. Cell cycle re-entry, accompanied by several signaling pathways and regulatory proteins (including non-canonical Wnt signaling, phosphoinositide signaling, calcium signaling, PDGFR β signaling, HDAC2 and Pifo), can trigger cilium disassembly via the activation of Aurora A. Aurora A then phosphorylates and stimulates the histone deacetylase HDAC6, which de-acetylates and destabilizes microtubules within the axoneme. During cilium disassembly, Plk1 and Nek2 activate the kinesins Kif2a and Kif24, respectively, which are required for the depolymerization of microtubules. Plk1 is recruited by PCM1 with the help of CDK1. Cilium disassembly also requires the modulation of IFT transport: KDM3A, for example, inhibits entry of the IFT complex into the cilium, whereas Nde1 regulates retrograde IFT transport. Growth signaling also triggers the removal of IFT-B particles through ciliary ectosomes released from the ciliary tip, which is also under the control of Aurora A. Cilium disassembly also requires remodeling of the ciliary pocket, accompanied by the enhancement of clathrin-mediated endocytosis. This process is controlled by Tctex1 and associated proteins (such as ANXA2, Cdc42 and ARPC2) and can be induced by IGF1 signaling, PDGFR β , platelet-derived growth factor receptor β .

Two kinesins that are able to depolymerize microtubules, Kif2a and Kif24, have also been implicated in the disassembly of primary cilia before mitosis (Fig. 4) (Kim et al., 2015b; Kobayashi et al., 2011; Miyamoto et al., 2015). Kif2a, which is recruited to the SDAs of the MC and to the proximal ends of both centrioles, is activated by Plk1 during G2/M phase (Miyamoto et al., 2015). Activation of this kinesin in the wake of a proliferative signal promotes ciliary microtubule depolymerization and cilium disassembly; in quiescent cells, by contrast, Kif2a is degraded through the APC/C-mediated ubiquitin/proteasome system to facilitate ciliogenesis. Kif24, identified through its association with CP110, also negatively regulates primary cilium assembly (Kobayashi et al., 2011). The ablation of this kinesin promotes aberrant assembly of cilia in growing cells, similar to CP110 loss. The microtubule depolymerizing activity of Kif24 can be enhanced by phosphorylation through Nek2, which is expressed during S and G2 phase (Kim et al., 2015b). Therefore, in a manner analogous to Kif2a, the cell cycle-specific phosphorylation of Kif24 ties the activation of this enzyme to cilium disassembly before mitosis. As this step is distinct from the initiation of cilium disassembly by Aurora A and HDAC6, microtubule depolymerization by Nek2/Kif24 could favor the irreversibility of this process once S phase begins, and thereby safeguard against aberrant assembly of cilia. It is notable that the cell invests a considerable amount of energy in maintaining a deciliated state, and the fact that relatives of Kif24 and Nek2 – as well as Aurora A – play a role in axonemal assembly and disassembly in flagellated and ciliated species (Bradley and Quarmby, 2005; Hilton et al., 2013; Mahjoub et al., 2002; Pan et al., 2004; Piao et al., 2009; Wloga et al., 2006) attests to the conservation and importance of this process. Future studies will be required to determine whether the abrogation of these pathways leads to pathological states, akin to defects in the cilium assembly process that lead to ciliopathies.

Ciliary membrane remodeling during cilium disassembly

Cilium disassembly also requires the remodeling of ciliary membranes (Fig. 4), and several recent studies have identified key mechanisms and proteins that play a role in this process. The ciliary

pocket (CiPo) is an actin-rich, periciliary subdomain that surrounds the proximal region of the ciliary axoneme (Fig. 1). It is a dynamic center for endocytosis and, upon cilium resorption, the CiPo membrane undergoes active remodeling, accompanied by enhanced endocytosis (Phua et al., 2017). Importantly, the perturbation of CiPo membrane endocytosis by depletion of clathrin heavy chain or expression of a dominant-negative Rab5 (S34N) mutant specifically blocks ciliary resorption, suggesting that CiPo membrane endocytosis is actively involved in ciliary disassembly/resorption. At the molecular level, remodeling of the CiPo membrane and enhancement of clathrin-mediated endocytosis is dependent on actin polymerization and is regulated by Tctex1 (also known as Dynlt1) (Saito et al., 2017), a protein that has previously been identified as a dynein light chain (Lader et al., 1989). Before S-phase entry, phospho (T94) Tctex1, the functionally active form of Tctex1, is recruited to the transition zone. Tctex1 directly binds to F-actin and interacts with three actin polymerization regulators, ANXA2, ARPC2 and Cdc42 (Saito et al., 2017); perturbing the expression and/or function of any of these three proteins blocks ciliary resorption. The recruitment of phospho (T94) Tctex1 to the transition zone is regulated by the IGF1 signaling pathway, which thus provides a link between mitogenic stimulation and cilium disassembly. Upon IGF binding, ciliary IGF1R translocates to the base of the cilium to activate G $\beta\gamma$, which competes with the dynein intermediate chain for binding to Tctex1 and thus facilitates the generation of the dynein-free Tctex1 necessary for Thr94 phosphorylation (Li et al., 2011; Saito et al., 2017; Yeh et al., 2013).

Recent studies indicate that the distal ciliary membrane also undergoes active remodeling during cilium disassembly (Fig. 4) (Nager et al., 2017; Phua et al., 2017). In particular, the release of CVs from the distal region of cilia (through ectocytosis; Figs 1 and 4) was periodically observed after growth stimulation, and this was achieved through cilium decapitation mediated by intra-ciliary actin polymerization (Nager et al., 2017; Phua et al., 2017). The exact position of ciliary decapitation is determined by the ciliary distribution of phosphatidylinositol 4,5-bisphosphate [PI(4,5)P $_2$], which induces actin polymerization in coordination with the actin regulators cofilin 1, fascin and Kras (Phua et al., 2017). Upon

growth stimulation, Aurora A drives INPP5E depletion and PI(4,5)P₂ re-distribution in the cilium to facilitate actin nucleation at a specific location. As IFT complexes are actively released by vesicles formed through growth-induced ciliary decapitation at the ciliary tip, this mechanism provides another layer of IFT regulation. Notably, proteomic analyses have demonstrated that CV release preferentially removes IFT-B, rather than IFT-A, from primary cilia, and that the removal of IFT-B from primary cilia can limit cilia re-growth and thereby promote cilia disassembly (Phua et al., 2017). As perturbation of ciliary decapitation could abolish cilium disassembly (Nager et al., 2017; Phua et al., 2017), future studies will be required to understand the role of this process in normal and pathological conditions.

Other factors that regulate cilium disassembly

As mentioned above, IFT is important for axonemal extension and length control, and, as such, this process – and the proteins that regulate it – also participates in cilium disassembly (Fig. 4). A number of factors (discussed above) are known to promote the recruitment of IFT complexes to cilia. By contrast, this recruitment process is restricted by local actin networks (Ishikawa and Marshall, 2017). Interestingly, the histone lysine demethylase KDM3A promotes the formation of actin bundles by regulating actin gene expression and by binding to the actin cytoskeleton (Yeyati et al., 2017); in its absence, the actin network is depolymerized, resulting in a delay in cilium resorption and an abnormal distribution of IFT within cilia. Nde1, which localizes at the transition zone, is another negative regulator of cilium length that controls cilium disassembly (Gabriel et al., 2016; Kim et al., 2011; Maskey et al., 2015). Nde1 is highly expressed in mitotic cells but is depleted in G0/G1 cells through CDK5-mediated phosphorylation, which targets the protein for ubiquitylation by the F-box protein Fbxw7, leading to its subsequent destruction. During cell cycle re-entry, CDK5 activity decreases, allowing Nde1 levels to accumulate and promote ciliary resorption. However, it is not known how Nde1 regulates cilium disassembly mechanistically. One Nde1 effector protein, LC8, the dynein light chain (also known as Dynl1), is tethered to Nde1 at the basal body. As LC8 is important for IFT transport and cilium assembly, Nde1 may regulate cilium disassembly in part through perturbation of IFT transport.

Additional mechanisms that induce deciliation have also been described. For example, cilia can be removed by severing mechanisms, as occurs in the green alga *Chlamydomonas*, in which deciliation can be enforced through the action of katanin, a microtubule-severing enzyme that separates basal bodies from axonemes before mitosis (Lohret et al., 1998; Rasi et al., 2009). In neurons, deciliation or apical abscission can also be accomplished by pinching off the cilium from the centrosome via another actomyosin-dependent process (Das and Storey, 2014). The pervasiveness of this abscission mechanism has not been determined, and it is unknown whether it can be implemented in a cell type- and context-dependent manner to regulate key signaling events under proliferative conditions or during differentiation.

Recent insights into the developmental control of ciliogenesis

It is clear that the correct formation of cilia plays exceptionally important and widespread roles in mammalian development (for a review, see Goetz and Anderson, 2010). By contrast, the dynamic regulation of cilium assembly and disassembly in development has been less thoroughly studied. However, in recent years, new and interesting insights have been reported that now link cilium assembly to diverse developmental states.

In multicellular organisms, the initiation of cilium assembly is regulated by intricate transcriptional programs (reviewed in Choksi et al., 2014; Spassky and Meunier, 2017). Our current knowledge of the transcriptional control of ciliogenesis primarily stems from studies in multiciliated cells, whereas the transcriptional program in monociliated cells has been largely left unexplored. Recently, the evolutionarily conserved RFX family of transcriptional factors was found to regulate cilium assembly in both types of cells by controlling the expression of core ciliary genes, including components of the transition zone, the BBsome and IFT (Choksi et al., 2014). The timely and spatially accurate expression of RFX transcription factors is also determined by key signaling factors, including FGF, as well as the neural transcription factors atonal and noto (Beckers et al., 2007; Cachero et al., 2011; Neugebauer et al., 2009). Ciliogenesis can also be regulated during development through posttranscriptional mechanisms involving microRNAs. For example, miR-129-3p initiates ciliogenesis in diverse tissues by downregulating CP110 and repressing branched F-actin formation (Cao et al., 2012).

In certain tissues, such as blood vessels, the heart, myoblasts and adipocytes (Fu et al., 2014; Goetz et al., 2014; Marion et al., 2009; Mohieldin et al., 2016), primary cilium assembly occurs transiently and is linked to a specific developmental phase, after which the structure disappears, suggesting that a cilium disassembly program may be involved. In these tissues, the transient appearance of primary cilia plays important, but poorly defined, roles during development. A good example here is the endothelial cilia, which are mechanical sensors of fluid flow, that are required for blood vessel maturation and homeostasis (Mohieldin et al., 2016). In zebrafish, endothelial cilia are exclusively present between 24 and 28 h after fertilization, and their disappearance can be ascribed, in part, to cilium disassembly induced by fluid shear stress (Goetz et al., 2014; Mohieldin et al., 2016). However, how shear stress leads to cilium disassembly remains unknown.

In other tissues, the developmental program can shift from a primary ciliated to multiciliated state through inhibition of Notch signaling, as occurs in the mammalian respiratory system and the zebrafish pronephros (Jain et al., 2010; Liu et al., 2007; Spassky and Meunier, 2017). Moreover, during mammalian brain development, the active resorption of primary cilia from progenitor cells is required for maintenance of the progenitor cell pool and for the control of brain size (Li et al., 2011; Yeh et al., 2013). This process is controlled by the cilia repressor *Tctex1* and its regulators and effectors, as mentioned above, although it is not yet known how the disappearance of cilia is regulated. Therefore, although much progress has been made, additional studies will be required to understand the precise mechanisms that induce the assembly and disassembly of cilia upon activation of diverse developmental programs.

Defects associated with cilium assembly and disassembly

A range of developmental disorders has been linked to ciliary defects, and manifestations include brain malformations, congenital heart defects and skeletal malformations (for a comprehensive review, see Reiter and Leroux, 2017). Here, we focus on recent studies of ciliopathies and ciliary aberrations that are caused by cell cycle perturbations and, specifically, cancer.

Cilia as tumor suppressors

Loss of cilia has been observed in a multitude of tumors including, but not limited to, pancreatic ductal adenocarcinoma, renal cell carcinoma, thyroid cancer, breast cancer, ovarian cancer, prostate

cancer, cholangiocarcinoma, glioblastoma and melanoma (Egeberg et al., 2012; Gradilone et al., 2013; Han et al., 2009; Hassounah et al., 2013; Lee et al., 2016a; Moser et al., 2009; Schraml et al., 2009; Seeley et al., 2009; Yuan et al., 2010). The importance of this cilia loss in tumor initiation, maintenance and progression, as well as in chemotherapeutic resistance, is now beginning to emerge, and it appears to be linked to the key roles played by cilia in various signaling pathways (Fig. 5).

Primary cilia are important in Hh signaling (for a review, see Bangs and Anderson, 2017), which plays an essential role in development and the abnormal activation of which is crucial for the development of many cancers (Pak and Segal, 2016). In a breast cancer model, inhibition of ciliogenesis was shown to result in non-canonical activation of Hh signaling, thereby accelerating tumor formation and enhancing the growth of malignant lesions (Hassounah et al., 2017). Moreover, disruption of ciliogenesis promotes pancreatic intraepithelial neoplasia (PanIN) formation during oncogenic Kras (G12D)-driven tumorigenesis (Seeley et al., 2009). Cilia are also known to restrain activation of β catenin-T cell factor (TCF) signaling (Lancaster et al., 2011), and a study using a pancreatic cancer model showed that disruption of ciliogenesis activates the mevalonate (MVA) pathway through β catenin-TCF signaling, which further boosts oncogenic Ras-Erk signaling (Deng et al., 2018). In glioblastoma, mitogenic signaling through lysophosphatidic acid is restricted in normal cells with a primary cilium because of the segregation of lysophosphatidic acid receptor (LPAR1) in the cilium from its downstream G-protein effectors: $G\alpha_{12}$ and $G\alpha_q$ (Loskutov et al., 2018). However, during tumorigenesis and upon loss of primary cilia, LPAR1 redistributes to the plasma membrane, allowing $G\alpha_{12}$ and $G\alpha_q$ to bind to the receptor, which promotes increased mitogenic signaling and proliferation of tumor cells. These data demonstrate that the absence of cilia observed in tumors could mediate, or repurpose, multiple signaling pathways and promote the formation of tumors.

Notably, a recent study suggested how the loss of cilia promotes tumor survival after chemotherapy (Zhao et al., 2017). Resistance to an inhibitor of smoothened (SMO), an activator of

the Hh pathway, is frequently observed in Hh pathway-dependent cancers. In a transposon mutagenesis screen aimed at understanding the mechanism underlying this resistance in medulloblastomas, recurrent mutations in *OFD1* – a gene that is defective in ciliopathies – were identified. Following on from this, it was shown that loss of cilia by depletion of *OFD1* and other ciliogenesis genes confers resistance to SMO inhibition by achieving a cilium-independent state that is able to transduce low-level Hh signaling and is capable of evolving into a more-aggressive tumor. This study pinpoints an important role for cilia in tumor evolution and drug resistance and, given the pivotal role of cilia in Hh and growth factor signaling, it is likely that many additional mediators of chemo-resistance that localize to centrosomes and cilia will be identified in the future.

Cilia as tumor promoters

In contrast with the above examples, cilia have been shown to persist in a range of tumors (Fu et al., 2014; Yasar et al., 2017) and can be found in medulloblastomas exhibiting activation of Hh or Wnt signaling (Han et al., 2009). Strikingly, tumorigenesis is blocked in a medulloblastoma mouse model driven by constitutively active SMO when primary cilia are genetically ablated (Han et al., 2009). In the same model, INPP5P inactivation increases cilia-localized PI3-kinase/AKT signaling, which promotes cilia loss, thereby reducing both oncogenic Hh signaling and tumor growth (Conduit et al., 2017). Furthermore, inhibiting cilia-dependent oncogenic sonic hedgehog overactivation, through depletion of the ciliary GTPase Arl13b, can also suppress medulloblastoma growth without ablating cilia (Bay et al., 2018). Similarly, the loss of cilia protects mice from tumorigenesis in a basal cell carcinoma model driven by constitutively active SmoM2 (Wong et al., 2009). In this context, the expression of *Intu* (Intu), a planar cell polarity effector required for cilium assembly that regulates apical actin networks, is aberrantly elevated, whereas disruption of *Intu* prevents the formation of basal cell carcinoma by suppressing primary cilia formation and Hh signaling (Yang et al., 2017).

In a novel example of ciliary repurposing by tumors, cells were able to switch fates to allow assembly of a primary cilium and

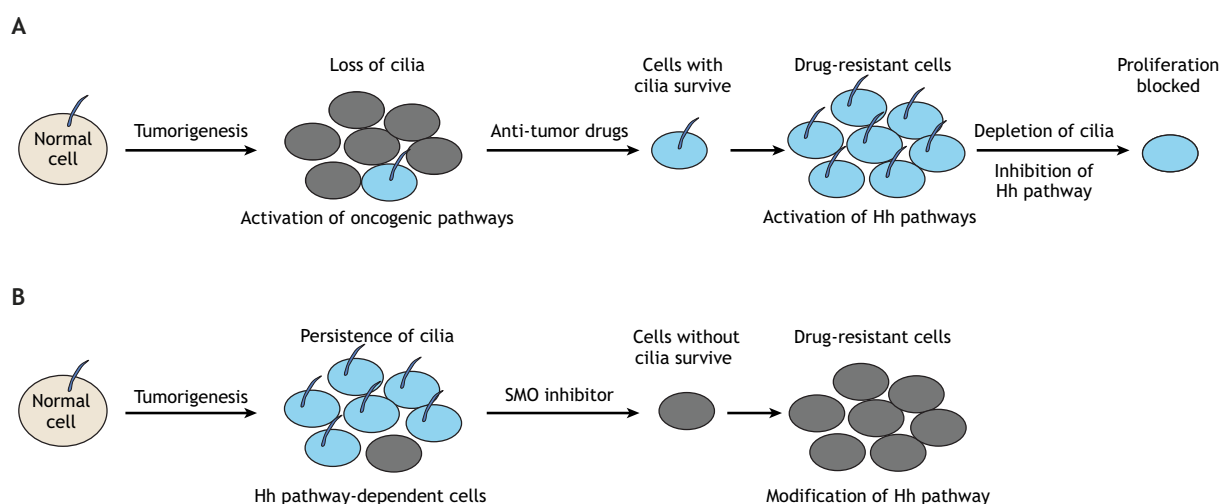


Fig. 5. The function of primary cilia in cancer. (A) Loss of cilia has been observed in several types of tumors and can lead to aberrant activation of many oncogenic pathways. After treatment with anti-tumor drugs, tumor cells with cilia, and hence aberrant activation of Hh pathway, survive and can further proliferate. Depletion of cilia or inhibition of Hh signal pathway can block the proliferation of these drug-resistant cells. (B) The persistence of cilia can also be observed in a range of tumors, in which they appear to help maintain the oncogenic Hh pathway. After treatment with an SMO inhibitor, tumor cells with cilia die and the surviving cells (without cilia) evolve a modified Hh pathway that confers resistance to SMO inhibition.

activation of Hh signaling (Li et al., 2016); in this example – a choroid plexus (CP) tumor model driven by sustained expression of Notch – monociliated CP tumor cells arise from multiciliated CP epithelial cells following elevated Notch signaling, which suppresses multiciliation in favor of primary ciliogenesis. This leads to enhanced Hh signaling that promotes CP tumor cell proliferation. Together, these data demonstrate that the presence of primary cilia in tumors can mediate Hh signaling and promote the formation of tumors. Furthermore, a recent study suggested that the acquisition of cilia, ciliary tip fragmentation and increased cilium length are frequently observed in tumor cells after anti-neoplastic drug treatment (Jenks et al., 2018), including in EGFR-mutant non-small cell lung carcinoma cells treated with an EGFR inhibitor, in rhabdoid tumors treated with a tyrosine kinase inhibitor, in EML4-ALK-fusion-positive lung cancers after ALK inhibitor treatment and in KRAS mutant lung cancer cells treated with a MEK inhibitor. The aberrant ciliogenesis is accompanied by activation of Hh signaling, and depletion of cilia or inhibition of Hh signaling can thus reduce the viability of drug-resistant cells. This study highlights that cilium assembly pathways can be hijacked by tumor cells to gain resistance to anti-tumor drugs, opening up exciting new avenues for the treatment of drug-resistant tumors.

Conclusions and future directions

In the past few years, significant advances have been made in understanding the events required during cilium assembly. In particular, new DA and SDA components required for centriole maturation have been identified, their localization defined with high-resolution methods, and their assembly pathways and function during vesicle docking and cytoskeleton connection elucidated. Importantly, novel markers of vesicles and regulators of vesicle trafficking, fusion and growth have also been revealed. Future studies will need to uncover the signals that mediate the onset of basal body maturation and cilium assembly, as well as the remodeling events – and specific molecules – at basal bodies that facilitate capture and growth of early ciliary vesicles, and extension of the nascent axoneme. In terms of cilium disassembly, we have a better understanding of the regulation of axonemal microtubule depolymerization and ciliary membrane remodeling, and additional signaling pathways have been found to control cilium disassembly. Given the pivotal role of cilia in development and disease, it will be essential to continue unraveling the mechanisms that link ciliogenesis and cilium disassembly to the cell cycle, mitogen deprivation and developmental cues. Improvements in real-time microscopy and lineage-tracing, as well as in single-cell sequencing technology, will hopefully lead to a better understanding of the developmental control of ciliogenesis in specific lineages and help us to understand the cilium-related mechanisms that govern chemoresistance in specific tumor types. It will also be interesting to understand the co-evolution of cilia structures and ciliary signaling pathways, in particular whether, and how, the ciliogenic program and related ciliary signaling pathways are coordinately switched on and off in a specific cell type or during certain developmental processes.

The role of cilia in tumorigenesis is further complicated by recent studies implicating this organelle in drug resistance. It is unclear how tumor cells manipulate cilium assembly or disassembly pathways for their own survival and how these pathways are harnessed by tumors to promote resistance to chemotherapeutic agents. Understanding these basic issues could contribute to the early detection of cancer and assist with the development of new anti-cancer regimens.

Acknowledgements

We apologize to the many researchers whose work could not be cited owing to space constraints.

Competing interests

The authors declare no competing or financial interests.

Funding

This work was supported by a U.S. Department of Defense fellowship (W81XWH-16-1-0392) to L.W., and a National Institutes of Health grant (9R01GM120776) to B.D.D. Deposited in PMC for release after 12 months.

References

- Absalon, S., Blisnick, T., Kohl, L., Toutirais, G., Doré, G., Julkowska, D., Tavenet, A. and Bastin, P. (2008). Intraflagellar transport and functional analysis of genes required for flagellum formation in trypanosomes. *Mol. Biol. Cell* **19**, 929-944.
- Adams, M., Simms, R. J., Abdelhamed, Z., Dawe, H. R., Szymanska, K., Logan, C. V., Wheway, G., Pitt, E., Gull, K., Knowles, M. A. et al. (2012). A meckelin-filamin A interaction mediates ciliogenesis. *Hum. Mol. Genet.* **21**, 1272-1286.
- Agbu, S. O., Liang, Y., Liu, A. and Anderson, K. V. (2018). The small GTPase RSG1 controls a final step in primary cilia initiation. *J. Cell Biol.* **217**, 413-427.
- Antoniades, I., Stylianou, P. and Skourides, P. A. (2014). Making the connection: ciliary adhesion complexes anchor basal bodies to the actin cytoskeleton. *Dev. Cell* **28**, 70-80.
- Aughstee, A. A. (2001). The ultrastructure of primary cilia in the endocrine and excretory duct cells of the pancreas of mice and rats. *Eur. J. Morphol.* **39**, 277-283.
- Bangs, F. and Anderson, K. V. (2017). Primary cilia and mammalian hedgehog signaling. *Cold Spring Harb. Perspect. Biol.* **9**, a028175.
- Bay, S. N., Long, A. B. and Casparly, T. (2018). Disruption of the ciliary GTPase Arl13b suppresses Sonic hedgehog overactivation and inhibits medulloblastoma formation. *Proc. Natl. Acad. Sci. USA* **115**, 1570-1575.
- Beckers, A., Alten, L., Viebahn, C., Andre, P. and Gossler, A. (2007). The mouse homeobox gene Noto regulates node morphogenesis, notochordal ciliogenesis, and left right patterning. *Proc. Natl. Acad. Sci. USA* **104**, 15765-15770.
- Bernabé-Rubio, M. and Alonso, M. A. (2017). Routes and machinery of primary cilium biogenesis. *Cell. Mol. Life Sci.* **74**, 4077-4095.
- Besschetnova, T. Y., Kolpakova-Hart, E., Guan, Y., Zhou, J., Olsen, B. R. and Shah, J. V. (2010). Identification of signaling pathways regulating primary cilium length and flow-mediated adaptation. *Curr. Biol.* **20**, 182-187.
- Bhattacharyya, S., Rainey, M. A., Arya, P., Dutta, S., George, M., Storck, M. D., McComb, R. D., Muirhead, D., Todd, G. L., Gould, K. et al. (2016). Endocytic recycling protein EHD1 regulates primary cilia morphogenesis and SHH signaling during neural tube development. *Sci. Rep.* **6**, 20727.
- Bradley, B. A. and Quarmby, L. M. (2005). A NIMA-related kinase, Cnk2p, regulates both flagellar length and cell size in *Chlamydomonas*. *J. Cell Sci.* **118**, 3317-3326.
- Burghoorn, J., Dekkers, M. P. J., Rademakers, S., de Jong, T., Willemsen, R. and Jansen, G. (2007). Mutation of the MAP kinase DYF-5 affects docking and undocking of kinesin-2 motors and reduces their speed in the cilia of *Caenorhabditis elegans*. *Proc. Natl. Acad. Sci. USA* **104**, 7157-7162.
- Burke, M. C., Li, F.-Q., Cyge, B., Arashiro, T., Brechbuhl, H. M., Chen, X., Siller, S. S., Weiss, M. A., O'Connell, C. B., Love, D. et al. (2014). Chibby promotes ciliary vesicle formation and basal body docking during airway cell differentiation. *J. Cell Biol.* **207**, 123-137.
- Cachero, S., Simpson, T. I., Zur Lage, P. I., Ma, L., Newton, F. G., Holohan, E. E., Armstrong, J. D. and Jarman, A. P. (2011). The gene regulatory cascade linking proneural specification with differentiation in *Drosophila* sensory neurons. *PLoS Biol.* **9**, e1000568.
- Cajane, L. and Nigg, E. A. (2014). Cep164 triggers ciliogenesis by recruiting Tau tubulin kinase 2 to the mother centriole. *Proc. Natl. Acad. Sci. USA* **111**, E2841-E2850.
- Cao, J., Shen, Y., Zhu, L., Xu, Y., Zhou, Y., Wu, Z., Li, Y., Yan, X. and Zhu, X. (2012). miR-129-3p controls cilia assembly by regulating CP110 and actin dynamics. *Nat. Cell Biol.* **14**, 697-706.
- Choksi, S. P., Lauter, G., Swoboda, P. and Roy, S. (2014). Switching on cilia: transcriptional networks regulating ciliogenesis. *Development* **141**, 1427-1441.
- Conduit, S. E., Ramaswamy, V., Remke, M., Watkins, D. N., Wainwright, B. J., Taylor, M. D., Mitchell, C. A. and Dyson, J. M. (2017). A compartmentalized phosphoinositide signaling axis at cilia is regulated by INPP5E to maintain cilia and promote Sonic Hedgehog medulloblastoma. *Oncogene* **36**, 5969-5984.
- Das, R. M. and Storey, K. G. (2014). Apical abscission alters cell polarity and dismantles the primary cilium during neurogenesis. *Science* **343**, 200-204.
- Deng, Y.-Z., Cai, Z., Shi, S., Jiang, H., Shang, Y. R., Ma, N., Wang, J.-J., Guan, D.-X., Chen, T.-W., Rong, Y.-F. et al. (2018). Cilia loss sensitizes cells to transformation by activating the mevalonate pathway. *J. Exp. Med.* **215**, 177-195.

- Egeberg, D. L., Lethan, M., Manguso, R., Schneider, L., Awan, A., Jorgensen, T. S., Byskov, A. G., Pedersen, L. B. and Christensen, S. T. (2012). Primary cilia and aberrant cell signaling in epithelial ovarian cancer. *Cilia* **1**, 15.
- Elliott, K. H. and Brugmann, S. A. (2018). Sending mixed signals: Cilia-dependent signaling during development and disease. *Dev. Biol.*
- Farina, F., Gaillard, J., Guerin, C., Coute, Y., Sillibourne, J., Blanchoin, L. and Théry, M. (2016). The centrosome is an actin-organizing centre. *Nat. Cell Biol.* **18**, 65-75.
- Fu, W., Asp, P., Canter, B. and Dynlacht, B. D. (2014). Primary cilia control hedgehog signaling during muscle differentiation and are deregulated in rhabdomyosarcoma. *Proc. Natl. Acad. Sci. USA* **111**, 9151-9156.
- Fu, W., Wang, L., Kim, S., Li, J. and Dynlacht, B. D. (2016). Role for the IFT-A complex in selective transport to the primary cilium. *Cell Rep* **17**, 1505-1517.
- Gabriel, E., Wason, A., Ramani, A., Gooi, L. M., Keller, P., Pozniakovskiy, A., Poser, I., Noack, F., Telugu, N. S., Calegari, F. et al. (2016). CPAP promotes timely cilium disassembly to maintain neural progenitor pool. *EMBO J.* **35**, 803-819.
- Goetz, S. C. and Anderson, K. V. (2010). The primary cilium: a signalling centre during vertebrate development. *Nat. Rev. Genet.* **11**, 331-344.
- Goetz, S. C., Liem, K. F., Jr. and Anderson, K. V. (2012). The spinocerebellar ataxia-associated gene Tau tubulin kinase 2 controls the initiation of ciliogenesis. *Cell* **151**, 847-858.
- Goetz, J. G., Steed, E., Ferreira, R. R., Roth, S., Ramspacher, C., Boselli, F., Charvin, G., Liebling, M., Wyart, C., Schwab, Y. et al. (2014). Endothelial cilia mediate low flow sensing during zebrafish vascular development. *Cell Rep* **6**, 799-808.
- Gradilone, S. A., Radtke, B. N., Bogert, P. S., Huang, B. Q., Gajdos, G. B. and LaRusso, N. F. (2013). HDAC6 inhibition restores ciliary expression and decreases tumor growth. *Cancer Res.* **73**, 2259-2270.
- Graser, S., Stierhof, Y.-D., Lavoie, S. B., Gassner, O. S., Lamla, S., Le Clech, M. and Nigg, E. A. (2007). Cep164, a novel centriole appendage protein required for primary cilium formation. *J. Cell Biol.* **179**, 321-330.
- Gupta, G. D., Coyaud, E., Goncalves, J., Mojarad, B. A., Liu, Y., Wu, Q., Gheiratmand, L., Comartin, D., Tkach, J. M., Cheung, S. W. et al. (2015). A dynamic protein interaction landscape of the human centrosome-cilium interface. *Cell* **163**, 1484-1499.
- Hamze-Komaihi, O., Sarr, S., Arlot-Bonnemains, Y., Samuel, D. and Gassama-Diagne, A. (2016). SHIP2 regulates lumen generation, cell division, and ciliogenesis through the control of basolateral to apical lumen localization of aurora A and HEF 1. *Cell Rep* **17**, 2738-2752.
- Han, Y.-G., Kim, H. J., Dlugosz, A. A., Ellison, D. W., Gilbertson, R. J. and Alvarez-Buylla, A. (2009). Dual and opposing roles of primary cilia in medulloblastoma development. *Nat. Med.* **15**, 1062-1065.
- Harris, J. A., Van De Weghe, J. M., Kubo, T., Witman, G. B. and Lechtreck, K. (2018). Diffusion rather than IFT provides most of the tubulin required for axonemal assembly. *bioRxiv*.
- Hassounah, N. B., Nagle, R., Saboda, K., Roe, D. J., Dalkin, B. L. and McDermott, K. M. (2013). Primary cilia are lost in preinvasive and invasive prostate cancer. *PLoS ONE* **8**, e68521.
- Hassounah, N. B., Nunez, M., Fordyce, C., Roe, D., Nagle, R., Bunch, T. and McDermott, K. M. (2017). Inhibition of ciliogenesis promotes hedgehog signaling, tumorigenesis, and metastasis in breast cancer. *Mol. Cancer Res.* **15**, 1421-1430.
- Hilton, L. K., Gunawardane, K., Kim, J. W., Schwarz, M. C. and Quarmby, L. M. (2013). The kinases LF4 and CNK2 control ciliary length by feedback regulation of assembly and disassembly rates. *Curr. Biol.* **23**, 2208-2214.
- Hori, A. and Toda, T. (2017). Regulation of centriolar satellite integrity and its physiology. *Cell. Mol. Life Sci.* **74**, 213-229.
- Hsiao, Y.-C., Tong, Z. J., Westfall, J. E., Ault, J. G., Page-McCaw, P. S. and Ferland, R. J. (2009). Ahi1, whose human ortholog is mutated in Joubert syndrome, is required for Rab8a localization, ciliogenesis and vesicle trafficking. *Hum. Mol. Genet.* **18**, 3926-3941.
- Huang, N., Xia, Y., Zhang, D., Wang, S., Bao, Y., He, R., Teng, J. and Chen, J. (2017). Hierarchical assembly of centriole subdistal appendages via centrosome binding proteins CCDC120 and CCDC68. *Nat. Commun.* **8**, 15057.
- Ibi, M., Zou, P., Inoko, A., Shimozu, T., Matsuyama, M., Hayashi, Y., Enomoto, M., Mori, D., Hirotsune, S., Kiyono, T. et al. (2011). Trichoplein controls microtubule anchoring at the centrosome by binding to Odf2 and ninein. *J. Cell Sci.* **124**, 857-864.
- Inaba, H., Goto, H., Kasahara, K., Kumamoto, K., Yonemura, S., Inoko, A., Yamano, S., Wanibuchi, H., He, D., Goshima, N. et al. (2016). Ndel1 suppresses ciliogenesis in proliferating cells by regulating the trichoplein-Aurora A pathway. *J. Cell Biol.* **212**, 409-423.
- Inoko, A., Matsuyama, M., Goto, H., Ohmuro-Matsuyama, Y., Hayashi, Y., Enomoto, M., Ibi, M., Urano, T., Yonemura, S., Kiyono, T. et al. (2012). Trichoplein and Aurora A block aberrant primary cilia assembly in proliferating cells. *J. Cell Biol.* **197**, 391-405.
- Ishikawa, H. and Marshall, W. F. (2017). Intraflagellar transport and ciliary dynamics. *Cold Spring Harb. Perspect. Biol.* **9**.
- Jain, R., Pan, J., Driscoll, J. A., Wisner, J. W., Huang, T., Gunsten, S. P., You, Y. and Brody, S. L. (2010). Temporal relationship between primary and motile ciliogenesis in airway epithelial cells. *Am. J. Respir. Cell Mol. Biol.* **43**, 731-739.
- Jain, R., Javidan-Nejad, C., Alexander-Brett, J., Horani, A., Cabellon, M. C., Walter, M. J. and Brody, S. L. (2012). Sensory functions of motile cilia and implication for bronchiectasis. *Front. Biosci. (Schol Ed)* **4**, 1088-1098.
- Jenks, A. D., Vyse, S., Wong, J. P., Kostaras, E., Keller, D., Burgoyne, T., Shoemark, A., Tsalikis, A., de la Roche, M., Michaelis, M. et al. (2018). Primary cilia mediate diverse kinase inhibitor resistance mechanisms in cancer. *Cell Rep* **23**, 3042-3055.
- Jensen, V. L. and Leroux, M. R. (2017). Gates for soluble and membrane proteins, and two trafficking systems (IFT and LIFT), establish a dynamic ciliary signaling compartment. *Curr. Opin. Cell Biol.* **47**, 83-91.
- Joo, K., Kim, C. G., Lee, M.-S., Moon, H.-Y., Lee, S.-H., Kim, M. J., Kweon, H.-S., Park, W.-Y., Kim, C.-H., Gleeson, J. G. et al. (2013). CCDC41 is required for ciliary vesicle docking to the mother centriole. *Proc. Natl. Acad. Sci. USA* **110**, 5987-5992.
- Kanie, T., Abbott, K. L., Mooney, N. A., Plowey, E. D., Demeter, J. and Jackson, P. K. (2017). The CEP19-RABL2 GTPase complex binds IFT-B to initiate intraflagellar transport at the ciliary base. *Dev. Cell* **42**, 22-36 e12.
- Kaplan, O. I., Doroquez, D. B., Cevik, S., Bowie, R. V., Clarke, L., Sanders, A. A., Kida, K., Rappoport, J. Z., Sengupta, P. and Blacque, O. E. (2012). Endocytosis genes facilitate protein and membrane transport in *C. elegans* sensory cilia. *Curr. Biol.* **22**, 451-460.
- Kasahara, K., Kawakami, Y., Kiyono, T., Yonemura, S., Kawamura, Y., Era, S., Matsuzaki, F., Goshima, N. and Inagaki, M. (2014). Ubiquitin-proteasome system controls ciliogenesis at the initial step of axoneme extension. *Nat. Commun.* **5**, 5081.
- Kasahara, K., Aoki, H., Kiyono, T., Wang, S., Kagiwada, H., Yuge, M., Tanaka, T., Nishimura, Y., Mizoguchi, A., Goshima, N. et al. (2018). EGF receptor kinase suppresses ciliogenesis through activation of USP8 deubiquitinase. *Nat. Commun.* **9**, 758.
- Kazatskaya, A., Kuhns, S., Lambacher, N. J., Kennedy, J. E., Brear, A. G., McManus, G. J., Sengupta, P. and Blacque, O. E. (2017). Primary cilium formation and ciliary protein trafficking is regulated by the atypical MAP kinase MAPK15 in *Caenorhabditis elegans* and human cells. *Genetics* **207**, 1423-1440.
- Kim, J., Krishnaswami, S. R. and Gleeson, J. G. (2008). CEP290 interacts with the centriolar satellite component PCM-1 and is required for Rab8 localization to the primary cilium. *Hum. Mol. Genet.* **17**, 3796-3805.
- Kim, S., Zaghloul, N. A., Bubenshchikova, E., Oh, E. C., Rankin, S., Katsanis, N., Obara, T. and Tsiokas, L. (2011). Nde1-mediated inhibition of ciliogenesis affects cell cycle re-entry. *Nat. Cell Biol.* **13**, 351-360.
- Kim, M., Kim, M., Lee, M.-S., Kim, C.-H. and Lim, D.-S. (2014). The MST1/2-SAV1 complex of the Hippo pathway promotes ciliogenesis. *Nat. Commun.* **5**, 5370.
- Kim, J., Jo, H., Hong, H., Kim, M. H., Kim, J. M., Lee, J.-K., Heo, W. D. and Kim, J. (2015a). Actin remodelling factors control ciliogenesis by regulating YAP/TAZ activity and vesicle trafficking. *Nat. Commun.* **6**, 6781.
- Kim, S., Lee, K., Choi, J.-H., Ringstad, N. and Dynlacht, B. D. (2015b). Nek2 activation of Kif24 ensures cilium disassembly during the cell cycle. *Nat. Commun.* **6**, 8087.
- Kinzel, D., Boldt, K., Davis, E. E., Burtscher, I., Trümbach, D., Diplas, B., Attié-Bitach, T., Wurst, W., Katsanis, N., Ueffing, M. et al. (2010). Pitchfork regulates primary cilia disassembly and left-right asymmetry. *Dev. Cell* **19**, 66-77.
- Klinger, M., Wang, W., Kuhns, S., Bärenz, F., Dräger-Meurer, S., Pereira, G. and Gruss, O. J. (2014). The novel centriolar satellite protein SSX2IP targets Cep290 to the ciliary transition zone. *Mol. Biol. Cell* **25**, 495-507.
- Kobayashi, T., Tsang, W. Y., Li, J., Lane, W. and Dynlacht, B. D. (2011). Centriolar kinesin Kif24 interacts with CP110 to remodel microtubules and regulate ciliogenesis. *Cell* **145**, 914-925.
- Kobayashi, T., Kim, S., Lin, Y.-C., Inoue, T. and Dynlacht, B. D. (2014). The CP110-interacting proteins Talpid3 and Cep290 play overlapping and distinct roles in cilia assembly. *J. Cell Biol.* **204**, 215-229.
- Kobayashi, T., Nakazono, K., Tokuda, M., Mashima, Y., Dynlacht, B. D. and Itoh, H. (2017). HDAC2 promotes loss of primary cilia in pancreatic ductal adenocarcinoma. *EMBO Rep.* **18**, 334-343.
- Kodani, A., Salome Sirerol-Piquer, M., Seol, A., Garcia-Verdugo, J. M. and Reiter, J. F. (2013). Kif3a interacts with Dynactin subunit p150 Glued to organize centriole subdistal appendages. *EMBO J.* **32**, 597-607.
- Kuhns, S., Schmidt, K. N., Reymann, J., Gilbert, D. F., Neuner, A., Hub, B., Carvalho, R., Wiedemann, P., Zentgraf, H., Erfle, H. et al. (2013). The microtubule affinity regulating kinase MARK4 promotes axoneme extension during early ciliogenesis. *J. Cell Biol.* **200**, 505-522.
- Kurtulmus, B., Wang, W., Ruppert, T., Neuner, A., Cerikan, B., Viol, L., Dueñas-Sánchez, R., Gruss, O. J. and Pereira, G. (2016). WDR8 is a centriolar satellite and centriole-associated protein that promotes ciliary vesicle docking during ciliogenesis. *J. Cell Sci.* **129**, 621-636.
- Kurtulmus, B., Yuan, C., Schuy, J., Neuner, A., Hata, S., Kalamakis, G., Martín-Villalba, A. and Pereira, G. (2017). Analysis of LRRC45 indicates cooperative functions of distal appendages at early steps of ciliogenesis. *bioRxiv*.

- Lader, E., Ha, H.-S., O'Neill, M., Artzt, K. and Bennett, D. (1989). *tctx-1*: a candidate gene family for a mouse t complex sterility locus. *Cell* **58**, 969-979.
- Lancaster, M. A., Schroth, J. and Gleeson, J. G. (2011). Subcellular spatial regulation of canonical Wnt signalling at the primary cilium. *Nat. Cell Biol.* **13**, 700-707.
- Latta, H., Maunsbach, A. B. and Madden, S. C. (1961). Cilia in different segments of the rat nephron. *J. Biophys. Biochem. Cytol.* **11**, 248-252.
- Lee, K. H., Johmura, Y., Yu, L.-R., Park, J. E., Gao, Y., Bang, J. K., Zhou, M., Veenstra, T. D., Yeon Kim, B. and Lee, K. S. (2012). Identification of a novel Wnt5a-CK1varepsilon-Dvl2-Plk1-mediated primary cilia disassembly pathway. *EMBO J.* **31**, 3104-3117.
- Lee, J., Yi, S., Kang, Y. E., Chang, J. Y., Kim, J. T., Sul, H. J., Kim, J. O., Kim, J. M., Kim, J., Porcelli, A. M. et al. (2016a). Defective ciliogenesis in thyroid hürthle cell tumors is associated with increased autophagy. *Oncotarget* **7**, 79117-79130.
- Lee, S.-H., Lee, M.-S., Choi, T.-I., Hong, H., Seo, J.-Y., Kim, C.-H. and Kim, J. (2016b). MCRS1 associates with cytoplasmic dynein and mediates pericentrosomal material recruitment. *Sci. Rep.* **6**, 27284.
- Lee, S. H., Joo, K., Jung, E. J., Hong, H., Seo, J. and Kim, J. (2017). Export of membrane proteins from the Golgi complex to the primary cilium requires the kinesin motor, KIFC1. *FASEB J.* **32**, 957-968.
- Li, A., Saito, M., Chuang, J.-Z., Tseng, Y.-Y., Dedesma, C., Tomizawa, K., Katsuka, T. and Sung, C.-H. (2011). Ciliary transition zone activation of phosphorylated Tctex-1 controls ciliary resorption, S-phase entry and fate of neural progenitors. *Nat. Cell Biol.* **13**, 402-411.
- Li, J., Kim, S., Kobayashi, T., Liang, F.-X., Korzeniewski, N., Duensing, S. and Dynlacht, B. D. (2012). *Neurl4*, a novel daughter centriole protein, prevents formation of ectopic microtubule organizing centres. *EMBO Rep.* **13**, 547-553.
- Li, L., Grausam, K. B., Wang, J., Lun, M. P., Ohli, J., Lidov, H. G. W., Calicchio, M. L., Zeng, E., Salisbury, J. L., Wechsler-Reya, R. J. et al. (2016). Sonic Hedgehog promotes proliferation of Notch-dependent monociliated choroid plexus tumour cells. *Nat. Cell Biol.* **18**, 418-430.
- Li, W., Yi, P., Zhu, Z., Zhang, X., Li, W. and Ou, G. (2017). Centriole translocation and degeneration during ciliogenesis in *Caenorhabditis elegans* neurons. *EMBO J.* **36**, 2553-2566.
- Liang, Y., Pang, Y., Wu, Q., Hu, Z., Han, X., Xu, Y., Deng, H. and Pan, J. (2014). FLA8/KIF3B phosphorylation regulates kinesin-II interaction with IFT-B to control IFT entry and turnaround. *Dev. Cell* **30**, 585-597.
- Liu, Y., Pathak, N., Kramer-Zucker, A. and Drummond, I. A. (2007). Notch signaling controls the differentiation of transporting epithelia and multiciliated cells in the zebrafish pronephros. *Development* **134**, 1111-1122.
- Lohret, T. A., McNally, F. J. and Quarmby, L. M. (1998). A role for katanin-mediated axonemal severing during *Chlamydomonas* deflagellation. *Mol. Biol. Cell* **9**, 1195-1207.
- Lopes, C. A. M., Prosser, S. L., Romio, L., Hirst, R. A., O'Callaghan, C., Woolf, A. S. and Fry, A. M. (2011). Centriolar satellites are assembly points for proteins implicated in human ciliopathies, including oral-facial-digital syndrome 1. *J. Cell Sci.* **124**, 600-612.
- Loskutov, Y. V., Griffin, C. L., Marinak, K. M., Bobko, A., Margaryan, N. V., Geldenhuys, W. J., Sarkaria, J. N. and Pugacheva, E. N. (2018). LPA signaling is regulated through the primary cilium: a novel target in glioblastoma. *Oncogene* **37**, 1457-1471.
- Lu, H., Toh, M. T., Narasimhan, V., Thamilselvan, S. K., Choksi, S. P. and Roy, S. (2015a). A function for the Joubert syndrome protein *Arl13b* in ciliary membrane extension and ciliary length regulation. *Dev. Biol.* **397**, 225-236.
- Lu, Q., Insinna, C., Ott, C., Stauffer, J., Pintado, P. A., Rahajeng, J., Baxa, U., Walia, V., Cuenca, A., Hwang, Y.-S. et al. (2015b). Early steps in primary cilium assembly require EHD1/EHD3-dependent ciliary vesicle formation. *Nat. Cell Biol.* **17**, 228-240.
- Mahjoub, M. R., Montpetit, B., Zhao, L., Finst, R. J., Goh, B., Kim, A. C. and Quarmby, L. M. (2002). The FA2 gene of *Chlamydomonas* encodes a NIMA family kinase with roles in cell cycle progression and microtubule severing during deflagellation. *J. Cell Sci.* **115**, 1759-1768.
- Mahjoub, M. R., Xie, Z. and Stearns, T. (2010). Cep120 is asymmetrically localized to the daughter centriole and is essential for centriole assembly. *J. Cell Biol.* **191**, 331-346.
- Marion, V., Stoetzel, C., Schlicht, D., Messaddeq, N., Koch, M., Flori, E., Danse, J. M., Mandel, J.-L. and Dollfus, H. (2009). Transient ciliogenesis involving Bardet-Biedl syndrome proteins is a fundamental characteristic of adipogenic differentiation. *Proc. Natl. Acad. Sci. USA* **106**, 1820-1825.
- Marshall, W. F. and Rosenbaum, J. L. (2001). Intraflagellar transport balances continuous turnover of outer doublet microtubules: implications for flagellar length control. *J. Cell Biol.* **155**, 405-414.
- Marshall, W. F., Qin, H., Rodrigo Brenni, M. and Rosenbaum, J. L. (2005). Flagellar length control system: testing a simple model based on intraflagellar transport and turnover. *Mol. Biol. Cell* **16**, 270-278.
- Maskey, D., Marlin, M. C., Kim, S., Kim, S., Ong, E.-C., Li, G. and Tsiokas, L. (2015). Cell cycle-dependent ubiquitylation and destruction of NDE1 by CDK5-FBW7 regulates ciliary length. *EMBO J.* **34**, 2424-2440.
- May-Simera, H. L., Gumerson, J. D., Gao, C., Campos, M., Cologna, S. M., Beyer, T., Boldt, K., Kaya, K. D., Patel, N., Kretschmer, F. et al. (2016). Loss of MACF1 abolishes ciliogenesis and disrupts apicobasal polarity establishment in the retina. *Cell Rep* **17**, 1399-1413.
- Mazo, G., Soplop, N., Wang, W.-J., Uryu, K. and Tsou, M.-F. B. (2016). Spatial control of primary ciliogenesis by subdistal appendages alters sensation-associated properties of cilia. *Dev. Cell* **39**, 424-437.
- Miyamoto, T., Hosoba, K., Ochiai, H., Royba, E., Izumi, H., Sakuma, T., Yamamoto, T., Dynlacht, B. D. and Matsuura, S. (2015). The microtubule-depolymerizing activity of a mitotic kinesin protein KIF2A drives primary cilia disassembly coupled with cell proliferation. *Cell Rep.*
- Mohieldin, A. M., Zubayer, H. S., Al Omran, A. J., Saternos, H. C., Zarban, A. A., Nauli, S. M. and AbouAlaiwi, W. A. (2016). Vascular endothelial primary cilia: mechanosensation and hypertension. *Curr. Hypertens Rev.* **12**, 57-67.
- Moser, J. J., Fritzler, M. J. and Rattner, J. B. (2009). Primary ciliogenesis defects are associated with human astrocytoma/glioblastoma cells. *BMC Cancer* **9**, 448.
- Munger, B. L. (1958). A light and electron microscopic study of cellular differentiation in the pancreatic islets of the mouse. *Am. J. Anat.* **103**, 275-311.
- Muthaiyan Shanmugam, M., Bhan, P., Huang, H. Y., Hsieh, J., Hua, T. E., Wu, G. H., Punjabi, H., Lee Aplicano, V. D., Chen, C. W. and Wagner, O. I. (2018). Cilium length and intraflagellar transport regulation by kinases PKG-1 and GCK-2 in *Caenorhabditis elegans* sensory neurons. *Mol. Cell Biol.* **38**.
- Nachury, M. V. (2018). The molecular machines that traffic signaling receptors into and out of cilia. *Curr. Opin. Cell Biol.* **51**, 124-131.
- Nachury, M. V., Loktev, A. V., Zhang, Q., Westlake, C. J., Peränen, J., Merdes, A., Slusarski, D. C., Scheller, R. H., Bazan, J. F., Sheffield, V. C. et al. (2007). A core complex of BBS proteins cooperates with the GTPase Rab8 to promote ciliary membrane biogenesis. *Cell* **129**, 1201-1213.
- Nager, A. R., Goldstein, J. S., Herranz-Perez, V., Portran, D., Ye, F., Garcia-Verdugo, J. M. and Nachury, M. V. (2017). An actin network dispatches ciliary GPCRs into extracellular vesicles to modulate signaling. *Cell* **168**, 252-263 e214.
- Neugebauer, J. M., Amack, J. D., Peterson, A. G., Bisgrove, B. W. and Yost, H. J. (2009). FGF signalling during embryo development regulates cilia length in diverse epithelia. *Nature* **458**, 651-654.
- Nielsen, B. S., Malinda, R. R., Schmid, F. M., Pedersen, S. F., Christensen, S. T. and Pedersen, L. B. (2015). PDGFRbeta and oncogenic mutant PDGFRalpha D842V promote disassembly of primary cilia through a PLCgamma- and AURKA-dependent mechanism. *J. Cell Sci.* **128**, 3543-3549.
- Nishijima, Y., Hagiya, Y., Kubo, T., Takei, R., Katoh, Y. and Nakayama, K. (2017). RABL2 interacts with the intraflagellar transport-B complex and CEP19 and participates in ciliary assembly. *Mol. Biol. Cell* **28**, 1652-1666.
- Ott, C., Nachmias, D., Adar, S., Jarnik, M., Sherman, S., Birnbaum, R. Y., Lippincott-Schwartz, J. and Elia, N. (2018). VPS4 is a dynamic component of the centrosome that regulates centrosome localization of gamma-tubulin, centriolar satellite stability and ciliogenesis. *Sci. Rep.* **8**, 3353.
- Pablo, J. L., DeCaen, P. G. and Clapham, D. E. (2017). Progress in ciliary ion channel physiology. *J. Gen. Physiol.* **149**, 37-47.
- Pak, E. and Segal, R. A. (2016). Hedgehog signal transduction: key players, oncogenic drivers, and cancer therapy. *Dev. Cell* **38**, 333-344.
- Pan, J. and Snell, W. J. (2014). Organelle size: a cilium length signal regulates IFT cargo loading. *Curr. Biol.* **24**, R75-R78.
- Pan, J., Wang, Q. and Snell, W. J. (2004). An aurora kinase is essential for flagellar disassembly in *Chlamydomonas*. *Dev. Cell* **6**, 445-451.
- Phirke, P., Efimenko, E., Mohan, S., Burghoorn, J., Crona, F., Bakhoum, M. W., Trieb, M., Schuske, K., Jorgensen, E. M., Piasecki, B. P. et al. (2011). Transcriptional profiling of *C. elegans* DAF-19 uncovers a ciliary base-associated protein and a CDK/CCRK/LF2p-related kinase required for intraflagellar transport. *Dev. Biol.* **357**, 235-247.
- Phua, S. C., Chiba, S., Suzuki, M., Su, E., Roberson, E. C., Pusapati, G. V., Setou, M., Rohatgi, R., Reiter, J. F., Ikegami, K. et al. (2017). Dynamic remodeling of membrane composition drives cell cycle through primary cilia excision. *Cell* **168**, 264-279 e215.
- Piao, T., Luo, M., Wang, L., Guo, Y., Li, D., Li, P., Snell, W. J. and Pan, J. (2009). A microtubule depolymerizing kinesin functions during both flagellar disassembly and flagellar assembly in *Chlamydomonas*. *Proc. Natl. Acad. Sci. USA* **106**, 4713-4718.
- Pitaval, A., Senger, F., Letort, G., Gidrol, X., Guyon, L., Sillibourne, J. and Théry, M. (2017). Microtubule stabilization drives 3D centrosome migration to initiate primary ciliogenesis. *J. Cell Biol.* **216**, 3713-3728.
- Plotnikova, O. V., Nikonova, A. S., Loskutov, Y. V., Kozyulina, P. Y., Pugacheva, E. N. and Golemis, E. A. (2012). Calmodulin activation of Aurora-A kinase (AURKA) is required during ciliary disassembly and in mitosis. *Mol. Biol. Cell* **23**, 2658-2670.
- Plotnikova, O. V., Seo, S., Cottle, D. L., Conduit, S., Hakim, S., Dyson, J. M., Mitchell, C. A. and Smyth, I. M. (2015). INPP5E interacts with AURKA, linking phosphoinositide signaling to primary cilium stability. *J. Cell Sci.* **128**, 364-372.
- Pugacheva, E. N., Jablonski, S. A., Hartman, T. R., Henske, E. P. and Golemis, E. A. (2007). HEF1-dependent Aurora A activation induces disassembly of the primary cilium. *Cell* **129**, 1351-1363.

- Ran, J., Yang, Y., Li, D., Liu, M. and Zhou, J. (2015). Deacetylation of alpha-tubulin and cortactin is required for HDAC6 to trigger ciliary disassembly. *Sci. Rep.* **5**, 12917.
- Rasi, M. Q., Parker, J. D., Feldman, J. L., Marshall, W. F. and Quarumby, L. M. (2009). Katanin knockdown supports a role for microtubule severing in release of basal bodies before mitosis in *Chlamydomonas*. *Mol. Biol. Cell* **20**, 379-388.
- Reiter, J. F. and Leroux, M. R. (2017). Genes and molecular pathways underpinning ciliopathies. *Nat. Rev. Mol. Cell Biol.* **18**, 533-547.
- Saito, M., Otsu, W., Hsu, K. S., Chuang, J. Z., Yanagisawa, T., Shieh, V., Kaitsuka, T., Wei, F. Y., Tomizawa, K. and Sung, C. H. (2017). Tctex-1 controls ciliary resorption by regulating branched actin polymerization and endocytosis. *EMBO Rep.* **18**, 1460-1472.
- Sánchez, I. and Dynlacht, B. D. (2016). Cilium assembly and disassembly. *Nat. Cell Biol.* **18**, 711-717.
- Scheidel, N., Kennedy, J. and Blacque, O. E. (2018). Endosome maturation factors Rabenosyn-5/VPS45 and caveolin-1 regulate ciliary membrane and polycystin-2 homeostasis. *EMBO J.* **37**, e98248.
- Schmidt, K. N., Kuhns, S., Neuner, A., Hub, B., Zentgraf, H. and Pereira, G. (2012). Cep164 mediates vesicular docking to the mother centriole during early steps of ciliogenesis. *J. Cell Biol.* **199**, 1083-1101.
- Schraml, P., Frew, I. J., Thoma, C. R., Boysen, G., Struckmann, K., Krek, W. and Moch, H. (2009). Sporadic clear cell renal cell carcinoma but not the papillary type is characterized by severely reduced frequency of primary cilia. *Mod. Pathol.* **22**, 31-36.
- Seeley, E. S., Carriere, C., Goetze, T., Longnecker, D. S. and Korc, M. (2009). Pancreatic cancer and precursor pancreatic intraepithelial neoplasia lesions are devoid of primary cilia. *Cancer Res.* **69**, 422-430.
- Shah, A. S., Ben-Shahar, Y., Moninger, T. O., Kline, J. N. and Welsh, M. J. (2009). Motile cilia of human airway epithelia are chemosensory. *Science* **325**, 1131-1134.
- Sharma, N., Kosan, Z. A., Stallworth, J. E., Berbari, N. F. and Yoder, B. K. (2011). Soluble levels of cytosolic tubulin regulate ciliary length control. *Mol. Biol. Cell* **22**, 806-816.
- Singla, V., Romaguera-Ros, M., Garcia-Verdugo, J. M. and Reiter, J. F. (2010). *Odf1*, a human disease gene, regulates the length and distal structure of centrioles. *Dev. Cell* **18**, 410-424.
- Sorokin, S. (1962). Centrioles and the formation of rudimentary cilia by fibroblasts and smooth muscle cells. *J. Cell Biol.* **15**, 363-377.
- Spasic, M. and Jacobs, C. R. (2017). Primary cilia: cell and molecular mechanosensors directing whole tissue function. *Semin. Cell Dev. Biol.* **71**, 42-52.
- Spassky, N. and Meunier, A. (2017). The development and functions of multiciliated epithelia. *Nat. Rev. Mol. Cell Biol.* **18**, 423-436.
- Spektor, A., Tsang, W. Y., Khoo, D. and Dynlacht, B. D. (2007). Cep97 and CP110 suppress a cilia assembly program. *Cell* **130**, 678-690.
- Tanos, B. E., Yang, H.-J., Soni, R., Wang, W.-J., Macaluso, F. P., Asara, J. M. and Tsou, M.-F. B. (2013). Centriole distal appendages promote membrane docking, leading to cilia initiation. *Genes Dev.* **27**, 163-168.
- Thauvin-Robinet, C., Lee, J. S., Lopez, E., Herranz-Pérez, V., Shida, T., Franco, B., Jego, L., Ye, F., Pasquier, L., Loget, P. et al. (2014). The oral-facial-digital syndrome gene *C2CD3* encodes a positive regulator of centriole elongation. *Nat. Genet.* **46**, 905-911.
- Tsang, W. Y., Bossard, C., Khanna, H., Peränen, J., Swaroop, A., Malhotra, V. and Dynlacht, B. D. (2008). CP110 suppresses primary cilia formation through its interaction with CEP290, a protein deficient in human ciliary disease. *Dev. Cell* **15**, 187-197.
- Tucker, R. W., Pardee, A. B. and Fujiwara, K. (1979a). Centriole ciliation is related to quiescence and DNA synthesis in 3T3 cells. *Cell* **17**, 527-535.
- Tucker, R. W., Scher, C. D. and Stiles, C. D. (1979b). Centriole deciliation associated with the early response of 3T3 cells to growth factors but not to SV40. *Cell* **18**, 1065-1072.
- Van der Vaart, A., Rademakers, S. and Jansen, G. (2015). DLK-1/p38 MAP kinase signaling controls cilium length by regulating RAB-5 mediated endocytosis in *Caenorhabditis elegans*. *PLoS Genet.* **11**, e1005733.
- Veleri, S., Manjunath, S. H., Fariss, R. N., May-Simera, H., Brooks, M., Foskett, T. A., Gao, C., Longo, T. A., Liu, P., Nagashima, K. et al. (2014). Ciliopathy-associated gene *Cc2d2a* promotes assembly of subdistal appendages on the mother centriole during cilia biogenesis. *Nat. Commun.* **5**, 4207.
- Wang, G., Chen, Q., Zhang, X., Zhang, B., Zhuo, X., Liu, J., Jiang, Q. and Zhang, C. (2013a). PCM1 recruits Plk1 to the pericentriolar matrix to promote primary cilia disassembly before mitotic entry. *J. Cell Sci.* **126**, 1355-1365.
- Wang, L., Piao, T., Cao, M., Qin, T., Huang, L., Deng, H., Mao, T. and Pan, J. (2013b). Flagellar regeneration requires cytoplasmic microtubule depolymerization and kinesin-13. *J. Cell Sci.* **126**, 1531-1540.
- Wang, L., Lee, K., Malonis, R., Sanchez, I. and Dynlacht, B. D. (2016). Tethering of an E3 ligase by PCM1 regulates the abundance of centrosomal KIAA0586/Talpid3 and promotes ciliogenesis. *Elife* **5**, e12950.
- Wei, Q., Zhang, Y., Li, Y., Zhang, Q., Ling, K. and Hu, J. (2012). The BBSome controls IFT assembly and turnaround in cilia. *Nat. Cell Biol.* **14**, 950-957.
- Wei, Q., Xu, Q., Zhang, Y., Li, Y., Zhang, Q., Hu, Z., Harris, P. C., Torres, V. E., Ling, K. and Hu, J. (2013). Transition fibre protein FBF1 is required for the ciliary entry of assembled intraflagellar transport complexes. *Nat. Commun.* **4**, 2750.
- Westlake, C. J., Baye, L. M., Nachury, M. V., Wright, K. J., Ervin, K. E., Phu, L., Chalouni, C., Beck, J. S., Kirkpatrick, D. S., Slusarski, D. C. et al. (2011). Primary cilia membrane assembly is initiated by Rab11 and transport protein particle II (TRAPP II) complex-dependent trafficking of Rabin8 to the centrosome. *Proc. Natl. Acad. Sci. USA* **108**, 2759-2764.
- Wheatley, D. N., Wang, A. M. and Strugnell, G. E. (1996). Expression of primary cilia in mammalian cells. *Cell Biol. Int.* **20**, 73-81.
- Wheway, G., Nazlamova, L. and Hancock, J. T. (2018). Signaling through the primary cilium. *Front. Cell Dev. Biol.* **6**, 8.
- Wloga, D., Camba, A., Rogowski, K., Manning, G., Jerka-Dziadosz, M. and Gaertig, J. (2006). Members of the NIMA-related kinase family promote disassembly of cilia by multiple mechanisms. *Mol. Biol. Cell* **17**, 2799-2810.
- Wong, S. Y., Seol, A. D., So, P.-L., Ermilov, A. N., Bichakjian, C. K., Epstein, E. H., Jr., Dlugosz, A. A. and Reiter, J. F. (2009). Primary cilia can both mediate and suppress Hedgehog pathway-dependent tumorigenesis. *Nat. Med.* **15**, 1055-1061.
- Wren, K. N., Craft, J. M., Tritschler, D., Schauer, A., Patel, D. K., Smith, E. F., Porter, M. E., Kner, P. and Lechtreck, K. F. (2013). A differential cargo-loading model of ciliary length regulation by IFT. *Curr. Biol.* **23**, 2463-2471.
- Wu, C.-T., Chen, H.-Y. and Tang, T. K. (2018). Myosin-Va is required for preciliary vesicle transportation to the mother centriole during ciliogenesis. *Nat. Cell Biol.* **20**, 175-185.
- Xu, Q., Zhang, Y., Wei, Q., Huang, Y., Hu, J. and Ling, K. (2016). Phosphatidylinositol phosphate kinase PIPKgamma and phosphatase INPP5E coordinate initiation of ciliogenesis. *Nat. Commun.* **7**, 10777.
- Yadav, S. P., Sharma, N. K., Liu, C., Dong, L., Li, T. and Swaroop, A. (2016). Centrosomal protein CP110 controls maturation of the mother centriole during cilia biogenesis. *Development* **143**, 1491-1501.
- Yang, N., Leung, E. L.-H., Liu, C., Li, L., Eguether, T., Jun Yao, X.-J., Jones, E. C., Norris, D. A., Liu, A., Clark, R. A. et al. (2017). INTU is essential for oncogenic Hh signaling through regulating primary cilia formation in basal cell carcinoma. *Oncogene* **36**, 4997-5005.
- Yang, T. T., Chong, W. M., Wang, W.-J., Mazo, G., Tanos, B., Chen, Z., Tran, T. M. N., Chen, Y.-D., Weng, R. R., Huang, C.-E. et al. (2018). Super-resolution architecture of mammalian centriole distal appendages reveals distinct blade and matrix functional components. *Nat. Commun.* **9**, 2023.
- Yasar, B., Linton, K., Slater, C. and Byers, R. (2017). Primary cilia are increased in number and demonstrate structural abnormalities in human cancer. *J. Clin. Pathol.* **70**, 571-574.
- Ye, X., Zeng, H., Ning, G., Reiter, J. F. and Liu, A. (2014). *C2cd3* is critical for centriolar distal appendage assembly and ciliary vesicle docking in mammals. *Proc. Natl. Acad. Sci. USA* **111**, 2164-2169.
- Yeh, C., Li, A., Chuang, J.-Z., Saito, M., Cáceres, A. and Sung, C.-H. (2013). IGF-1 activates a cilium-localized noncanonical Gbetagamma signaling pathway that regulates cell-cycle progression. *Dev. Cell* **26**, 358-368.
- Yeyati, P. L., Schiller, R., Mali, G., Kasioulis, I., Kawamura, A., Adams, I. R., Playfoot, C., Gilbert, N., van Heyningen, V., Wills, J. et al. (2017). KDM3A coordinates actin dynamics with intraflagellar transport to regulate cilia stability. *J. Cell Biol.* **216**, 999-1013.
- Yuan, K., Frolova, N., Xie, Y., Wang, D., Cook, L., Kwon, Y.-J., Steg, A. D., Serra, R. and Frost, A. R. (2010). Primary cilia are decreased in breast cancer: analysis of a collection of human breast cancer cell lines and tissues. *J. Histochem. Cytochem.* **58**, 857-870.
- Zhao, X., Pak, E., Ornell, K. J., Pazyra-Murphy, M. F., MacKenzie, E. L., Chadwick, E. J., Ponomaryov, T., Kelleher, J. F. and Segal, R. A. (2017). A transposon screen identifies loss of primary cilia as a mechanism of resistance to SMO inhibitors. *Cancer Discov.* **7**, 1436-1449.
- Zou, C., Li, J., Bai, Y., Gunning, W. T., Wazer, D. E., Band, V. and Gao, Q. (2005). Centrobin: a novel daughter centriole-associated protein that is required for centriole duplication. *J. Cell Biol.* **171**, 437-445.

ARTICLE

DOI: 10.1038/s41467-018-06286-y

OPEN

A distal centriolar protein network controls organelle maturation and asymmetry

Lei Wang¹, Marion Failler¹, Wenxiang Fu^{1,2} & Brian D. Dynlacht¹

A long-standing mystery in the centrosome field pertains to the origin of asymmetry within the organelle. The removal of daughter centriole-specific/enriched proteins (DCPs) and acquisition of distal appendages on the future mother centriole are two important steps in the generation of asymmetry. We find that DCPs are recruited sequentially, and their removal is abolished in cells lacking *Talpid3* or *C2CD3*. We show that removal of certain DCPs constitutes another level of control for distal appendage (DA) assembly. Remarkably, we also find that *Talpid3* forms a distal centriolar multi-functional hub that coordinates the removal of specific DCPs, DA assembly, and recruitment of ciliary vesicles through distinct regions mutated in ciliopathies. Finally, we show that *Talpid3*, *C2CD3*, and *OFD1* differentially regulate the assembly of sub-distal appendages, the CEP350/FOP/CEP19 module, centriolar satellites, and actin networks. Our work extends the spatial and functional understanding of proteins that control organelle maturation and asymmetry, ciliogenesis, and human disease.

¹Department of Pathology, New York University Cancer Institute, New York University School of Medicine, New York, NY 10016, USA. ²Present address: Biozentrum, University of Basel, 4056 Basel, Switzerland. Correspondence and requests for materials should be addressed to B.D.D. (email: brian.dynlacht@nyumc.org)

The centrosome is an asymmetric organelle comprised of a daughter centriole, a mother centriole, pericentriolar material, and pericentriolar satellites. The older, mother centriole is distinguished by distal appendages (DA) and sub-distal appendages (SDA), whereas the younger centriole is characterized by daughter centriole-specific/enriched proteins (DCPs). DCPs, including CEP120, Centrobins, and Neurl4, are recruited to nascent daughter centrioles after centriole duplication is initiated to regulate centriole elongation and homeostasis, and they are subsequently removed at the G1/S transition in the next cell cycle during mother centriole maturation^{1–6}. Subsequently, SDA and DA are assembled at the maturing mother centriole during the G2 phase and the G2/M transition, respectively. DA, assembled through the sequential recruitment of CEP83, CEP89, SCLT1, CEP164, and FBF1 proteins, are involved in vesicle docking and intraflagellar transport (IFT) during ciliogenesis and in immune synapse formation^{7–13}. SDA, composed of ODF2, Centriolin, CEP128, CEP170, and other proteins, are required for microtubule anchoring and cilium positioning^{14–18}. Mutations in genes linked to mother centriole maturation are associated with a plethora of human diseases, termed ciliopathies, including Joubert syndrome (JBTS), Jeune asphyxiating thoracic dystrophy, Bardet–Biedl syndrome, and oral–facial–digital (OFD) syndrome, among others^{19–23}.

Despite the above observations, the regulatory mechanisms linking the recruitment of SDA and DA and other distal-end proteins to mother centriole maturation are largely unknown. To our knowledge, only three proteins (C2CD3, OFD1, and ODF2) have been linked to mother centriole maturation. Intriguingly, however, C2CD3 and OFD1 localize on centriolar satellites (CS) and the distal ends of both mother and daughter centrioles, where they play antagonistic roles in centriole elongation. C2CD3 is involved in DA, and perhaps SDA, assembly^{24,25}, whereas its interacting partner, OFD1, appears to be required for DA assembly only²⁶. ODF2, a SDA component, initiates appendage assembly through direct interactions with other SDA proteins, but its role in DA assembly, if any, remains to be clarified^{14,16}. Further, although the constellation of DA and SDA proteins have been identified and localized with ever-increasing precision, the relationship between the assembly of these structures, removal of DCPs, and mother centriole maturation—the basis of asymmetry within the organelle—remains largely uncharacterized. To this end, it is attractive to speculate that mother and daughter centriole components display antagonistic relationships to suppress or promote their respective identities.

Talpid3 is an evolutionarily conserved gene essential for vertebrate development and ciliogenesis^{27–29}. Recently, several groups independently identified mutations in *Talpid3* as a cause of JBTS and lethal ciliopathies, such as hydrocephalus and short-rib polydactyly syndrome^{30–35}. Our previous studies showed that *Talpid3* localizes at the distal ends of both centrioles and regulates vesicle docking during ciliogenesis^{36,37}. Although *Talpid3* localizes to both centrioles, foregoing studies suggested that *Talpid3* could play an important role in mother centriole maturation. In this study, in an effort to begin understanding the molecular basis of centriole asymmetry and maturation, we identify *Talpid3* and C2CD3 as regulators of DCP removal. We find that the removal of DCPs is not required for centriole duplication, but it plays an essential role in centriole maturation. Remarkably, we show that *Talpid3* regulates centriole maturation and ciliary vesicle docking through distinct regions. Furthermore, we show that removal of certain DCPs acts as an additional layer of DA assembly control, via regulation of OFD1 recruitment. Importantly, although the location and function of *Talpid3*, C2CD3, and OFD1 are coordinated and, in some cases, interdependent, we found that each protein exhibits distinct roles in regulating the actin network, CS

organization, removal of DCPs, and assembly of appendages. Lastly, our data suggest potential mechanisms to explain how *Talpid3* mutations found in JBTS contribute to disease phenotypes.

Results

***Talpid3* regulates early and late centriole maturation events through distinct regions.** To gain further insight into the role of *Talpid3* in ciliogenesis, we used CRISPR/Cas9-mediated gene editing to generate a *Talpid3*^{−/−} retinal pigment epithelial (RPE1) cell line³⁷ and systematically observed the localization of DCPs, as well as markers of mother centriole/basal body maturation and ciliation, by immunofluorescence (IF). First, we found that *Talpid3* KO cells recapitulated the defects caused by depletion or loss of *Talpid3* using RNAi and genetic knock-outs^{27–29,36}, including the failure to dock ciliary vesicles and assemble primary cilia after serum withdrawal (Fig. 1a). Consistent with previous studies^{34,36}, we also observed elongated centrioles in *Talpid3*^{−/−} cells using electron microscopy (EM; Fig. 1b). Moreover, we found that DA proteins (CEP83, CEP89, CEP164, and FBF1) were not observed at centrosomes in *Talpid3* knock-out cells (Fig. 1a). Consistent with the role of DA in multiple processes, we found that IFT protein (IFT88 and IFT140) localization, TTBK2 recruitment, and CP110 removal were abrogated in *Talpid3*^{−/−} cells. In each case, we showed that these results could not be explained by altered protein levels (Fig. 1c), leading us to conclude that recruitment per se was impacted. We note that CP110 and CEP164 recruitment persisted in prior *Talpid3* knock-down experiments³⁶. Since residual *Talpid3* persists in siRNA-treated cells, our data suggest that recruitment of DA proteins is very sensitive to *Talpid3* dosage and that recruitment of these proteins fails completely in the absence of *Talpid3*. On the other hand, we observed that assembly of SDA was intact in knock-out cells, similar to siRNA-depleted cells. Examination of *Talpid3*^{−/−} cells by EM after serum withdrawal confirmed the absence of DA, ciliary vesicle docking, and ciliation, while confirming that normal SDA were assembled (Fig. 1b).

Remarkably, we also observed abnormal localization of DCPs (CEP120, Centrobins, and Neurl4) in *Talpid3* KO cells: rather than exhibiting asymmetric enrichment on daughter centrioles, DCPs were found on both mothers and daughters (Fig. 1a). Asymmetric localization of DCPs is maintained by removal of DCPs from daughter centrioles during the G1–S transition, when centriole duplication is initiated^{5,6}. However, DCP removal was completely blocked in *Talpid3*^{−/−} cells (Supplementary Fig. 1a). Since centriole duplication is grossly normal in *Talpid3*^{−/−} cells (Supplementary Fig. 1a), these data also suggest that removal of DCPs is not required for centriole duplication, but it might be involved in other processes. We showed that each of these phenotypes could be rescued by reintroducing full-length *Talpid3* into *Talpid3*^{−/−} cells, confirming that the observed defects were provoked specifically by the loss of *Talpid3* (Fig. 2a). To identify regions in *Talpid3* required for each stage of maturation and ciliogenesis, we performed rescue experiments in *Talpid3*^{−/−} cells with a series of *Talpid3* truncations. Strikingly, our data suggest that a region encompassing amino acids 466–700 is required for asymmetric localization of DCPs (Neurl4, Centrobins, and CEP120; Fig. 2a and Supplementary Fig. 1b), DA assembly (CEP83), and IFT complex recruitment (IFT88; Fig. 2b). We further confirmed the rescue of DA assembly by examining CEP164 rings using 3D-structured illumination microscopy (SIM, Supplementary Fig. 1c). In contrast, visualization of Rab8a and SmoM2, two early ciliary vesicle markers, or CP110 indicated that residues 701–1533 are essential for vesicle docking, CP110 removal, and ciliogenesis (GT335) (Fig. 2a, b). Importantly, these

data also (1) indicate that assembly of DA is sufficient for recruitment of the IFT machinery but not for initiation of vesicle docking or subsequent events during ciliogenesis and (2) pinpoint

a requirement for separable regions of Talpid3 in the maturation of mother centrioles/basal bodies versus the coordinated docking of vesicles and CP110 removal. In other words, a single protein,

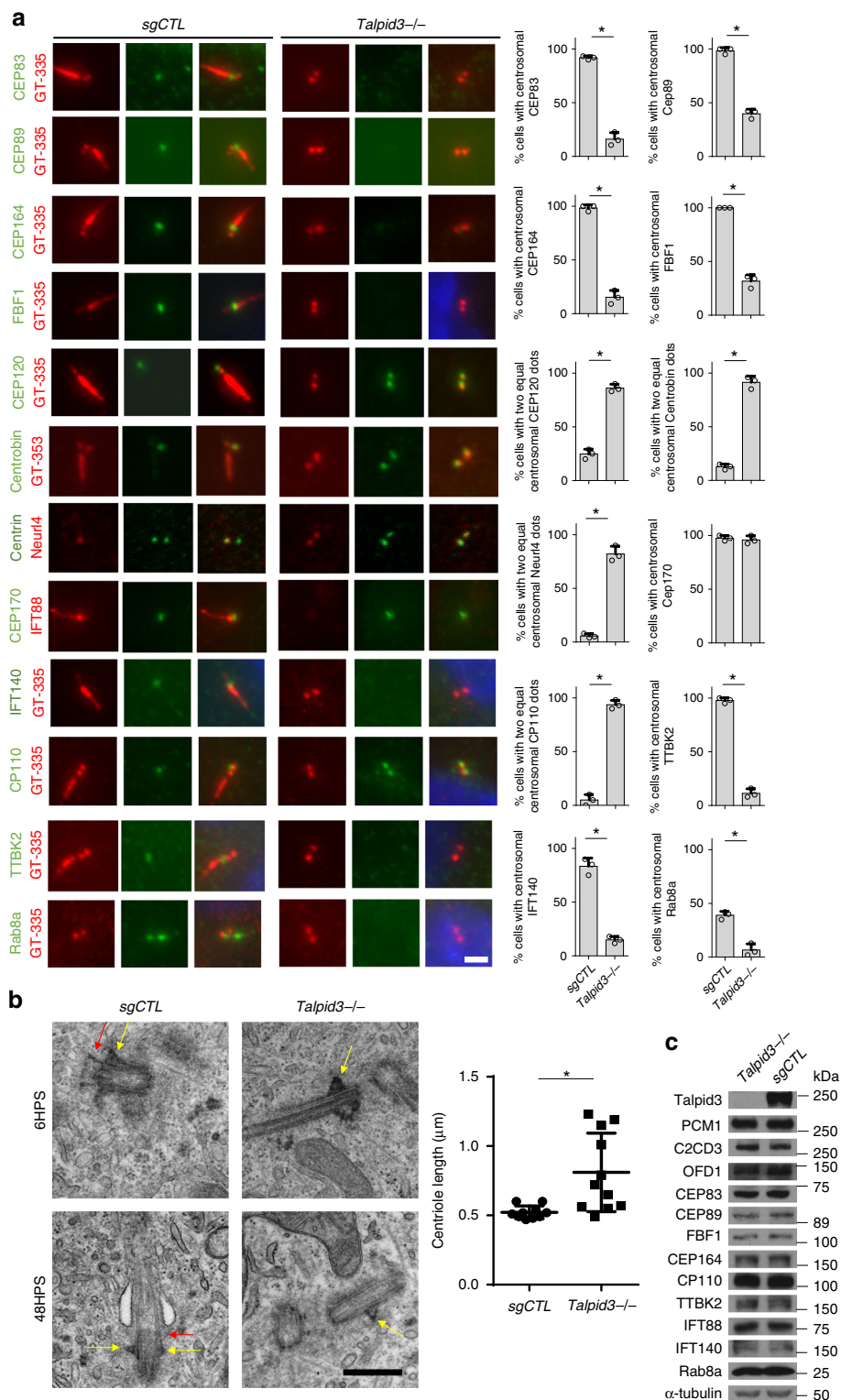


Fig. 1 Talpid3 regulates centriole maturation and vesicle docking. **a** Centrosomal proteins and vesicular proteins were examined in control and *Talpid3*^{-/-} cells by IF after 6 (Rab8a) or 48 h (all markers except for Rab8a) of serum-starvation using indicated antibodies. Scale bar = 2 μm. The protein level of these markers was examined by western blot (WB) in **c**. Cumulative data from three independent experiments are shown. For each group, a minimum of 100 cells/experiment was averaged. **b** Centrosome and primary cilium structure in control and *Talpid3*^{-/-} cells was examined by transmission electron microscopy (TEM) after 6 and 48 h of serum-starvation (HPS). Red arrows indicate DA/transitional fibers. Yellow arrows indicate SDA. Data from one experiment are shown (N = 10 for *sgCTL* and N = 11 for *Talpid3*^{-/-}). All data are presented as mean ± SD. *p < 0.05 (unpaired t-test). Scale bar = 0.5 μm

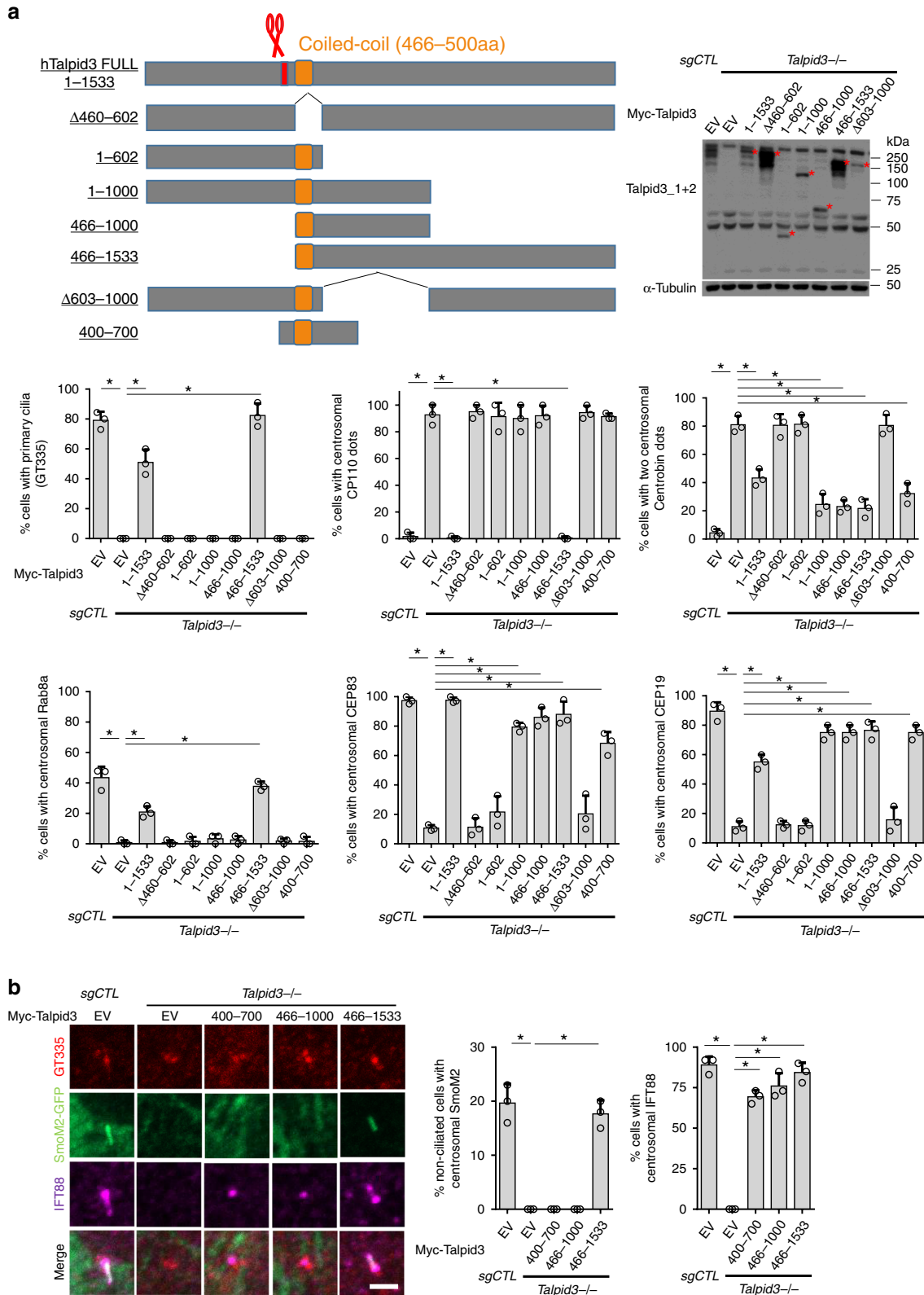


Fig. 2 Talpid3 regulates centriole maturation and vesicle docking through distinct regions. **a** Centrosomal and ciliary defects of *Talpid3*^{-/-} cells were rescued by infection with lentiviruses expressing different Myc-tagged Talpid3 constructs. Cells were serum-starved for 48 h and examined by IF with antibodies against indicated antibodies. Coiled-coil domain and CRISPR-targeted region of *Talpid3*^{-/-} cells are shown in orange and red (scissors), respectively. Specific truncation proteins are indicated with an asterisk. The fragment spanning residues 400-700 is not recognized by Talpid3 antibodies and thus was detected by Myc tag, shown in Supplementary Figure 1b. **b** Stable *Talpid3*^{-/-} cell lines expressing Talpid3 truncations were transduced with lentiviruses expressing SmoM2-GFP. Two days after transduction, cells were serum-starved for 6 h and stained with indicated antibodies. Cumulative data from three independent experiments are shown. For each group, a minimum of 100 cells/experiment was averaged. All data are presented as mean ± SD. **p* < 0.05 (unpaired t-test). Scale bar = 2 μm

Talpid3, coordinates three activities essential for ciliogenesis: removal of DCP, assembly of DA/maturation of basal bodies, and recruitment of ciliary vesicles.

Removal of specific DCPs is a prerequisite for DA assembly.

We were particularly intrigued by the centriole maturation defects observed in *Talpid3*^{-/-} cells for two reasons. First, DA assembly is thought to be the earliest obligatory step for the initiation of ciliogenesis³⁸, and the major defects observed in *Talpid3*^{-/-} cells, including the failure to dock vesicles, TTBK2 recruitment, CP110 removal, and IFT transport could be attributed to the DA assembly defect in *Talpid3* null cells. Secondly, little is known about the regulatory mechanisms underpinning the asymmetric localization of DCPs. We speculated that during the maturation of daughter centrioles, removal of DCPs at the G1/S transition could be a prerequisite for the acquisition of appendages occurring later in the G2 phase. To test this hypothesis, DCPs were forced to symmetrically localize on both centrioles in wild-type RPE1 cells by expressing fusion proteins containing the PACT domain³⁹. We found that PACT-CEP120 and PACT-Centrobilin, but not PACT-Neurl4, were able to disrupt the localization of DA proteins, CEP83 and CEP164 (Fig. 3a and Supplementary Fig. 2a). These results suggest that the persistence of specific daughter centriole proteins is sufficient to suppress DA assembly.

Conversely, to further examine whether the failure to remove CEP120 and Centrobilin inhibits DA assembly, we knocked down Centrobilin in *Talpid3*^{-/-} cells using siRNAs. Strikingly, we found that depletion of Centrobilin was able to substantially rescue the assembly of DA (Fig. 3b and Supplementary Figs. 2a, b). The rescue of DA assembly was further confirmed by measuring the diameter of CEP164 rings using SIM (Supplementary Fig. 2c). We note that rescue of DA assembly was unable to restore ciliogenesis in *Talpid3* KO cells, consistent with an additional role(s) of *Talpid3* in ciliogenesis beyond DCP removal and DA assembly. We also silenced CEP120, but knocking down this protein blocked centriole duplication and resulted in cells with one centriole or no centrioles (Supplementary Fig. 2b and Fig. 3d), as expected⁵, preventing us from confirming its role in inhibiting DA assembly. We next asked whether there was a reciprocal relationship between DA assembly and DCP appearance. However, disruption of DA assembly through depletion of CEP83 had no effect on the asymmetric localization of DCPs in wild type RPE1 cells (Fig. 3c). We found that DCPs were recruited in a sequential manner, with CEP120 localization required for recruitment of Centrobilin, and recruitment of Neurl4 dependent upon both CEP120 and Centrobilin, suggesting that removal of DCPs could also occur sequentially. Moreover, we found that Centrobilin is required for maintenance of CEP120 asymmetry, since depletion of Centrobilin led to symmetric localization of CEP120 on both centrioles (Fig. 3d). These data reveal a robust network underlying the daughter-to-mother centriole transition, wherein the removal of DCPs, Centrobilin, and perhaps CEP120, is a prerequisite for DA assembly but not vice versa.

Talpid3 and C2CD3 coordinately regulate mother centriole maturation. Next, we investigated how *Talpid3* regulates the asymmetric localization of DCPs, and we considered several possibilities. First, since DCPs were recruited in a sequential manner, *Talpid3* could regulate CEP120 localization through direct interactions with CEP120, as suggested previously⁴⁰. We tested the interaction between different *Talpid3* truncations and CEP120 and found that CEP120 interacted most robustly with a fragment spanning residues 466–1000, although this protein

interacted with multiple surfaces of *Talpid3* (Supplementary Fig. 3). We found that the localization of *Talpid3* to centrioles was important for this interaction, since a mutant protein from a JBTS patient (C.1697A>T) that failed to localize to centrosomes (see below) exhibited significantly impaired interactions with CEP120. Importantly, since the 1–602 fragment of *Talpid3* was able to interact with CEP120 without rescuing the centriole maturation defects observed in *Talpid3*^{-/-} cells, we conclude that *Talpid3*–CEP120 interactions are not sufficient to regulate asymmetric localization of DCPs. Secondly, since CS disorganization is observed in *Talpid3*^{-/-} cells, and *Talpid3* was shown to be required for vesicle docking³⁶, it was possible that *Talpid3* could regulate centriole maturation through CS. To test this possibility, we utilized the *PCMI*^{-/-} RPE1 cell line³⁷, which lacks CS. We found that the asymmetric localization of DCPs and DA assembly were normal in *PCMI* KO cells, demonstrating that the formation of CS is not required for these two events (Fig. 4a).

We speculated that *Talpid3* could also regulate the asymmetric localization of DCPs through other distal centriolar proteins. C2CD3 and OFD1 have been shown to regulate DA assembly, although their mechanisms remain obscure, and thus we investigated these candidates as regulators of asymmetric localization of daughter centriole proteins. We generated *C2CD3*^{-/-} and *OFD1*^{-/-} cell lines using CRISPR/Cas9 and found that, consistent with previous reports^{24–26}, both proteins were required for DA assembly, and these defects could be rescued with full-length C2CD3 and OFD1, respectively (Fig. 4a, Supplementary Fig. 4a). Interestingly, *C2CD3*^{-/-}, but not *OFD1*^{-/-} cells, displayed symmetric localization of CEP120 and Centrobilin (Fig. 4a, b), but this was not due to increased protein levels (Supplementary Fig. 4b). Strikingly, depletion of Centrobilin could partially rescue the localization of DA proteins in *C2CD3*^{-/-}, but not in *OFD1*^{-/-} cells (Fig. 4b). These data not only confirmed our previous conclusion that removal of certain DCPs is a prerequisite for DA assembly, but they also suggested that C2CD3 and *Talpid3* control asymmetric localization of DCPs, whereas OFD1 may be required primarily for DA assembly. Since maturation occurs during the G2/M phase, it was possible that the defects in maturation could result from cell cycle arrest prior to this stage. However, we confirmed that the centriole maturation defects found in *Talpid3*^{-/-}, *C2CD3*^{-/-}, and *OFD1*^{-/-} cells did not arise from aberrant cell cycle progression or the altered abundance of daughter centriole proteins (Supplementary Fig. 4b).

We next explored the functional interactions between *Talpid3*, C2CD3, and OFD1 in greater detail. First, to determine whether recruitment of these proteins occurred sequentially, we examined their localization in all three KO cell lines. We found that *Talpid3* and C2CD3 were coordinately recruited to mother and daughter centrioles, and both were also required to recruit OFD1 (Fig. 4c). In contrast, OFD1 was not required to recruit either *Talpid3* or C2CD3. Further, we found that *Talpid3* could interact most robustly with C2CD3 through residues 466–1533, whereas amino-terminal portions of *Talpid3* were unable to do so (Fig. 4d). Taken together with previous data suggesting a functional interaction between C2CD3 and OFD1, we conclude that *Talpid3*, C2CD3, and OFD1 form a complex at the distal ends of centrioles.

To extend our understanding of the critical role of C2CD3 and OFD1 recruitment by *Talpid3*, we examined the ability of *Talpid3*–C2CD3 and *Talpid3*–OFD1 fusion proteins to functionally reconstitute each step of the maturation process in *Talpid3*^{-/-} cells. We fused the *Talpid3* amino-terminal 1–602 aa fragment (*Talpid3*Nter), which is required for centrosome localization but is not sufficient for centriole maturation³⁶ (Fig. 2a), with C2CD3 or OFD1, thereby tethering each protein to centrioles in *Talpid3* KO cells. We observed that tethering of

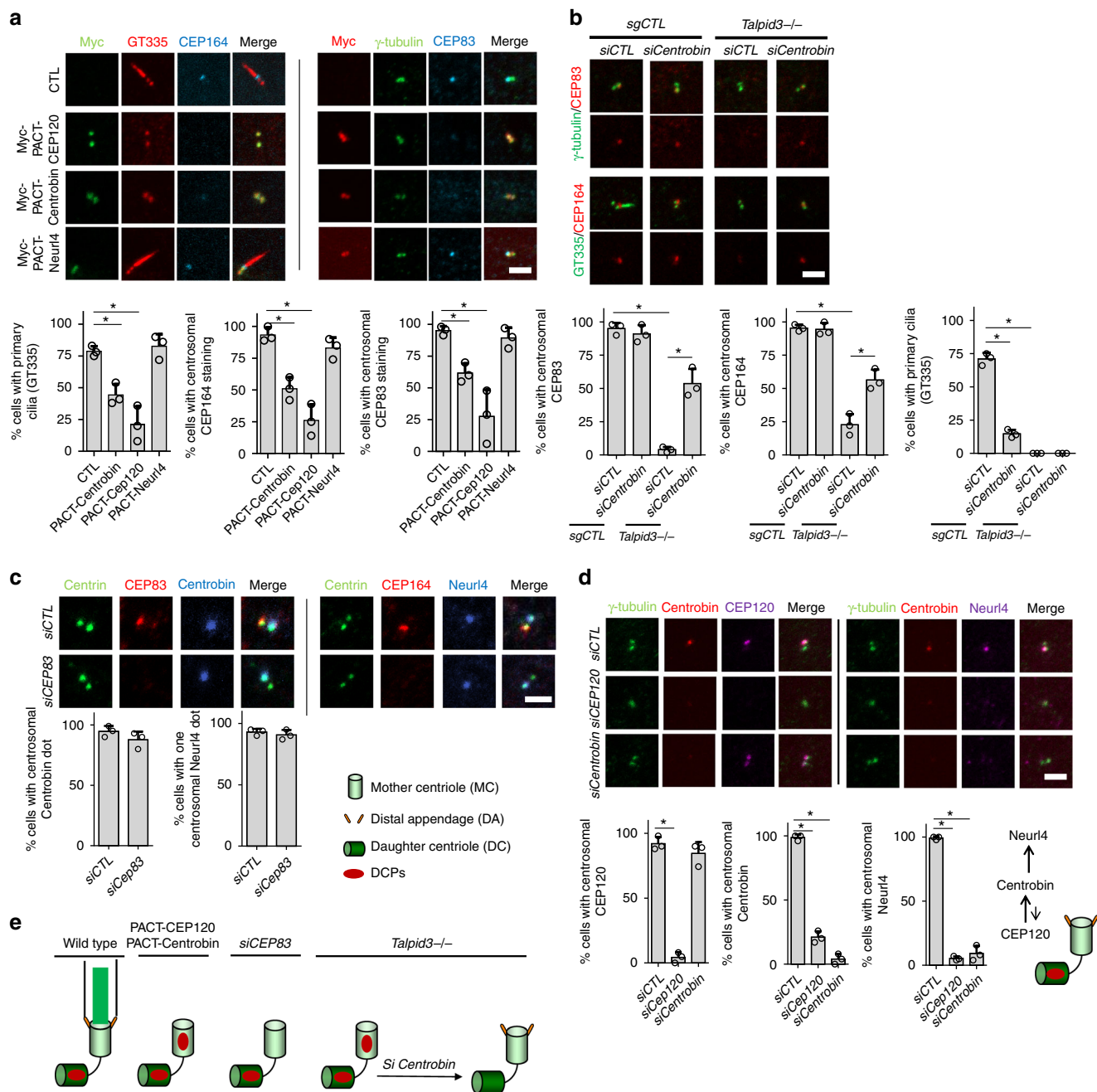


Fig. 3 Removal of specific DCPs is a prerequisite for DA assembly. **a** WT RPE1 cells were transfected with lentiviruses expressing Myc-PACT-CEP120, Myc-PACT-Centrobins, or Myc-PACT-Neur14, as indicated. Two days after transduction, cells were serum-starved for 48 h and examined by IF with antibodies against DA markers, CEP83 and CEP164. **b** Control and *Talpid3*^{-/-} cells were transfected with siRNAs against CEP120 (Supplementary Figures 2a, b) and Centrobins. Two days after transfection, cells were serum-starved for 24 h and examined by IF and WB using indicated antibodies. **c** WT RPE1 cells were transfected with siRNAs against CEP83. Two days after transfection, cells were serum-starved for 24 h and were visualized with indicated antibodies to check DA and DCPs. **d** WT RPE1 cells were transfected with siRNAs against CEP120 and Centrobins. Two days after transfection, cells were serum-starved for 24 h and then visualized with indicated antibodies to check the localization of DCPs, which are recruited as schematized (right). **e** Schematic of the relationship between removal of DCPs and DA assembly. Cumulative data from three independent experiments are shown. For each group, a minimum of 100 cells/experiment was averaged. All data are presented as mean \pm SD. **p* < 0.05 (unpaired *t*-test). Scale bars = 2 μ m

C2CD3 could substantially rescue defective recruitment of DA proteins in *Talpid3* KO cells (Fig. 4e). Tethering of OFD1 could also partially rescue the recruitment of DA proteins, although its impact was considerably less robust than that of C2CD3. These data suggest that centriolar recruitment of C2CD3 by *Talpid3* plays an important role in the regulation of asymmetric localization of DCPs, proper OFD1 localization, and subsequent DA assembly. Indeed, our data suggest that a key role for *Talpid3*

is the targeting and recruitment of other proteins, C2CD3 and OFD1, to the distal end and that such recruitment can largely bypass the loss of *Talpid3*.

Asymmetric localization of DC-enriched proteins is required for proper localization of OFD1. Given that abnormal, symmetric localization of DCPs is accompanied by the absence of

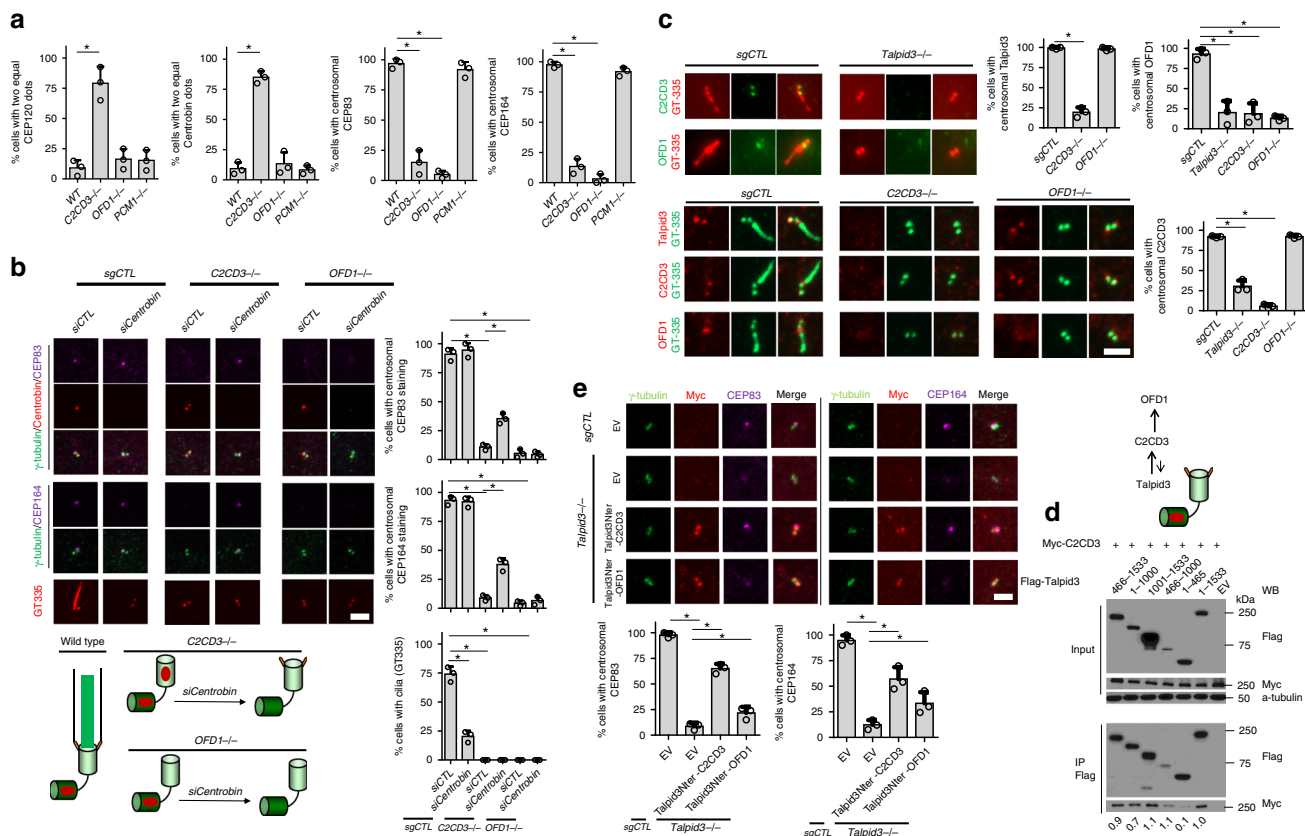


Fig. 4 Talpid3 and C2CD3 coordinately regulate mother centriole maturation. **a** Localization of DCPs and DA proteins were checked in control, *C2CD3*^{-/-}, *OFD1*^{-/-}, and *PCMI*^{-/-} cells. Cells were serum-starved for 24 h and then visualized with indicated antibodies. **b** Control, *C2CD3*^{-/-}, and *OFD1*^{-/-} cells were transfected with siRNAs against CEP83. Two days after transfection, cells were serum-starved for 24 h and were visualized with indicated antibodies to examine DA and DCPs. **c** Localization of Talpid3, C2CD3, and OFD1 was checked in control, *C2CD3*^{-/-}, *OFD1*^{-/-}, and *Talpid3*^{-/-} cells. Cells were serum-starved for 24 h and then visualized with indicated antibodies. **d** 293T cells stably expressing N-terminally Myc-tagged C2CD3 and N-terminally Flag-tagged Talpid3 were immunoprecipitated with anti-Flag antibody. Eluates were analyzed by immunoblotting with indicated antibodies. Numbers at the bottom of each lane represent the quantification of band intensities of immunoprecipitated Flag-CEP120, which was first normalized to the lane containing the full-length Talpid3 protein (1-1533) and then normalized to the intensities of each corresponding, co-immunoprecipitated Myc-Talpid3 truncation. **e** DA assembly in *Talpid3*^{-/-} cells was substantially or partially rescued by infection with lentiviruses expressing an amino-terminal fragment of Talpid3 (residues 1-602) fused to C2CD3 or OFD1. Cells were examined by IF after 48 h of serum starvation using the indicated antibodies. Cumulative data from three independent experiments are shown. For each group, a minimum of 100 cells/experiment was averaged. All data are presented as mean ± SD. **p* < 0.05 (unpaired *t*-test). Scale bars = 2 μm

OFD1 from centrioles in Talpid3 and C2CD3 KO cells (Figs. 1a and 4a, c), we hypothesized that the failure to remove DCPs during centriole maturation could prevent centrosomal localization of OFD1 and thus assembly of DA. To test our hypothesis, DCPs were again forced to symmetrically localize on both centrioles by expressing PACT domain fusions in wild-type RPE1 cells. We found that PACT-CEP120 and PACT-Centrobins, but not PACT-Neurl4, were able to disrupt the localization of OFD1 (Fig. 5a). To further examine whether failure to remove Centrobins plays an inhibitory role in OFD1 recruitment, we knocked down Centrobins in *Talpid3*^{-/-} and *C2CD3*^{-/-} cells with siRNAs and found that the localization of OFD1 was largely rescued (Fig. 5b). The rescue of centrosomal OFD1 was further confirmed by measuring the diameter of OFD1 rings using SIM (Supplementary Fig. 2c). Since tethering of C2CD3 to centrioles in *Talpid3*^{-/-} cells using an amino-terminal fusion could rescue the recruitment of DA proteins (Fig. 4e), we anticipated that the recruitment of OFD1 would also be rescued in these cells, and this was indeed the case (Fig. 5c). In total, these data demonstrate that the failure to remove DCPs blocks centrosomal OFD1 recruitment and thus abrogates DA assembly.

In addition to their centriolar localization, C2CD3 and OFD1 also partition to CS, and this could potentially contribute to centriole maturation. To address whether the CS pool of C2CD3 and OFD1 plays a role in centriole maturation, we first examined the CS localization of C2CD3 and OFD1 in *PCMI*^{-/-} cells using Myc-tagged C2CD3 and an anti-OFD1 antibody (OFD1-2) that are able to detect CS pools of C2CD3 and OFD1, respectively. Compared with control cells, the CS pools of C2CD3 and OFD1 were depleted in *PCMI*^{-/-} cells (Fig. 4a), and only centrosomal C2CD3 and OFD1 remained (Supplementary Fig. 5a). Since centriole maturation is normal in *PCMI*^{-/-} cells, these data suggest that the CS pools of C2CD3 and OFD1 are not required for centriole maturation. Moreover, we found that PACT-CEP120, PACT-Centrobins, and PACT-Neurl4 do not affect the CS pool of OFD1 (Supplementary Fig. 5b). Together, these data demonstrate that centriole-bound Talpid3 and C2CD3 regulate the removal of DCPs, which, in turn, controls the centrosomal recruitment of OFD1 and DA assembly (Fig. 5d).

Spatial coordination of Talpid3/C2CD3/OFD1 complex with DC protein asymmetry and DA assembly. To better understand the spatial basis for regulation of asymmetric localization of DC

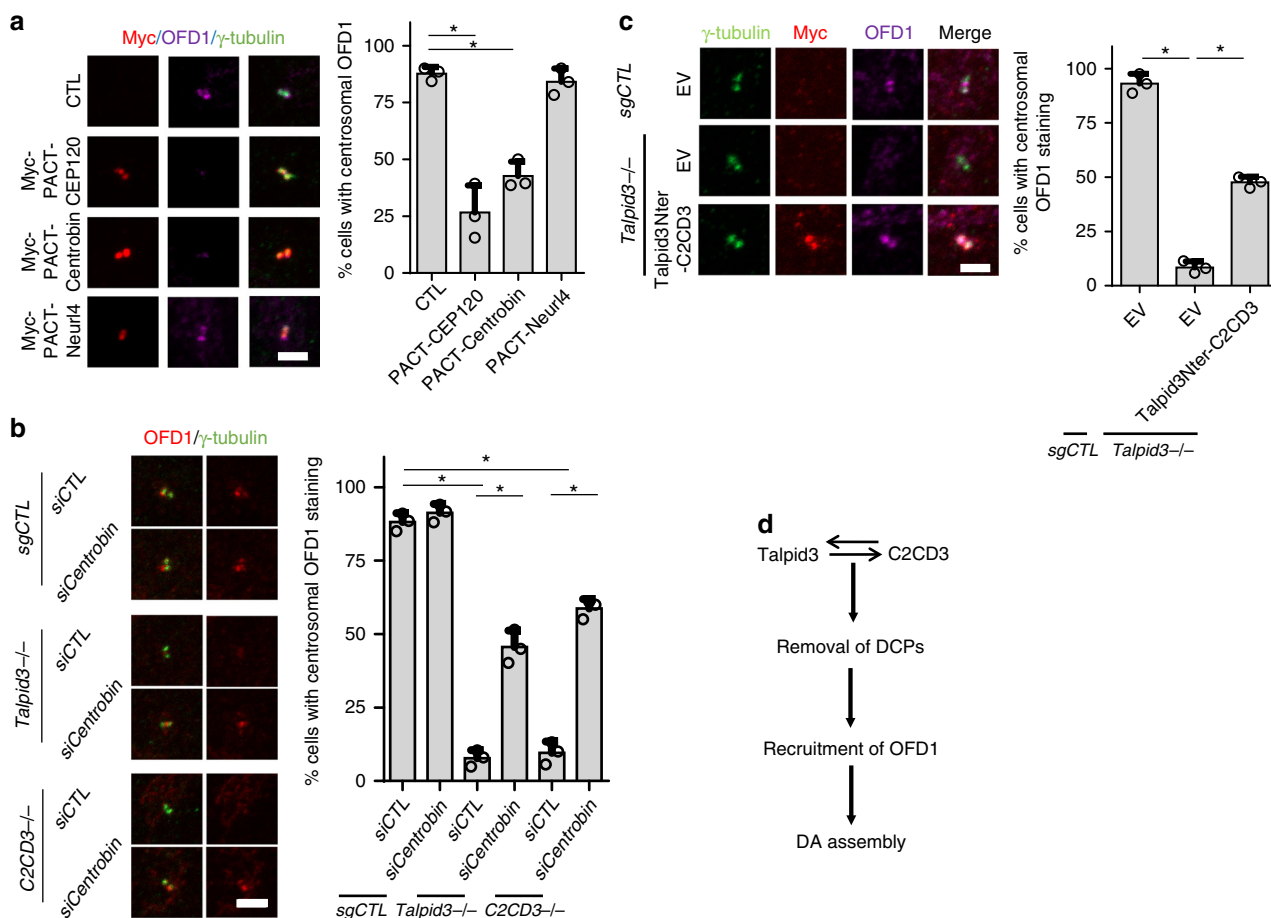


Fig. 5 Asymmetric localization of DC-enriched proteins is required for proper localization of OFD1. **a** WT RPE1 cells were transduced with lentiviruses expressing Myc-PACT-CEP120, Myc-PACT-Centrobins, or Myc-PACT-Neur14, as indicated. Two days after transduction, cells were serum-starved for 48 h and examined by IF with indicated antibodies. **b** Control, *C2CD3*^{-/-}, and *Talpid3*^{-/-} cells were transfected with siRNAs against Centrobins. Two days after transfection, cells were serum-starved for 24 h and were visualized with indicated antibodies. **c** OFD1 recruitment defect in *Talpid3*^{-/-} cells was rescued by infection with lentiviruses expressing the Talpid3-C2CD3 fusion protein described in Fig. 3e. Cells were examined by IF after 48 h of serum starvation using indicated antibodies. **d** Model indicating a centriole maturation regulatory mechanism. Cumulative data from three independent experiments are shown. For each group, a minimum of 100 cells/experiment was averaged. All data are presented as mean \pm SD. **p* < 0.05 (unpaired *t*-test). Scale bars = 2 μ m

proteins instigated by Talpid3 and C2CD3, we investigated the compartmentalization of distal end proteins and DCPs (Talpid3, C2CD3, CEP120, and Centrobins) using SIM (Fig. 6a). We observed that C2CD3 localized to a small dot at the extreme distal end of both centrioles, enveloped by a Talpid3 ring. Centrobins formed a ring in a middle segment of the daughter centriole, adjacent to the Talpid3 ring and distal to the proximal marker, GT335. Consistent with a previous report¹, CEP120 was distributed along the length of the DC centriole barrel, and it co-localized with Talpid3 at the distal end, in line with data indicating that these proteins interact (Fig. 6a and Supplementary Fig. 3). Our data demonstrate that a complex consisting of Talpid3 and C2CD3 at the distal end of centrioles partially co-localizes with CEP120 and is adjacent to the Centrobins ring, prompting speculation that the asymmetric localization of DC-enriched proteins could be controlled at the distal end of centrioles. OFD1 also displayed different localization patterns on the mother (MC) and daughter (DC) centrioles (Fig. 6a). On the DC, OFD1 formed a ring at the distal end that co-localized with the Talpid3 ring. On the MC, OFD1 formed a much larger ring at the distal end that co-localized with, and had the same diameter as, the CEP164 ring. These data suggest that OFD1 may be peripherally associated with DA structure and could play a more direct

role in DA assembly. We also examined the localization of CEP120 and Centrobins using SIM to determine how these DCPs partitioned in *Talpid3*^{-/-}, *C2CD3*^{-/-}, and *PCMI*^{-/-} cells. Using CP110 and GT335 as centriolar distal and proximal markers, respectively, we observed that CEP120 and Centrobins staining appeared identical along the barrels of both centrioles, from the proximal to distal ends, in *Talpid3*^{-/-} and *C2CD3*^{-/-} cells (Fig. 6b). In contrast, Cep120 and Centrobins partitioned preferentially to DC in control and *PCMI*^{-/-} cells. These data unequivocally demonstrate that removal of DCPs was completely blocked in *Talpid3*^{-/-} and *C2CD3*^{-/-} cells, resulting in a symmetrical distribution of DCPs on both centrioles. Interestingly, we found that PACT-domain fusions with DCPs localized along the barrels of both centrioles, mimicking the localization of CEP120 and Centrobins in *Talpid3*^{-/-} and *C2CD3*^{-/-} cells (Fig. 6b and Supplementary Fig. 5c). Specifically, the diameters of PACT-CEP120 (384 \pm 34 nm) and PACT-Centrobins (395 \pm 26 nm) rings are comparable to those of endogenous CEP120 (378 \pm 29 nm) and Centrobins (356 \pm 33 nm) proteins, which are consistent with previous reports showing that CEP120 and Centrobins localize close to the outer centriole wall^{5,6,41}. These data suggest that the “default” state for localization of DCPs could be on or near the barrels of both centrioles, but Talpid3 and C2CD3 act to

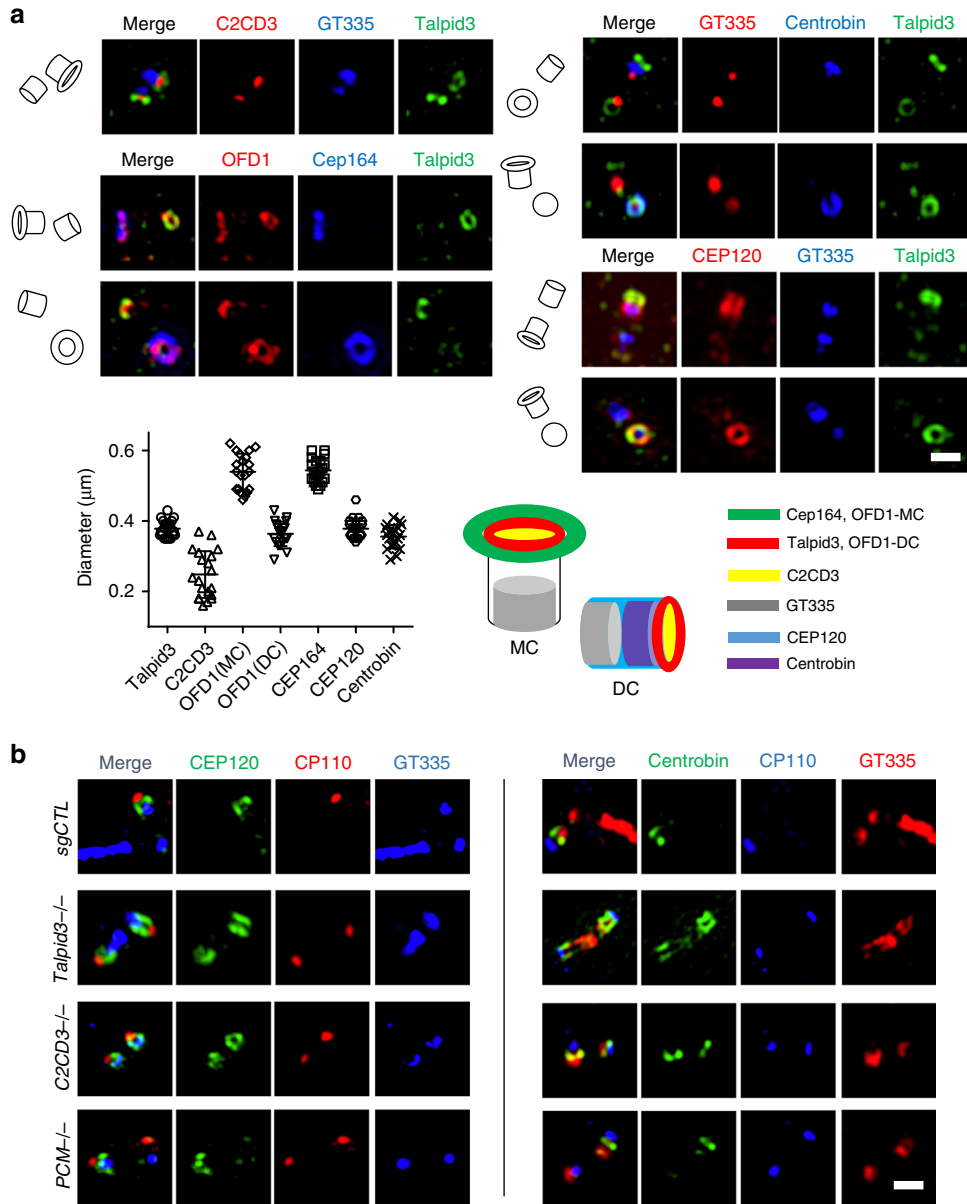


Fig. 6 Topography of distal and daughter centriolar proteins. **a** Growing RPE1 cells were stained with the indicated combinations of antibodies and visualized using structured illumination microscopy (SIM). Bottom left: diameter of the Talpid3/C2CD3/OFD1 complex, DCPs, and DA protein, CEP164 ($N = 20$). Cumulative data from two independent experiments are shown. Bottom right: schematic representation of the centrosome illustrates the localization of Talpid3/C2CD3/OFD1 complex, DCPs, and DA protein, CEP164. **b** Localization of CEP120 and Centrobin was examined in control, *Talpid3*^{-/-}, *C2CD3*^{-/-}, and *PCMI*^{-/-} cells using SIM. Cells were serum-starved for 24 h and then visualized with indicated antibodies. Scale bars = 0.5 μm

promote removal of DCPs from the mother centriole. Lastly, since ablation of Talpid3 leads to aberrantly long centrioles, and loss of C2CD3 leads to abnormally short centrioles (Figs. 1b and 6b²⁴), our data suggest that the observed centriole maturation defects are not solely due to excessively long centrioles.

Unique functions for Talpid3, C2CD3, and OFD1. Our findings provided definitive evidence to support a role for a distal centriolar network in promoting loss of DCPs as well as assembly of DA, major hallmarks of organelle asymmetry. To further explore the function of Talpid3, C2CD3, and OFD1 in the acquisition of centriolar asymmetry and the assembly of distal ends, we examined SDA assembly in all three knock-outs. We observed that C2CD3, but not Talpid3 or OFD1, was required for proper localization of SDA proteins (Figs. 7a and 1b), since the

percentage of *C2CD3*^{-/-} cells with centrosomal ODF2, CEP128, and Centriolin decreased by ~60% as compared to controls (Fig. 7a), consistent with EM studies in *C2cd3* and *Ofd1* mutant mouse embryonic fibroblasts (MEFs)^{24,26}. In contrast, removal of CEP128 and disruption of SDA did not affect the localization of Talpid3, C2CD3, and OFD1. These data also suggest that assembly of SDA is independent of DCP removal and DA assembly.

Next, we examined the centrosomal localization of the recently identified CEP350/FOP/CEP19 module⁴²⁻⁴⁴ in all three KO cell lines. On mother centrioles, the CEP350/FOP/CEP19 complex partitions to a region near the SDA (CEP350/FOP) or between sub-distal and distal (CEP19) appendages, and it is essential for IFT trafficking and ciliogenesis. Further, whereas CEP350 and FOP can be recruited to either centriole, CEP19 is enriched at the

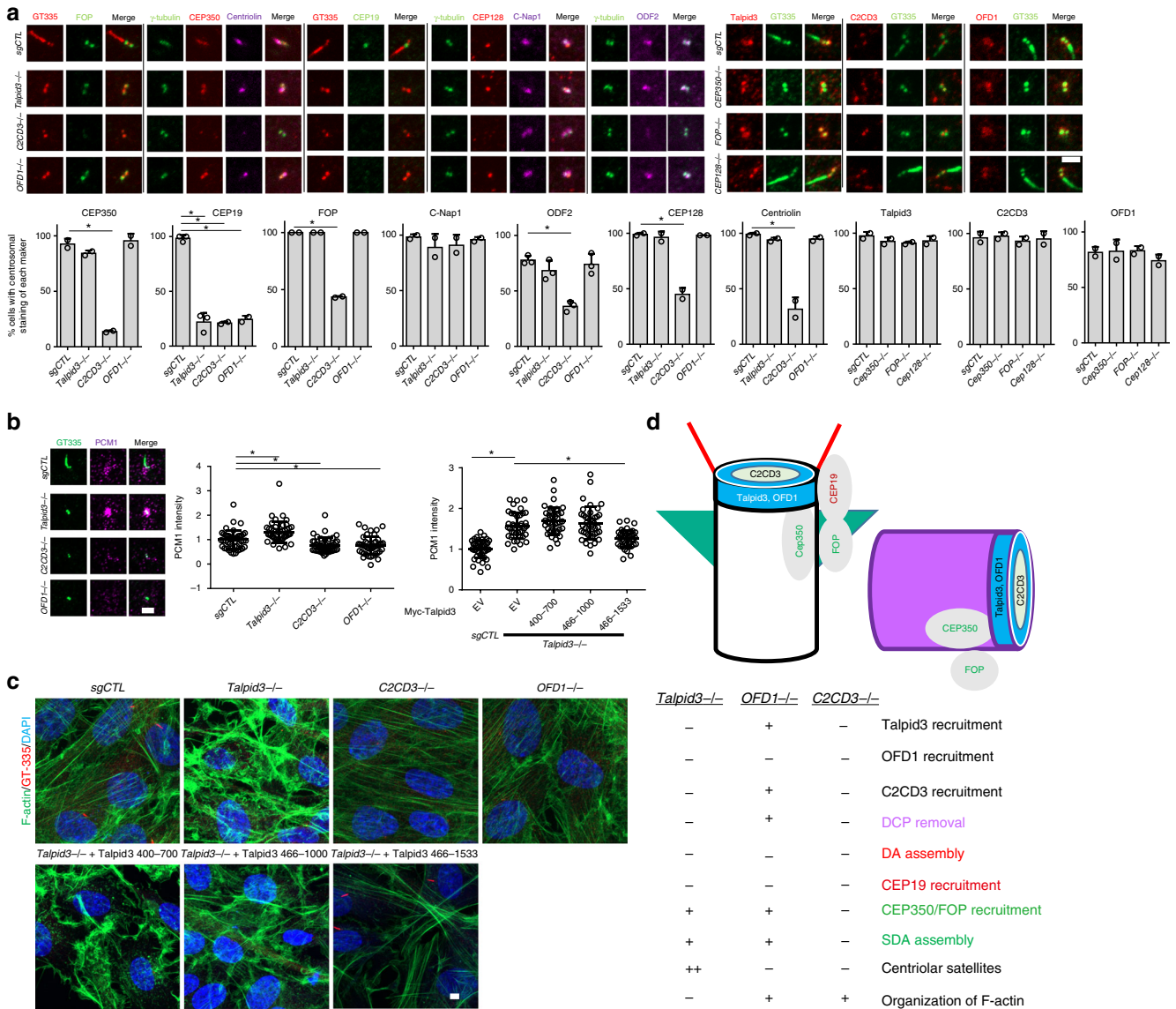


Fig. 7 Unique functions for Talpid3, C2CD3, and OFD1 in assembling distal-end structures. **a** Localization of CEP350/FOP/CEP19 module, SDA proteins, and **b**, **c** the organization of cytoplasmic actin and centriolar satellites (CS) was examined in control, *C2CD3*^{-/-}, *OFD1*^{-/-}, and *Talpid3*^{-/-} cells. Localization of Talpid3, C2CD3, and OFD1 was examined in control, *CEP350*^{-/-}, *FOP*^{-/-}, and *CEP128*^{-/-} cells. Cells were serum-starved for 24 h and then visualized with indicated antibodies. Cumulative data from two or three independent experiments are shown in **a**, as indicated by data dots. For each group, a minimum of 100 cells/experiment was averaged. Data from one experiment are shown in **b**, with 40 cells per group in the left panel and 45 cells per group in the right panel. Experiments were repeated independently two times with similar results. **d** Schematic of the unique functions for Talpid3, C2CD3, and OFD1 in assembling distal-end structures, CS and actin network (-, defective; +, normal; ++, enhanced). All data are presented as mean ± SD. **p* < 0.05 (unpaired t-test). Scale bars = 2 μm

mother centriole/basal body upon serum starvation⁴⁵ (Fig. 7a). Strikingly, we observed that CEP19 localization was defective in all three KO cell lines, whereas CEP350 was absent only in *C2CD3*^{-/-} cells. Similarly, FOP staining was lost from ~60% of *C2CD3*^{-/-} cells, but it appeared normal in *Talpid3*^{-/-} and *OFD1*^{-/-} cells (Fig. 7a). In an effort to determine whether restoration of CEP19 could be tied to other mother centriole-specific maturation-associated events, we attempted to rescue its localization in *Talpid3*^{-/-} cells. Interestingly, residues 466–700 of Talpid3 were sufficient to restore proper localization of CEP19 in *Talpid3* KO cells (Figs. 2a and 7a), indicating that recruitment of CEP19 may be tightly linked to critical steps in maturation, namely, removal of DCP and acquisition of DAs. The rescue of CEP19 localization was further confirmed by measuring the diameter of CEP19 rings using SIM

(Supplementary Fig. 1c). Conversely, ablation of *CEP350* or *FOP* does not affect the localization of Talpid3, C2CD3, and OFD1. These data suggest that the Talpid3–OFD1–C2CD3 network, together with FOP and CEP350, play a prominent role in recruitment of CEP19. C2CD3 can be placed higher in a regulatory hierarchy by controlling recruitment of OFD1, FOP, and CEP350, and Talpid3 could regulate CEP19 localization through OFD1 (see Discussion).

Previous studies from our lab and others^{36,46} suggested a functional antagonism between Talpid3 and OFD1 in the organization of CS. To confirm previous discoveries and compare the functions of Talpid3, C2CD3, and OFD1 in CS organization, we investigated the PCM1 staining pattern in *Talpid3*^{-/-}, *C2CD3*^{-/-}, and *OFD1*^{-/-} cells. Consistent with previous studies, we observed accumulation and increased intensity of CS near centrioles in

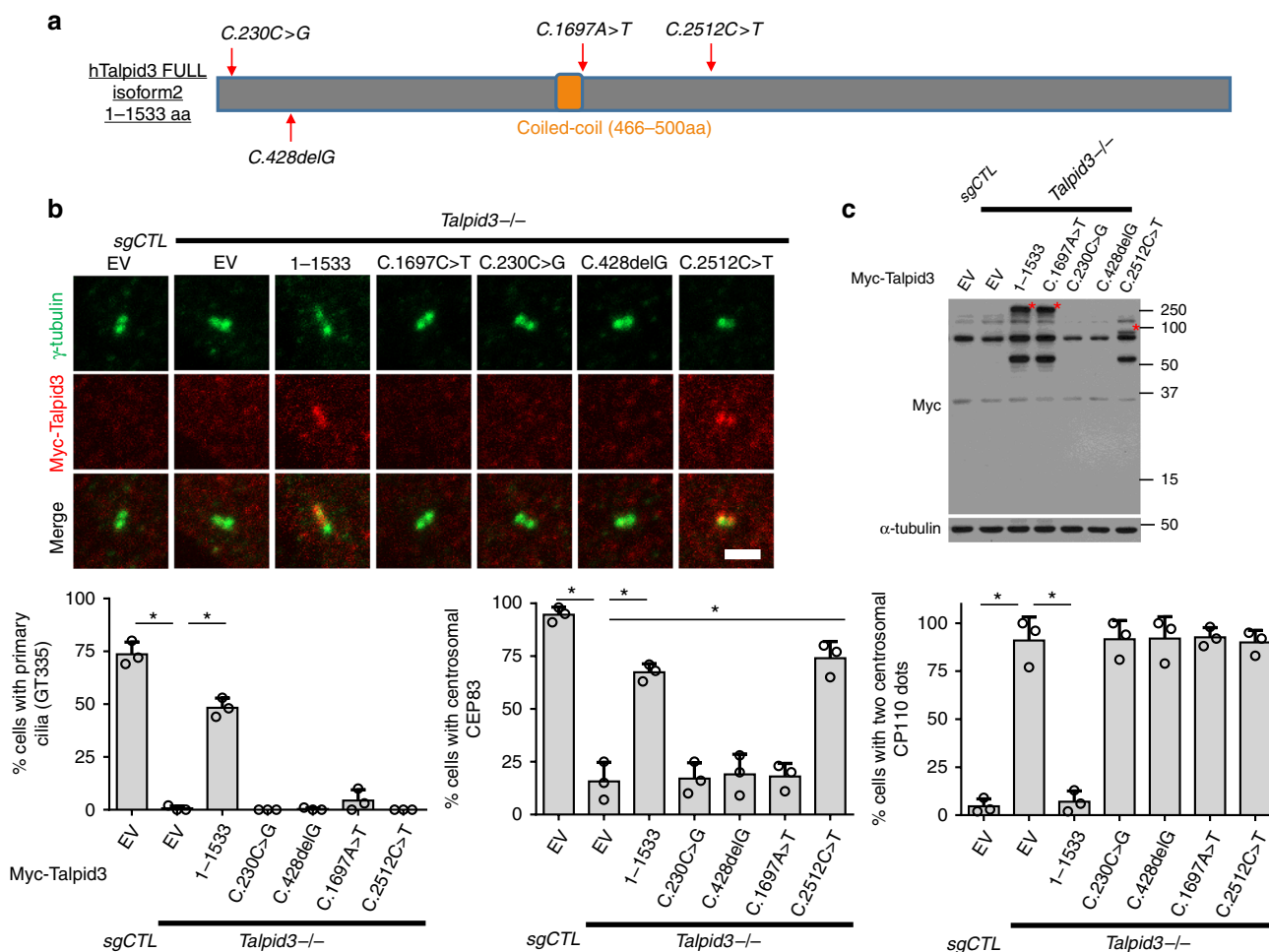


Fig. 8 Talpid3 mutants associated with JBTS and other lethal ciliopathies display centriole maturation defects. **a** Summary of Talpid3 mutations under investigation and their locations (red arrows) in Talpid3 protein. Centrosomal and ciliary defects in *Talpid3* KO cells were rescued by infection with lentiviruses expressing Myc-tagged Talpid3 constructs. Cells were examined by IF (**b**) and WB (**c**) after 48 h of serum starvation using indicated antibodies. Specific truncation proteins are indicated with an asterisk. Cumulative data from three independent experiments are shown. For each group, a minimum of 100 cells/experiment was averaged. All data are presented as mean ± SD. **p* < 0.05 (unpaired *t*-test). Scale bar = 2 μm

Talpid3^{-/-} cells compared to controls (Fig. 7b), and in rescue experiments, residues 1001–1533 of Talpid3 were required to promote proper CS organization in null cells. Moreover, in *C2CD3*^{-/-} and *OFD1*^{-/-} cells, we observed a significant decrease in CS staining near centrosomes (Fig. 7b). These data demonstrate that both *C2CD3* and *OFD1* are required for maintenance of CS organization, and *C2CD3* may exert its role by regulating the localization of *OFD1*. These data also suggest that Talpid3 inhibits CS accumulation through other unknown regulators and that the absence of SDA or DA in these knock-out cells is not a result of aberrant organization of CS around centrosomes.

The distal ends of centrioles also play a role in assembling the actin network. This may be due in part to interactions between CP110, ciliary adhesion complexes, and components of the actin cytoskeleton^{47,48}. In addition, loss of Talpid3 provokes remodeling of actin filaments in mouse and chicken mutants^{28,49}. Indeed, we observed disorganization of the actin network, marked by reduced stress fibers and punctate staining in *Talpid3* KO cells (Fig. 7c). In rescue experiments, the required regulatory region included residues 1001–1533 of Talpid3 (Fig. 7c). Interestingly, *C2CD3* and *OFD1* ablation did not disrupt actin organization (Fig. 7c). These studies suggest that Talpid3, a CP110-interacting protein, may be uniquely required among this group of distal proteins to organize actin networks. Moreover, our results suggest

that the absence of SDA or DA is not sufficient to promote remodeling of the actin cytoskeleton, and conversely, the ability to maintain the actin and CS networks does not guarantee the normal assembly of appendages.

Altogether, these data demonstrate that Talpid3, *C2CD3*, and *OFD1* commonly regulate the assembly of DA, but they play distinct roles in DCP removal as well as in the assembly of SDA, CS, the actin cytoskeleton, and the CEP350/FOP/CEP19 module (Fig. 7d).

Talpid3 mutations associated with ciliopathies affect centriole maturation and ciliogenesis. Mutations in human *KIAA0586/Talpid3* have been linked to JBTS and other lethal ciliopathies^{30–35}. It is not well understood how these mutations affect the centriolar structure and promote disease phenotypes. In an effort to determine which functions of Talpid3 are most critical, we expressed patient-derived *Talpid3* alleles and asked whether they are compromised for one or more of the functions that we have analyzed in our studies. We generated human Talpid3 constructs harboring a variety of mutations described previously and compared the ability of wild-type Talpid3 and four patient-derived mutant proteins to localize to the centriole and to rescue centriolar defects observed in

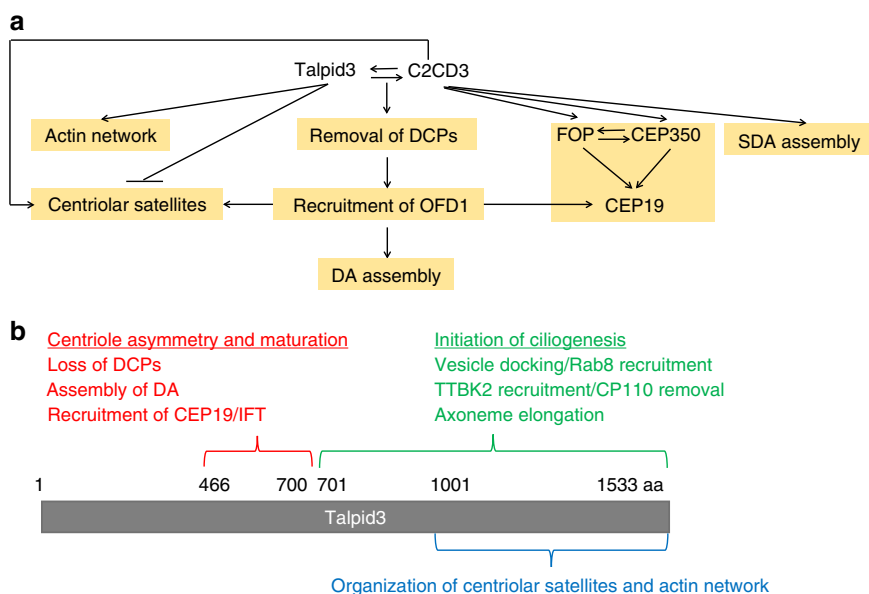


Fig. 9 The Talpid3-C2CD3-OFD1 complex as a multi-functional hub that promotes centriole maturation and asymmetry. **a** Model summarizing how Talpid3, C2CD3, and OFD1 promote centriole maturation and assembly of distal structures. **b** Schematic of the functional and interacting regions of Talpid3. See text for details

Talpid3^{-/-} RPE1 cells (Fig. 8). The substitution mutation, *C.230C>G*, and deletion mutation, *C.428delG*, are predicted to result in truncated proteins of 77 and 147 amino acids, respectively. The predicted truncations were not detected by immunoblotting, were unable to localize to centriole by IF, and were therefore unable to rescue centriole maturation or ciliogenesis (Fig. 8). The substitution mutation, *C.1697A>T*, causes a single amino acid change (p.D566V) near the conserved coiled-coil domain, which is required for centrosomal localization of Talpid3. Surprisingly, this mutant protein, though expressed at the same level as endogenous Talpid3, was unable to localize to centrosomes, and it was unable to rescue centriole maturation and ciliogenesis. Therefore, correct localization of Talpid3 at centrioles is essential for its ability to promote centriole asymmetry and maturation (Fig. 8). The substitution mutation, *C.2512C>T*, is predicted to result in a truncated protein of 838 amino acids. This mutant protein correctly localized to the centrosome and was able to rescue centriole maturation but not CP110 removal or cilia formation. These data are consistent with our functional mapping of Talpid3 fragments (Figs. 8 and 2a). We conclude that the Talpid3 mutations found in JBTS and other lethal ciliopathies patients can be classified into three groups. One group of mutations resides in the amino-terminal portion (residues 1–465) of Talpid3, results in early termination and/or production of highly unstable proteins, and fails to support centriole maturation and ciliogenesis. The second group of mutations maps near the coil-coil domain (466–500 aa), disrupts the localization of Talpid3 to centrosomes, and abrogates centriole maturation and ciliogenesis. The third group of mutations partitions to the carboxy-terminal region (700–1533 aa) and results in truncation mutants that include residues 400–700, which enable normal centriole maturation but abrogate ciliogenesis. Although additional experiments are required, our data also suggest that diverse Talpid3 mutations, which result in defects at different stages of centriole maturation and ciliogenesis, could explain the spectrum of pathologies observed in JBTS and other lethal ciliopathies patients.

Discussion

In this study, we identified Talpid3 and C2CD3 as critical regulators of DCP removal and revealed that removal of certain DCPs constitutes another level of control for DA assembly. We also revealed that a centriolar protein network, comprised of Talpid3, C2CD3, and OFD1, differentially regulates the assembly of other distal centriole structures, CS, and the actin network. Our studies could ultimately link defects in Talpid3 function to Joubert Syndrome and other lethal ciliopathies and explain the spectrum of pathologies associated with human mutations in *OFD1* and *C2CD3*.

Until now, the controlled removal of DCPs and its relationship with DA assembly have not been methodically studied. This is due, in part, to the paucity of daughter centriole proteins identified thus far (three to-date). Indeed, it is intriguing that few daughter proteins have been identified, given that a substantially larger number of mother-specific proteins have been uncovered. We found that the removal of these three DCPs is an all-or-none event, such that future mother centrioles either remove or retain each of them (Fig. 1a and Supplementary Fig. 1a). This could be partially explained by the hierarchical recruitment/organization of DCPs (Fig. 3d). We found that control of CEP120 removal is critical for the removal of the other two DCPs. Since the CS pools of C2CD3 and OFD1 are not required for centriole maturation (Fig. 4a and Supplementary Fig. 5), and the centrosomal pools of Talpid3, C2CD3, and OFD1 reside exclusively at the distal ends of centrioles, our data imply that the removal of DCPs may be triggered or regulated at the distal end of the maturing mother centriole, where CEP120 and Centrobilin co-localize with, or are juxtaposed to, Talpid3 and C2CD3. However, future studies will be required to determine how Talpid3 and C2CD3 regulate the removal of DCPs, given that the overall abundance of DCPs is not affected by the loss of Talpid3 or C2CD3 (Supplementary Fig. 4b). One possibility is that Talpid3 and C2CD3 enforce localized, centrosome-specific protein degradation of DCPs. It is also possible that Talpid3 and C2CD3 recruit an enzyme, such as a protein kinase, that alters the conformation and recruitment of DCPs. Also, since CEP120 and Centrobilin interact with microtubules and regulate their stability^{2,4},

the modifications/decorations of microtubules during centriole maturation could also affect the localization of DCPs. The possibility that *Talpid3* and *C2CD3* regulate such modifications cannot be excluded at this time.

We established that removal of DCPs constitutes another layer of DA assembly control based on the following evidence. First, defects in the removal of DCPs are accompanied by aberrant DA assembly in *Talpid3* and *C2CD3* KO cells (Figs. 1a and 4a) and, potentially, in patients harboring mutations in these genes. Both defects can be rescued by the same *Talpid3* fragment, consisting of residues 400–700, in *Talpid3*^{-/-} cells (Fig. 2a). Second, mimicking defective DCP removal observed in KO cells—by targeting CEP120 and Centrobins to both centrioles—suppressed DA assembly, and disruption of symmetrical localization of Centrobins in *Talpid3*^{-/-} and *C2CD3*^{-/-} cells reversed this inhibitory effect (Fig. 3a, b). Furthermore, we found that removal of DCPs is important for proper OFD1 localization, which in turn initiates DA assembly (Fig. 5). Therefore, our observations suggest how DCPs removal is mechanistically and temporally linked to subsequent maturation events such as appendage formation (Fig. 9a). How removal of DCPs promotes OFD1 recruitment remains to be determined. One possibility is that the inability to remove DCPs could sterically prevent the proper recruitment or localization of OFD1, and this mechanism is supported by the observations that PACT–CEP120 and PACT–Centrobins expression blocked OFD1 recruitment (Fig. 5a). It is also possible that removal of DCPs constitutes a checkpoint monitored by unknown regulatory protein(s) that also control the recruitment of OFD1 and initiation of DA assembly. Moreover, loss of DA has also been found recently in *Talpid3*^{-/-} chicken cells³⁴, suggesting that the function of *Talpid3* in mother centriole maturation is evolutionarily conserved. We previously found that knock-down of *Talpid3* did not cause a centriole maturation defect³⁶, which we ascribe to the incomplete knock-down of *Talpid3* afforded by RNAi, reinforcing the importance of using genetically null cells for studying centriolar protein function. Our work could thus explain certain genotype–phenotype relationships in ciliopathies, as particular patient alleles may reduce the abundance of *Talpid3* protein on centrosomes, whereas other alleles—such as the ones shown here (Fig. 8)—may abolish *Talpid3* protein expression altogether.

Our work may also shed further light on another important question, namely, how vesicle docking to basal bodies is intricately coupled to DA assembly. We speculate that *Talpid3* is a bi-functional protein: whereas a middle fragment of the protein is required for organelle asymmetry and maturation as well as IFT recruitment, the carboxy-terminal half of *Talpid3* could engage with determinants on early ciliary vesicles and initiate ciliogenesis (Fig. 9b). Our previous study showed that *Talpid3* directly interacts with Rab8a and Rabin8, and this event could promote vesicle docking³⁶.

In this study, we have also unveiled both overlapping and distinct roles for *Talpid3*, *C2CD3*, and OFD1 in assembling distal-end structures, CS, and the actin network (Fig. 7), allowing us to study their interdependencies and functional relationships in DCP removal and DA assembly. Among these three proteins, *Talpid3* plays a unique role in the organization of cytoplasmic actin, while *C2CD3* is specifically required for SDA assembly. In terms of CS organization, *Talpid3* antagonizes the function of *C2CD3* and OFD1. Importantly, these data suggest that assembly of the SDA, CS, and actin network are independent of DCP removal and DA assembly. We also uncovered distinct roles for *Talpid3*, *C2CD3*, and OFD1 in assembling the distal end CEP350/FOP/CEP19 complex and demonstrated that the recruitment of CEP19, but not CEP350 or FOP, is linked to DCP removal and DA assembly (Figs. 7d and 9a). On the other hand, *C2CD3* plays a unique role in regulating the recruitment of CEP350 and FOP. Considering

the proximity of CEP350 and FOP to SDA, these data also suggest *C2CD3* as a key organizer of sub-distal structures.

Our results are interesting in light of recent findings on *C2CD3* and OFD1, both of which traffic from CS to centrioles^{25,46}. *C2CD3* is conserved in worms (*SAS-1*)⁵⁰ and birds (*Talpid2*). Interestingly, the avian *Talpid2* mutation results from a 120 amino acid carboxy-terminal deletion, which produces Hh and limb phenotypes also seen in *Talpid3* mutants, and, interestingly, *Talpid2* and *Talpid3* animals exhibit cranio-facial defects⁵¹. *C2CD3* is required for ciliogenesis, and human mutations in this gene lead to JBTS and OFD-type syndrome with additional features of JBTS^{24,52,53}, suggesting potentially overlapping disease mechanisms. Furthermore, SDA and DA assembly and CV recruitment are nearly abolished after depleting human *C2CD3* and in *Talpid2* mutant cells^{24,51}. Moreover, *C2cd3* and *Ofd1* silencing leads to abnormally short or long centrioles^{24,26}, respectively, and *Talpid3* ablation similarly promotes aberrant centriole elongation (Fig. 1b and refs. 34,36). Given that all three genes (*Talpid3*, *Ofd1*, and *C2cd3*) have been implicated in ciliopathies and that several inter-related sets of defects result from the loss of each gene, these findings point to a potentially important and intimate relationship between *Talpid3*, OFD1, and *C2CD3* in assembling an essential functional complex at basal body distal ends, defects in which lead to human ciliopathies.

Our work has revealed an extensive, overlapping set of functional similarities between *Talpid3* and OFD1, which is also mutated in JBTS^{54,55}. It will be important to understand the molecular basis for anomalies observed in JBTS patient cells by assessing phenotypes known to be associated with *Talpid3* loss. It will also be interesting to determine whether disease-associated *Ofd1* and *C2CD3* mutations result in defects in recruitment or localization of *Talpid3*, DCP removal, basal body maturation, Rab trafficking, and ciliogenesis. JBTS patients with *Talpid3* mutations show brain defects, although they exhibit varying degrees of pathology. In this study, we identified three types of *Talpid3* mutations that affect different stages of centriole maturation and ciliogenesis, suggesting a potential causative link between defects in these events and varying degrees of pathology in JBTS patients. Future experiments will determine whether disease mutations map to distinct fragments with specific functions that we have identified herein, thereby producing unique disease phenotypes of differing severity.

Methods

Cell culture and gene-editing using CRISPR/Cas9. Human retinal pigment epithelial (RPE1-hTERT) and human embryonic kidney (HEK293T) cells were obtained from ATCC. Cells were grown in DMEM supplemented with 10% FBS. To induce cilia formation, RPE1 were incubated in DMEM without FBS for 24 or 48 h. To generate CRISPR KO cells, RPE1 cells were infected with lentivirus expressing Flag-Cas9 and sgRNA and grown for 10 days, after which the cells were examined by IF and separated as single cells into 96-well plates. After 2 weeks, the colonies were analyzed for genome editing. sgRNAs used included: sgCTL (5'-GAGACGTCTAGCA CGTCTCT-3'), sg*Talpid3* (5'-GATGATGTTCTTCATGACCT-3'), sg*C2CD3* (5'-GGAGGAGGTGATCTTCAATG-3'), sgOFD1 (5'-GGTGCTTGTGAATCTT TCA-3'), and sgCEP128 (5'-GCTGCCAGATCAACGCACAGGG-3').

Transfection and lentivirus infection. Polyethylenimine (PEI) was used for plasmid transfection in 293T cells. DNA and PEI (1 mg/ml) were added at 1:5 to 1:8 ratio. Lentiviral supernatant was prepared by co-transfection of the lentiviral plasmid with Δ8.2 envelope and VsVG packaging plasmids into 293T cells using PEI. Lentivirus supernatants were harvested 48–72 h post-transfection. RPE1 cells were incubated with virus supernatants in the presence of 8 μg/ml polybrene for 6–10 h, and medium was changed thereafter. siRNAs were transfected into RPE1 cells using RNAiMAX (Invitrogen, Carlsbad, CA) according to the manufacturer's protocol. siRNAs were synthesized by Dharmacon with the following sequences: non-specific control (5'-AATTCTCCGAACGTGTACAGT-3'), Centrobins (5'-GGATGGTTCT AAGCATATC-3'), CEP120 (5'-GAUGAGAACGGGUGUGUUAU-3', 5'-AAACCG AGCGACAAGAAUU-3', and 5'-GGAUUUAAGAACCGCUCUAA-3') siRNAs, and the siRNA pool against CEP83 (L-021034-02-0005).

DNA constructs. To generate Myc-tagged Talpid3 proteins, human Talpid3 truncations were amplified by PCR and sub-cloned into the PCDH-Myc-Neo vector. Talpid3 mutants were generated by site-directed mutagenesis. The expression of Talpid3 truncations and mutants was confirmed by immunoblotting using a mixture of Talpid3_1 and Talpid3_2 antibodies or anti-Myc antibody. To generate Myc-tagged C2CD3 protein, a human C2CD3 cDNA was obtained from Kazusa DNA Research Institute (Kazusa-kamatari, Chiba, Japan) and cloned into PCDH-Myc-Neo vector. A plasmid expressing Myc-tagged OFD1 was obtained from Andrew M. Fry (University of Leicester, Leicester, UK). EGFP-SmoM2 was a gift from J.F. Reiter (University of California, San Francisco, USA). To generate Myc-tagged PACT-CEP120 and PACT-Centrobins, the PACT domain, CEP120, and Centrobins were amplified by PCR and sub-cloned into Plvx-Myc vector. Myc-tagged PACT-Neurl4 was generated by sub-cloning the PACT domain and Neurl4 into the PCDH-Myc-Neo vector. To generate Myc-tagged Talpid3Nter-C2CD3 and Talpid3Nter-OFD1, Talpid3Nter, C2CD3, and OFD1 were amplified by PCR and sub-cloned into PCDH-Myc-Neo vector. All PCR reactions were performed using high fidelity PfuTurbo DNA polymerases (Agilent), and the PCR-generated plasmids were further verified by DNA sequencing.

Immunoprecipitation. 293T or RPE1 cells were lysed in ELB buffer (50 mM Hepes pH 7, 150 mM NaCl, 5 mM EDTA pH 8, 0.1% NP-40, 1 mM DTT, 0.5 mM AEBBSF, 2 µg/ml leupeptin, 2 µg/ml aprotinin, 10 mM NaF, 50 mM β-glycerophosphate, and 10% glycerol) on ice for 10 min, lysates were centrifuged at 16,000×g for 15 min, and supernatants were incubated with 2 µg anti-Myc antibody (sc-40, Santa Cruz) and 15 µl Protein G Sepharose (17-0618-01, GE Healthcare) or 15 µl Flag beads (A2220, Sigma-Aldrich). For immunoprecipitation, 2 mg of the resulting supernatant was immunoprecipitated, and beads were washed with ELB buffer and analyzed by immunoblotting. Protein band intensities were quantified using Image J software. The uncropped blots are shown in Supplementary Fig. 6.

Immunofluorescence microscopy. Cells were fixed with cold methanol for 10 min or with 10% formalin solution (Sigma-Aldrich) for 15 min and permeabilized with 0.3% Triton X-100/PBS for 10 min. Slides were blocked with 3% BSA in PBS before incubation with primary antibodies. Secondary antibodies used were Cy3-conjugated (Jackson ImmunoResearch Laboratories, Inc.), Alexa Fluor 488-conjugated or Alexa Fluor 647-conjugated (Invitrogen) donkey anti-mouse, anti-rabbit, or anti-goat IgG. Cells were stained with DAPI, and slides were mounted, observed, and photographed using a microscope (63× or 100×, NA 1.4; Axiovert 200M, Carl Zeiss) equipped with a cooled CCD (Retiga 2000R; QImaging) and MetaMorph Software (Molecular Devices). Alternatively, an LSM 800 confocal microscope (63×, NA 1.4 Carl Zeiss) with Zen software (Carl Zeiss) was used. Super-resolution microscopy was performed using a structured-illumination microscopy (SIM) system (DeltaVision OMX 3D; Applied Precision). For SIM, a 100×, 1.4 NA oil objective (Olympus) was used with 405, 488, and 593 nm laser illumination and standard excitation and emission filter sets. 125-nm z-steps were applied to acquire raw images, which were reconstructed in 3D using SoftWoRx software (Applied Precision). Image analysis was performed using Photoshop (Adobe). Intensity of CS and DA proteins was quantified by Image J. Briefly, regions of interest were defined by drawing a circle (radius of 2.5 µm for PCM1 and 0.8 µm for CEP83 and CEP164) centered on the centrosome. Background values were measured from the same-sized circle in an adjacent region. Staining was analyzed in G0/G1 phase cells (serum-starved for 24 or 48 h) to achieve uniformity and to avoid oscillations in abundance during the cell cycle.

Transmission electron microscopy (TEM). RPE1 cells were washed with PBS followed by fixation with 0.1 M sodium cacodylate buffer (pH 7.4) supplemented with 2% paraformaldehyde, 2.5% glutaraldehyde, and 0.1% Ruthenium red. Cells were post-fixed with 1% osmium tetroxide for 1.5 h at room temperature, and stained with 1% uranyl acetate, processed in a standard manner, and embedded in EMbed 812 (Electron Microscopy Sciences) for TEM. Serial thin (60 nm) sections were cut, mounted on 200 mesh or slotted copper grids, and stained with uranyl acetate and lead citrate. Stained grids were examined using an electron microscope (model CM-12; Philips/FEI) and photographed with a 4-k × 2.7-k digital camera (Gatan, Inc.).

Antibodies. Antibodies used include: Talpid3_1 (antigen:1–180, 1:500 for WB), Talpid3_2 (antigen: 847–1026, 1:500 for IF and WB), centrin (1:2500 for IF, 04-1624; Millipore), Rabbit anti-Flag (1:2000 for WB, F7425, Sigma), mouse anti-Flag (1:2000 for WB and 1:500 for IF, F1804, Sigma), goat anti-GFP (1:500 for IF, ab545025, Abcam), mouse anti-α-tubulin (1:5000 for WB, T5168, Sigma), goat anti-γ-tubulin (1:500 for IF, sc-7396, Santa Cruz), mouse anti-polyglutamylated tubulin (GT335) (1:2500 for IF, AG-20B-0020-C100, Adipogen), rabbit anti-IFT88 (1:1000 for WB and 1:500 for IF, 13967-1-AP, Proteintech), rabbit anti-IFT140 (1:200 for IF, 17460-1-AP, Proteintech), rabbit anti-Arl13b (1:2000 for WB and 1:2000 for IF, 17711-1-AP, Proteintech), rabbit anti-Rab8 (1:200 for IF, gift from J. Peränen), rabbit anti-TTBK2 (1:500 for IF, HPA018113, sigma), rabbit anti-CP110 (1:1000 for WB and 1:200 for IF), rabbit anti-OFD1 (1:2000 for WB and 1:500 for IF, gift of J.F. Reiter), rabbit anti-OFD1-2 (1:1000 for WB and 1:250 for IF, gift of A. Fry), mouse anti-CEP170 (1:500 for IF, 72-413-1, Invitrogen), rabbit anti-Neurl4 (1:500 for IF),

mouse anti-Centrobins (1:1000 for IF, ab70448, Abcam), rabbit anti-CEP120 (1:5000 for IF, gift from LH Tsai), rabbit anti-FBF1 (1:500 for IF, 11531-1-AP, Proteintech), rabbit anti-CEP83 (1:500 for IF, HPA038161, Sigma), rabbit anti-C2CD3 (1:500 for IF, HPA038552, Sigma), rabbit anti-CEP89 (1:50 for IF, gift from M. Bornens), rabbit anti-CEP164 (1:500 for IF, 45330002, Novus), rabbit anti-CEP19 (1:2000 for IF, ab74989, Abcam), rabbit anti-FOP (1:2000 for IF, A301-860A, Bethyl), rabbit anti-CEP350 (1:1000 for IF, NB100-59811, NOVUS), rabbit anti-ODF2 (1:100 for IF, H00004957-M01, NOVUS), rabbit anti CEP128 (1:2000 for IF; A303-348, Bethyl), and mouse anti-Centriolin (1:200 for IF; sc-365521, Santa Cruz).

Statistics and reproducibility. The statistical significance of the difference between two means was determined using a two-tailed unpaired Student's *t*-test. All data are presented as mean ± SD as specified in the figure legends. Differences were considered significant when *p* < 0.05. Results reported are from 2–3 independent biological replicates as noted in legends with reproducible findings each time. For all experiments, except as noted, *N* ≥ 100 cells per sample were counted in three biologically independent experiments.

Data availability

The uncropped western blots are shown in Supplementary Fig. 6. The data that support the findings of this study are available from the corresponding author (B.D.D.) upon reasonable request.

Received: 22 January 2018 Accepted: 24 August 2018

Published online: 26 September 2018

References

- Comartin, D. et al. CEP120 and SPICE1 cooperate with CPAP in centriole elongation. *Curr. Biol.* **23**, 1360–1366 (2013).
- Gudi, R., Zou, C., Li, J. & Gao, Q. Centrobins-tubulin interaction is required for centriole elongation and stability. *J. Cell Biol.* **193**, 711–725 (2011).
- Li, J. et al. Neurl4, a novel daughter centriole protein, prevents formation of ectopic microtubule organizing centres. *EMBO Rep.* **13**, 547–553 (2012).
- Lin, Y. N. et al. CEP120 interacts with CPAP and positively regulates centriole elongation. *J. Cell Biol.* **202**, 211–219 (2013).
- Mahjoub, M. R., Xie, Z. & Stearns, T. Cep120 is asymmetrically localized to the daughter centriole and is essential for centriole assembly. *J. Cell Biol.* **191**, 331–346 (2010).
- Zou, C. et al. Centrobins: a novel daughter centriole-associated protein that is required for centriole duplication. *J. Cell Biol.* **171**, 437–445 (2005).
- Cajane, L. & Nigg, E. A. Cep164 triggers ciliogenesis by recruiting Tau tubulin kinase 2 to the mother centriole. *Proc. Natl Acad. Sci. USA* **111**, E2841–E2850 (2014).
- Joo, K. et al. CCDC41 is required for ciliary vesicle docking to the mother centriole. *Proc. Natl Acad. Sci. USA* **110**, 5987–5992 (2013).
- Sillibourne, J. E. et al. Primary ciliogenesis requires the distal appendage component Cep123. *Biol. Open* **2**, 535–545 (2013).
- Stinchcombe, J. C. et al. Mother centriole distal appendages mediate centrosome docking at the immunological synapse and reveal mechanistic parallels with ciliogenesis. *Curr. Biol.* **25**, 3239–3244 (2015).
- Tanos, B. E. et al. Centriole distal appendages promote membrane docking, leading to cilia initiation. *Genes Dev.* **27**, 163–168 (2013).
- Wei, Q. et al. Transition fibre protein FBF1 is required for the ciliary entry of assembled intraflagellar transport complexes. *Nat. Commun.* **4**, 2750 (2013).
- Graser, S. et al. Cep164, a novel centriole appendage protein required for primary cilium formation. *J. Cell Biol.* **179**, 321–330 (2007).
- Mazo, G., Soplop, N., Wang, W. J., Uryu, K. & Tsou, M. B. Spatial control of primary ciliogenesis by subdistal appendages alters sensation-associated properties of cilia. *Dev. Cell* **39**, 424–437 (2016).
- Nakagawa, Y., Yamane, Y., Okanou, T., Tsukita, S. & Tsukita, S. Outer dense fiber 2 is a widespread centrosome scaffold component preferentially associated with mother centrioles: its identification from isolated centrosomes. *Mol. Biol. Cell* **12**, 1687–1697 (2001).
- Ishikawa, H., Kubo, A., Tsukita, S. & Tsukita, S. Odf2-deficient mother centrioles lack distal/subdistal appendages and the ability to generate primary cilia. *Nat. Cell Biol.* **7**, 517–524 (2005).
- Gromley, A. et al. A novel human protein of the maternal centriole is required for the final stages of cytokinesis and entry into S phase. *J. Cell Biol.* **161**, 535–545 (2003).
- Guarguaglini, G. et al. The forkhead-associated domain protein Cep170 interacts with Polo-like kinase 1 and serves as a marker for mature centrioles. *Mol. Biol. Cell* **16**, 1095–1107 (2005).
- Adly, N., Alhashem, A., Ammari, A. & Alkuraya, F. S. Ciliary genes TBC1D32/C6orf170 and SCLT1 are mutated in patients with OFD type IX. *Hum. Mutat.* **35**, 36–40 (2014).

20. Failler, M. et al. Mutations of CEP83 cause infantile nephronophthisis and intellectual disability. *Am. J. Hum. Genet.* **94**, 905–914 (2014).
21. Shaheen, R. et al. A founder CEP120 mutation in Jeune asphyxiating thoracic dystrophy expands the role of centriolar proteins in skeletal ciliopathies. *Hum. Mol. Genet.* **24**, 1410–1419 (2015).
22. Maria, M. et al. Genetic and clinical characterization of Pakistani families with Bardet–Biedl syndrome extends the genetic and phenotypic spectrum. *Sci. Rep.* **6**, 34764 (2016).
23. Li, J. et al. Sclt1 deficiency causes cystic kidney by activating ERK and STAT3 signaling. *Hum. Mol. Genet.* **26**, 2949–2960 (2017).
24. Thauvin-Robinet, C. et al. The oral–facial–digital syndrome gene C2CD3 encodes a positive regulator of centriole elongation. *Nat. Genet.* **46**, 905–911 (2014).
25. Ye, X., Zeng, H., Ning, G., Reiter, J. F. & Liu, A. C2cd3 is critical for centriolar distal appendage assembly and ciliary vesicle docking in mammals. *Proc. Natl Acad. Sci. USA* **111**, 2164–2169 (2014).
26. Singla, V., Romaguera-Ros, M., Garcia-Verdugo, J. M. & Reiter, J. F. Ofd1, a human disease gene, regulates the length and distal structure of centrioles. *Dev. Cell* **18**, 410–424 (2010).
27. Davey, M. G. et al. The chicken talpid3 gene encodes a novel protein essential for Hedgehog signaling. *Genes Dev.* **20**, 1365–1377 (2006).
28. Bangs, F. et al. Generation of mice with functional inactivation of talpid3, a gene first identified in chicken. *Development* **138**, 3261–3272 (2011).
29. Ben, J., Elworthy, S., Ng, A. S., van Eeden, F. & Ingham, P. W. Targeted mutation of the talpid3 gene in zebrafish reveals its conserved requirement for ciliogenesis and Hedgehog signalling across the vertebrates. *Development* **138**, 4969–4978 (2011).
30. Alby, C. et al. Mutations in KIAA0586 cause lethal ciliopathies ranging from a hydroletharus phenotype to short-rib polydactyly syndrome. *Am. J. Hum. Genet.* **97**, 311–318 (2015).
31. Bachmann-Gagescu, R. et al. KIAA0586 is mutated in Joubert syndrome. *Hum. Mutat.* **36**, 831–835 (2015).
32. Malicdan, M. C. et al. Mutations in human homologue of chicken talpid3 gene (KIAA0586) cause a hybrid ciliopathy with overlapping features of Jeune and Joubert syndromes. *J. Med. Genet.* **52**, 830–839 (2015).
33. Roosing, S. et al. Functional genome-wide siRNA screen identifies KIAA0586 as mutated in Joubert syndrome. *eLife* **4**, e06602 (2015).
34. Stephen, L. A. et al. TALPID3 controls centrosome and cell polarity and the human ortholog KIAA0586 is mutated in Joubert syndrome (JBTS23). *eLife* **4**, e08077 (2015).
35. Vilboux, T. et al. Molecular genetic findings and clinical correlations in 100 patients with Joubert syndrome and related disorders prospectively evaluated at a single center. *Genet. Med.* **19**, 875–882 (2017).
36. Kobayashi, T., Kim, S., Lin, Y. C., Inoue, T. & Dynlacht, B. D. The CP110-interacting proteins Talpid3 and Cep290 play overlapping and distinct roles in cilia assembly. *J. Cell Biol.* **204**, 215–229 (2014).
37. Wang, L., Lee, K., Malonis, R., Sanchez, I. & Dynlacht, B. D. Tethering of an E3 ligase by PCM1 regulates the abundance of centrosomal KIAA0586/Talpid3 and promotes ciliogenesis. *eLife* **5**, e12950 (2016).
38. Sanchez, I. & Dynlacht, B. D. Cilium assembly and disassembly. *Nat. Cell Biol.* **18**, 711–717 (2016).
39. Gillingham, A. K. & Munro, S. The PACT domain, a conserved centrosomal targeting motif in the coiled-coil proteins AKAP450 and pericentrin. *EMBO Rep.* **1**, 524–529 (2000).
40. Wu, C. et al. Talpid3-binding centrosomal protein Cep120 is required for centriole duplication and proliferation of cerebellar granule neuron progenitors. *PLoS ONE* **9**, e107943 (2014).
41. Lawo, S., Hasegan, M., Gupta, G. D. & Pelletier, L. Subdiffraction imaging of centrosomes reveals higher-order organizational features of pericentriolar material. *Nat. Cell Biol.* **14**, 1148–1158 (2012).
42. Kanie, T. et al. The CEP19-RABL2 GTPase complex binds IFT-B to initiate intraflagellar transport at the ciliary base. *Dev. Cell* **42**, 22–36 (2017).
43. Mojarad, B. A. et al. CEP19 cooperates with FOP and CEP350 to drive early steps in the ciliogenesis programme. *Open Biol.* **7**, 170114 (2017).
44. Nishijima, Y. et al. RABL2 interacts with the intraflagellar transport-B complex and CEP19 and participates in ciliary assembly. *Mol. Biol. Cell* **28**, 1652–1666 (2017).
45. Shalata, A. et al. Morbid obesity resulting from inactivation of the ciliary protein CEP19 in humans and mice. *Am. J. Hum. Genet.* **93**, 1061–1071 (2013).
46. Lopes, C. A. et al. Centriolar satellites are assembly points for proteins implicated in human ciliopathies, including oral–facial–digital syndrome 1. *J. Cell Sci.* **124**, 600–612 (2011).
47. Antoniadis, I., Stylianou, P. & Skourides, P. A. Making the connection: ciliary adhesion complexes anchor basal bodies to the actin cytoskeleton. *Dev. Cell* **28**, 70–80 (2014).
48. Walentek, P. et al. Ciliary transcription factors and miRNAs precisely regulate Cp110 levels required for ciliary adhesions and ciliogenesis. *eLife* **5**, e17557 (2016).
49. Yin, Y. et al. The Talpid3 gene (KIAA0586) encodes a centrosomal protein that is essential for primary cilia formation. *Development* **136**, 655–664 (2009).
50. von Tobel, L. et al. SAS-1 is a C2 domain protein critical for centriole integrity in *C. elegans*. *PLoS Genet.* **10**, e1004777 (2014).
51. Chang, C. F. et al. The cellular and molecular etiology of the craniofacial defects in the avian ciliopathic mutant talpid2. *Development* **141**, 3003–3012 (2014).
52. Hoover, A. N. et al. C2cd3 is required for cilia formation and Hedgehog signaling in mouse. *Development* **135**, 4049–4058 (2008).
53. Srouf, M. et al. Joubert Syndrome in French Canadians and identification of mutations in CEP104. *Am. J. Hum. Genet.* **97**, 744–753 (2015).
54. Coene, K. L. et al. OFD1 is mutated in X-linked Joubert syndrome and interacts with LCA5-encoded lebercilin. *Am. J. Hum. Genet.* **85**, 465–481 (2009).
55. Field, M. et al. Expanding the molecular basis and phenotypic spectrum of X-linked Joubert syndrome associated with OFD1 mutations. *Eur. J. Hum. Genet.* **20**, 806–809 (2012).

Acknowledgements

We thank M. Owa for helpful comments on our manuscript. We thank M. Bornens, A. Fry, and J. Reiter for plasmids and antibodies detailed in the Methods section. We are especially grateful to T. Kanie and P. Jackson for CEP350 and FOP null RPE1 cells. We thank F. Liang and the NYU School of Medicine Imaging core for assistance with EM. The Rockefeller University Bio-Imaging Center provided assistance. The project described was supported by Award Number S10RR031855 from the National Center for Research Resources. The content is solely the responsibility of the authors and does not necessarily represent the official views of the National Center for Research Resources or the National Institutes of Health. Work in BDD's laboratory was supported by 9R01GM120776-05A1 and a DOD prostate cancer postdoctoral training award W81XWH-16-1-0392 to L.W.

Author contributions

L.W. and B.D.D. designed the experiments, and L.W. conducted the experiments. M.F. generated *Cep128^{-/-}* cell line and contributed to the SIM experiments. W.F. contributed to the CRISPR knock-out experiments and EM studies. L.W. and B.D.D. analyzed the data and wrote the paper, and all authors were involved in reading and correcting the manuscript.

Additional information

Supplementary Information accompanies this paper at <https://doi.org/10.1038/s41467-018-06286-y>.

Competing interests: The authors declare no competing interests.

Reprints and permission information is available online at <http://npg.nature.com/reprintsandpermissions/>

Publisher's note: Springer Nature remains neutral with regard to jurisdictional claims in published maps and institutional affiliations.



Open Access This article is licensed under a Creative Commons Attribution 4.0 International License, which permits use, sharing, adaptation, distribution and reproduction in any medium or format, as long as you give appropriate credit to the original author(s) and the source, provide a link to the Creative Commons license, and indicate if changes were made. The images or other third party material in this article are included in the article's Creative Commons license, unless indicated otherwise in a credit line to the material. If material is not included in the article's Creative Commons license and your intended use is not permitted by statutory regulation or exceeds the permitted use, you will need to obtain permission directly from the copyright holder. To view a copy of this license, visit <http://creativecommons.org/licenses/by/4.0/>.

© The Author(s) 2018